

Electronic Supplementary Information

Bridging the opposite chemistries of tantalum and tungsten polyoxometalates

Pedro I. Molina^a, Dylan J. Sures^a, Pere Miró^b Lev N. Zakharov,^a May Nyman^{a*}

^aDepartment of Chemistry, Oregon State University, 107 Gilbert Hall, Corvallis, OR, 97331-4003, USA.

^cSchool of Engineering and Science, Jacobs University, Bremen, Germany

* Correspondence to May.Nyman@oregonstate.edu

Pedro I. Molina: Twitter, @scifanz; ORCID, 0000-0002-4491-3739.

List of figures and tables

Crystallographic summary	Table S1
Representations of the crystal structure of CsNa{Ta ₃ W ₃ }, Cs{Ta ₂ W ₈ } and Cs{NbW ₉ }.....	Fig S2-S6
Representations of the molecular structures of the Lindqvist ion and of decatungstate.....	Fig S7
Bond-Valence Summation (BVS) analysis	Table S8-S15
Assignments of the ESI-MS spectra	Table S16
UV-Vis spectra	Fig S17
CV of CsNa{Ta ₃ W ₃ }.....	Fig S18
TGA plots	Fig S19-S22
SEM micrographs	Fig S23
EDX spectra.....	Fig S24
ATR-FTIR spectra of starting materials.....	Fig S25
ATR-FTIR spectra of reported compounds.....	Fig S26-S30
Labelled representation of the structure of [W ₁₀ O ₃₂] ⁴⁻ {W ₁₀ }	Fig S31
Molecular structures of the substitutional isomers of {MW ₉ } (M= Nb, Ta).	Fig S32
Molecular structures of the substitutional isomers of {M ₂ W ₈ } (M= Nb, Ta).	Fig S33
HOMO/LUMO orbitals of {NbW ₉ } and {TaW ₉ }	Fig S34
HOMO/LUMO orbitals of {W ₁₀ }, {Ta ₂ W ₈ }, and [Nb ₂ W ₈ O ₃₂] ⁶⁻	Fig S35
Mulliken spin density on the metal centres of {W ₁₀ }, 2 and 3.....	Table S36-S38
HOMO/LUMO energies and E _{gap} of {W ₁₀ }, {NbW ₉ }, {TaW ₉ } and {Ta ₂ W ₈ } and their reduced derivatives.....	Table S39-S41
Experimental and calculated E _{gap} of {W ₁₀ }, {NbW ₉ }, {TaW ₉ } and {Ta ₂ W ₈ }	Table S42
Calculated redox potentials for {W ₁₀ }, {NbW ₉ }, {TaW ₉ } and {Ta ₂ W ₈ } and their reduced derivatives	Table S41
Calculated and experimental redox potentials for {W ₁₀ }, {NbW ₉ }, {TaW ₉ }.....	Table S42
Relative energies of the different {MW ₉ } isomers (M=Nb, Ta).....	Table S43
Relative energies of the different {MW ₉ } isomers (M=Nb, Ta).....	Table S44

Calculated redox potentials for the stepwise one- and two- electron reductions of $[W_{10}O_{32}]^{n-}$, $[TaW_9O_{32}]^{n-}$, $[NbW_9O_{32}]^{n-}$, $[Ta_2W_8O_{32}]^{n-}$ and $[Nb_2W_8O_{32}]^n$Table S45

Experimental and calculated (B3LYP) redox potentials for $[W_{10}O_{32}]^{4-}$, $[TaW_9O_{32}]^{5-}$, $[NbW_9O_{32}]^{5-}$, (vs. Ag/AgCl).....Table S46

Density of States (DOS) plots for $\{W_{10}\}$, $\{NbW_9\}$, $\{TaW_9\}$ and $\{Ta_2W_8\}$ and their reduced derivatives.....Fig S47-S74

Cartesian coordinate tables of $\{W_{10}\}$, $\{NbW_9\}$, $\{TaW_9\}$ and $\{Ta_2W_8\}$ and their reduced derivatives.....Tables S75-S103

Materials and Methods

Starting materials

All reagents starting materials were purchased from VWR and used without further purification: $TaCl_5$ (Puratronic®, 99.99 %), $Na_2WO_4 \cdot 2H_2O$ (95 %), $CsCl$ (99 %), Cs_2WO_4 (99 %), KOH (85-100 %), $CsOH$ (99.9 %), $NaCl$ (99.5 %), isopropyl alcohol and methanol. Literature procedures were used in the synthesis of $K_3[Ta(O_2)_4]^1$ and $[N(C_4H_9)_4][W_{10}O_{32}]^2$ and their identities were confirmed by FTIR and UV-Vis spectroscopies.

Cyclic Voltammetry (CV)

Electrochemical measurements were performed on an Epsilon Electrochemical Workstation (BASi). The stability of the cluster in solution for the duration of a typical CV experiment was confirmed by means of UV-Vis spectroscopy (Fig S17). The working, reference and auxiliary electrodes (BASi) were respectively glassy carbon (3 mm diam.), $Ag/AgCl$ (3M $NaCl$) and Pt wire. Before recording the voltammograms, the analyte solutions were purged with Ar for at least 15 min while the working electrode was polished with diamond suspensions of decreasing grain size (15, 6 and 1 μm), rinsed with water after each of the polishing routines and finally rinsed with methanol.

Fourier-transform Infrared Spectroscopy (FTIR)

Infrared spectra were recorded in attenuated reflectance mode (ATR) using a NicoletTM iSTM 10 spectrometer (Thermo Scientific).

Electrospray-ionisation mass spectrometry (ESI-MS)

Mass spectra were obtained from an Agilent 6230 ESI-MS system comprised of a Time-of-Flight (TOF) mass spectrometer coupled to an electrospray ioniser. 100 μL volumes of compound solutions (0.1 mM in

$\text{H}_2\text{O}:\text{CH}_3\text{CN}$, 4:1, v/v), were first mixed with a mobile phase of the same composition as the solvent, and then infused into the ESI-MS system at a flow rate of 0.5 mL min^{-1} using an Agilent 1260 Infinity quaternary pump. The solutions were nebulized with the aid of heated N_2 (325°C) flowing at 8 L min^{-1} and a pressure of 35 psig (241 kPa). The voltages of the capillary, skimmer and RT octopole were set at 3500, 65 and 750 V respectively, while the voltage of the fragmentor was set at 100 V.

pH measurements

The pH of the reaction mixtures was measured using an OrionTM VERSA STARTM pH/ISE Benchtop Multiparameter Meter. The instrument was calibrated using standard solutions before each round of measurements.

Thermogravimetric analysis (TGA)

Crystalline samples (20-40 mg) were placed in alumina crucibles and the corresponding thermograms were recorded under air flow (100 mL min^{-1}) on a SDT Q600 instrument (TA).

Scanning Electron Microscopy (SEM) / Energy Dispersive X-ray Spectroscopy (EDS)

Micrographs and elemental analysis of the crystalline materials were obtained from a Quanta 600F instrument (FEI).

X-ray crystallography

Data collection, reduction and refinement details

Diffraction intensities were collected at $173(2)$ K ($\text{CsNa}\{\text{Ta}_3\text{W}_3\}$, $\text{Cs}\{\text{NbW}_9\}$), $193(2)$ K ($\text{Cs}\{\text{TaW}_9\}$) and $200(2)$ K ($\text{Cs}\{\text{Ta}_2\text{W}_8\}$) on a Bruker Apex2 CCD diffractometer using MoK α radiation, $\lambda = 0.71073 \text{ \AA}$. Space groups were determined based on systematic absences ($\text{CsNa}\{\text{Ta}_3\text{W}_3\}$) and intensity statistics ($\text{Cs}\{\text{NbW}_9\}$, $\text{Cs}\{\text{TaW}_9\}$ and $\text{Cs}\{\text{Ta}_2\text{W}_8\}$). Absorption corrections were applied by SADABS.³ Structures were solved by direct methods and Fourier techniques and refined on F^2 using full matrix least-squares procedures. All calculations were performed by using the Bruker SHELXTL package.⁴

Notes on the refinement of the metal positions in the clusters

The crystal structure of $\{\text{Ta}_3\text{W}_3\}$ shows only one symmetrically independent metal position. Ta and W share this position in a 1:1 ratio as shown from a free refinement of the occupation factors for this position. These occupation factors were fixed to 0.5/0.5 in the final refinement of this structure.

The crystal structure of $\text{Cs}\{\text{NbW}_9\}$ is centrosymmetrical and there are five symmetrically independent positions of which the four equatorial ones (M2, Fig S7) are occupied by Nb/W and the apical position (M1, Fig S7) is fully occupied by W. This differential assignment of the equatorial and apical positions of

the structure is based on the significant disparity of electron number in Nb and W. Free refinement of W occupation factors on the M1/M2 positions yield a value very close to 1 for M1 and considerably lower than 1 for M2. The occupation factors at these four M2 positions obtained from a refinement in which such positions were treated as mixed Nb/W were 0.88/0.12, 0.89/0.11, 0.88/0.12 and 0.88/0.18. The eventual refinement of Cs{NbW₉} was performed by fixing the M1 apical position as fully occupied by W and the four M2 equatorial positions as Nb/W at a 0.125/0.875 ratio to correctly balance the charge of the compound. Finally, this assignment of the metal positions in the Cs{NbW₉} structure is supported by theory as substitution of Nb/Ta at the apical position is energetically disfavoured (Table S43). In the case of {TaW₉} and {Ta₂W₈}, the difference of electron number in Ta^V and W^{VI} is just one and therefore the analysis of the X-ray diffraction data cannot assign any of the metal positions as occupied solely by W or Ta. Hence, the final refinement of these two structures were performed in a similar fashion as for Cs{NbW₉} and confirmed by calculation (Table S43), *i.e.* the occupation of the apical M1 position was fixed as pure W while the remaining four equatorial M2 positions were fixed as Ta/W at ratios of 0.875/0.125 ({TaW₉}) and 0.75/0.25 ({Ta₂W₈}).

Notes on the refinement of the countercation and solvent molecules positions

The final refinements of countercation positions in the structures of Cs{NbW₉}, Cs{TaW₉} and Cs{Ta₂W₈} indicated that there are two types of such positions in the crystal structures. One of these types, *i.e.* the positions labelled as Cs1 and Cs2, are fully occupied by Cs. The second type (Cs3) is partially occupied (0.25) and disordered over two closely located positions in both Cs{NbW₉} and Cs{TaW₉}. However, this third Cs3 position is fully occupied by Cs in Cs{Ta₂W₈} in the same fashion as Cs1 and Cs2.

The solvent water molecules were refined isotropically. Some relatively high peaks on residual density in Cs{Ta₂W₈} are close to the terminal O atoms in the cluster and probably related to the fact that positions of terminal O atoms in W-O and Ta-O bonds are different.

Ultraviolet-Visible spectroscopy (UV-Vis)

Electronic absorption spectra were recorded on an Evolution™ 220 spectrophotometer (Thermo Scientific).

Experimental

Synthesis of starting materials

The ATR-FTIR spectra of K₃[Nb(O₂)₄], K₃[Ta(O₂)₄] and Cs₃[Ta(O₂)₄] are shown in Fig S25.

Synthesis of K₃[Nb(O₂)₄]

The procedure to prepare K₃[Nb(O₂)₄] is analogous to the one use for the synthesis of Cs₃[Ta(O₂)₄] except for the use of NbCl₅ (3.4 g, 12.6 mmol) and 4M KOH (35 mL) in the place of TaCl₅ and 4M

CsOH, respectively. Yield = 4.2 g (98 %, Nb). K₃NbO₈, MW = 337.8 g mol⁻¹. Characteristic IR bands (cm⁻¹): 429 (vsh), 536 (vsh), 590 (s), 812 (vsh).

Synthesis of Cs₃[Ta(O₂)₄]

The synthesis of Cs₃[Ta(O₂)₄] was adapted from a literature procedure.⁵ Aqueous H₂O₂ (30% v/v, 40 mL) was vigorously stirred in a 600 mL beaker placed in an ice bath. TaCl₅ (4.6 g, 12.8 mmol) was added to the cold solution (*ca.* 8 °C) and the resulting thin suspension was allowed to cool back down to *ca.* 8°C under moderate stirring. 4M aqueous CsOH (32 mL) was subsequently added in small volumes and in several steps, *i.e.* the addition of base was interrupted when the temperature of the mixture was close to 20 °C and resumed once the mixture had cooled back down to *ca.* 8 °C. A white precipitate formed and then dissolved fully during this base addition step. Cs₃[Ta(O₂)₄] was finally precipitated by adding methanol (150 mL) to the cold, clear solution; isolated by vacuum filtration, washed with more methanol (20 mL) and dried in air. Yield = 3.0 g (85 %, Ta). Cs₃O₈Ta, MW = 707.6 g mol⁻¹. Characteristic IR bands (cm⁻¹): 418 (vsh), 520 (vsh), 549 (s), 803 (vsh).

Synthesis of K₄W₁₀O₃₂·xH₂O (K{W₁₀})

The synthesis of K₄W₁₀O₃₂·xH₂O was adapted from the literature.⁶ Boiling 1M HCl (200 mL) was added to a boiling solution of Na₂WO₄·2H₂O (33 g, 100 mmol) and the resulting bright yellow clear solution was quickly cooled down to 0 °C with the aid of a dry ice/acetone bath. Saturated KCl solution (100 mL) was subsequently added to this solution under vigorous stirring and the light yellow-green precipitated produced was firstly isolated *via* vacuum filtration and finally dried under suction for 4h. Yield: 13.2 g (53 %, W). K₄W₁₀O₃₂, MW = 2507.2 g mol⁻¹. Characteristic IR bands (cm⁻¹): 433 (s), 574 (s), 790 (vs), 955 (vs).

Synthesis of mixed metal polyoxometalates

TGA/DSC plots for these compounds are shown in Fig S19-S22. SEM images and EDX spectra are also shown in Fig S23-S24. ATR-FTIR spectra of the compounds are shown in Fig S26-S30.

Synthesis of Cs₄Na[Ta₃W₃O₁₉]·6H₂O (CsNa{Ta₃W₃})

Cs₃[Ta(O₂)₄] (3.0 g, 4.2 mmol) was added to a solution of Na₂WO₄·2H₂O (3.3 g, 10.0 mmol) 30 mL of H₂O. The pH of the resulting turbid solution was adjusted to 8.0 by the dropwise addition of HCl (37%, v/v). The thin suspension thus obtained was refluxed for 5 h and the resulting mixture was centrifuged at room temperature. Colourless crystals plates of CsNa{Ta₃W₃} formed overnight in the supernatant placed at 4 °C in a cold chamber. Yield (crystals): 0.783 g (25% based on Ta). Cs₄H₁₂NaO₃₀Ta₃W₃, MW = 2061.4 g mol⁻¹. Atomic ratios (EDX), calculated (found): W/Ta 1.0 (1.0), W/Cs 0.8 (0.7). Characteristic IR bands (cm⁻¹): 537 (sh), 572 (sh), 772 (sh), 887 (w), 934 (s). UV absorption: λ (O→M) = 256 nm, ϵ = 2.0 × 10⁴ mol⁻¹ L cm⁻¹. Water content (%), crystallographic (TGA crystals, 22-200 °C, in air): 5.2 (5.4).

Crystallographic Data for CsNa{Ta₃W₃}: Cs₄H₁₂NaO₂₅Ta₃W₃, M = 2061.13, 0.16 x 0.12 x 0.04 mm, T = 173 K, Trigonal, space group R-3, a = 9.3948(3) Å, b = 9.3948(3) Å, c = 28.2796(11) Å, V =

$2161.62(16)$ Å 3 , $Z = 3$, $D_c = 4.750$ Mg/m 3 , $\mu = 28.348$ mm $^{-1}$, $F(000) = 2652$, $2\theta_{\max} = 74.29^\circ$, 14994 reflections, 2432 independent reflections [$R_{\text{int}} = 0.0455$], $R1 = 0.0342$, $wR2 = 0.0849$ and GOF = 1.116 for 2432 reflections (57 parameters) with $I > 2\sigma(I)$, $R1 = 0.0423$, $wR2 = 0.0880$ and GOF = 1.116 for all reflections, max/min residual electron density +3.436/-3.627 eÅ 3 .

Synthesis of Cs₅[NbW₉O₃₂]·7H₂O (Cs{NbW₉})

K₃[Nb(O₂)₄] (1.1 g, 3.3 mmol) was dissolved in 25 mL of H₂O at 70 °C. In a separate beaker, Na₂WO₄·2H₂O (3.6 g, 11 mmol) was dissolved in a mixture of H₂O (11.9 mL) and H₂O₂ (0.65 mL, 30% v/v). The contents of the two beakers were then combined and stirred for 30 min at 70 °C to afford a clear solution. The pH of this solution was adjusted to 2.0 (3M H₂SO₄) and the resulting mixture was first refluxed for 2 h and then centrifuged at room temperature. CsCl (5.6 g, 33 mmol) was added to the supernatant under vigorous stirring and the thick yellow suspension thus obtained was stirred for *ca.* 3 min and filtrated under vacuum. The isolated yellow precipitate was finally washed with cold water (2 mL) and dried under suction. Yield (crude product) = 2.089 g (21%, Nb). Analytically pure crystals of Cs{NbW₉} were obtained by recrystallizing this crude product twice from the minimum amount of boiling water and these crystals were subsequently used for further characterization. Cs₅H₁₄NbO₃₉W₉, MW = 3050.9 g mol $^{-1}$. Atomic ratios (EDX), calculated (found): W/Nb 9.0 (8.7), W/Cs 1.8 (1.8). Characteristic IR bands (cm $^{-1}$): 565 (s), 572 (s), 656 (s), 754 (vs), 879 (sh), 948 (vsh) 991 (vw). UV absorption: λ_1 (O→M, shoulder) = 260 nm, $\epsilon_1 = 13.2 \times 10^4$ mol $^{-1}$ L cm $^{-1}$, λ_2 (O→M, band) = 309 nm, $\epsilon_2 = 10.1 \times 10^4$ mol $^{-1}$ L cm $^{-1}$. Water content (%), crystallographic (TGA, 22-200 °C, in air): 4.1 (4.0).

Crystallographic data for Cs{NbW₉}: Cs₅H₁₅O_{39.50}NbW₉, M = 3051.67, 0.14 x 0.13 x 0.09 mm, T = 193(2) K, Triclinic, space group P-1, $a = 9.8464(4)$ Å, $b = 10.2634(4)$ Å, $c = 11.5535(4)$ Å, $\alpha = 99.160(2)^\circ$, $\beta = 100.815(2)^\circ$, $\gamma = 115.949(2)^\circ$, $V = 991.98(7)$ Å 3 , $Z = 1$, $D_c = 5.108$ Mg/m 3 , $\mu = 30.880$ mm $^{-1}$, $F(000) = 1306$, $2\theta_{\max} = 56.0^\circ$, 17629 reflections, 4770 independent reflections [$R_{\text{int}} = 0.0643$], $R1 = 0.0365$, $wR2 = 0.0690$ and GOF = 1.021 for 4770 reflections (268 parameters) with $I > 2\sigma(I)$, $R1 = 0.0561$, $wR2 = 0.0760$ and GOF = 1.021 for all reflections, max/min residual electron density +1.838/-1.809 eÅ 3 .

Synthesis of Cs₅[TaW₉O₃₂]·6.5H₂O (Cs{TaW₉})

K₃[Ta(O₂)₄] (2.0 g, 4.7 mmol) was added at room temperature to a stirred solution of Na₂WO₄·2H₂O (6.6 g, 20.0 mmol) in 40 mL of hot (ca 60 °C) H₂O. The pH of the resulting mixture was carefully adjusted to 2.0 by the dropwise addition of HCl (37% w/w). The yellow suspension was refluxed for 2 h and centrifuged at room temperature. CsCl (10.0 g, 59.4 mmol) was added to the isolated bright yellow supernatant and a mass of light orange solids was isolated from the resulting suspension by centrifugation, washed twice with 5 mL of water, twice with 20 mL of 2-propanol and finally dried under vacuum. This crude product was dissolved in 30 mL of boiling H₂O and yellow crystal plates formed overnight at 40°C. Yield (crude product) = 2.55 g (17.3 %, Ta) Cs₅H₁₃O_{38.5}TaW₉, MW = 3129.3 g mol $^{-1}$. Atomic ratios (EDX), calculated (found): W/Ta 9.0 (7.4), W/Cs 1.8 (1.9). Characteristic IR bands (cm $^{-1}$): 549 (s), 572 (s), 655 (s), 772 (vs), 885 (s), 953 (vs). UV absorption: λ_1 (O→M, shoulder) = 260 nm, $\epsilon_1 = 3.7 \times 10^4$ mol $^{-1}$ L cm $^{-1}$, λ_2 (O→M, band) = 305 nm, $\epsilon_2 = 2.8 \times 10^4$ mol $^{-1}$ L cm $^{-1}$. Water content (%), crystallographic (TGA, 22-200 °C, in air): 4.0 (4.5).

Crystallographic data for Cs{TaW₉} : Cs₅H₁₃O_{38.50}TaW₉, M = 3129.25, 0.08 x 0.06 x 0.04 mm, T = 193(2) K, Triclinic, space group P-1, $a = 9.783(3)$ Å, $b = 10.175(3)$ Å, $c = 11.464(3)$ Å, $\alpha = 99.025(5)$ °, $\beta = 100.999(5)$ °, $\gamma = 115.804(6)$ °, $V = 970.6(5)$ Å³, Z = 1, $D_c = 5.354$ Mg/m³, $\mu = 34.077$ mm⁻¹, $F(000) = 1335$, $2\theta_{\max} = 56.0$ °, 16826 reflections, 4675 independent reflections [$R_{\text{int}} = 0.0621$], $R_1 = 0.0322$, $wR_2 = 0.0698$ and GOF = 1.036 for 4675 reflections (253 parameters) with I>2σ(I), $R_1 = 0.0480$, $wR_2 = 0.0756$ and GOF = 1.036 for all reflections, max/min residual electron density +2.913/-1.928 eÅ⁻³.

Synthesis of Cs₆[Ta₂W₈O₃₂]·6H₂O (Cs{Ta₂W₈})

The synthetic procedure to prepare this compound was analogous to the one used for Cs{TaW₉} save for the amount of Na₂WO₄·2H₂O (3.3 g, 10.0 mmol). Yield (crude product) = 0.165 g (1 %, Ta). H₁₂Cs₆Ta₂W₈O₃₈, MW = 3118.9 g mol⁻¹. Atomic ratios (EDX), calculated (found): W/Ta 4.0 (3.8), W/Cs 1.3 (1.5). Characteristic IR bands (cm⁻¹): 534 (s), 648(s), 769 (sh), 880 (s), 946 (vsh). UV absorption: λ_1 (O→M, shoulder) = 260 nm, $\epsilon_1 = 3.3 \times 10^4$ mol⁻¹ L cm⁻¹, λ_2 (O→M, band) = 298 nm, $\epsilon_2 = 3.3 \times 10^4$ mol⁻¹ L cm⁻¹. Water content (%), crystallographic (TGA, 26-200 °C, in air): 3.5 (3.5).

Crystallographic Data for Cs{Ta₂W₈} : Cs₆H₁₂O₃₈Ta₂W₈, M = 3250.26, 0.07 x 0.04 x 0.02 mm, T = 200(2) K, Triclinic, space group P-1, $a = 9.798(6)$ Å, $b = 10.273(6)$ Å, $c = 11.322(7)$ Å, $\alpha = 92.172(9)$ °, $\beta = 101.597(9)$ °, $\gamma = 115.836(7)$ °, $V = 994.6(11)$ Å³, Z = 1, $D_c = 5.426$ Mg/m³, $\mu = 34.014$ mm⁻¹, $F(000) = 1384$, $2\theta_{\max} = 56.0$ °, 12962 reflections, 4791 independent reflections [$R_{\text{int}} = 0.0783$], $R_1 = 0.0502$, $wR_2 = 0.0912$ and GOF = 1.025 for 4791 reflections (241 parameters) with I>2σ(I), $R_1 = 0.0938$, $wR_2 = 0.1087$ and GOF = 1.025 for all reflections, max/min residual electron density +5.545/-2.705 eÅ⁻³.

Table S1. Summary of the crystallographic collection and refinement data for $CsNa\{Ta_3W_3\}$, $Cs\{NbW_9\}$, $Cs\{TaW_9\}$ and $Cs\{Ta_2W_8\}$.

	$Cs\{Ta_3W_3\}$	$Cs\{NbW_9\}$	$Cs\{TaW_9\}$	$Cs\{Ta_2W_8\}$
Empirical Formula	$Cs_4H_{12}NaO_{25}Ta_3W_3$	$Cs_5H_{15}O_{39.5}NbW_9$	$Cs_5H_{13}O_{38.5}TaW_9$	$Cs_6H_{12}O_{38}Ta_2W_8$
FW (g mol⁻¹)	2061.13	3051.67	3129.25	3250.26
T (K)	173(2)	173(2)	193(2)	200(2)
Crystal system	Trigonal	Triclinic	Triclinic	Triclinic
Space group	R-3	P-1	P-1	P-1
a (Å)	9.3948(3)	9.8464(4)	9.783(3)	9.798(6)
b (Å)	9.3948(3)	10.2634(4)	10.175(3)	10.273(6)
c (Å)	28.2796(11)	11.5535(4)	11.464(3)	11.322(7)
α (°)	90	99.160(2)	99.025(5)	92.172(9)
β (°)	90	100.815(2)	100.999(5)	101.597(9)
γ (°)	120	115.949(2)	115.804	115.836(7)
V (Å³)	2161.62(16)	991.98(7)	970.6(5)	994.6(11)
Z	3	1	1	1
μ (mm⁻¹)	28.348	30.880	34.077	34.014
$F(000)$	2652	1306	1335	1384
Crystal size (mm³)	0.16 x 0.12 x 0.04	0.14 x 0.13 x 0.09	0.08 x 0.06 x 0.04	0.07 x 0.04 x 0.02
Reflections collected /unique [R(int)]	14994 / 2432 [0.0455]	17629 / 4770 [0.0643]	16826 / 4675 [0.0621]	12962/ 4791 [0.0783]
GOF (F^2)	1.116	1.021	1.036	1.025
Final R indices [$I>2\sigma(I)$]	$R1^a = 0.0342$, wR2 = 0.0849	$R1^a = 0.0365$, wR2 = 0.0690	$R1^a = 0.0322$, wR2 = 0.0698	$R1^a = 0.0502$, wR2 = 0.0912
R indices (all data)	$R1^a = 0.0423$, wR2 = 0.0880	$R1^a = 0.0561$, wR2 = 0.0760	$R1^a = 0.0480$, wR2 = 0.0756	$R1^a = 0.0938$, wR2 = 0.1087
Largest difference peak and hole (e Å⁻³)	3.436 and -3.627	1.838 and -1.809	2.913 and -1.928	5.545 and -2.705

^a RI = $(\sum|F_0|-|F_c|)/(\sum|F_0|)$ ^bwR2 = $\{\sum[w(F_o^2 - F_c^2)^2]/\sum w(F_o^2)^2\}^{1/2}$

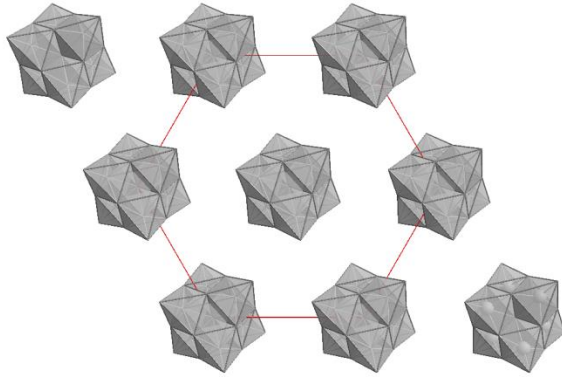


Fig S2. Representation of the crystal structure of $\text{CsNa}\{\text{Ta}_3\text{W}_3\}$ viewed along the crystallographic ‘c’ axis.

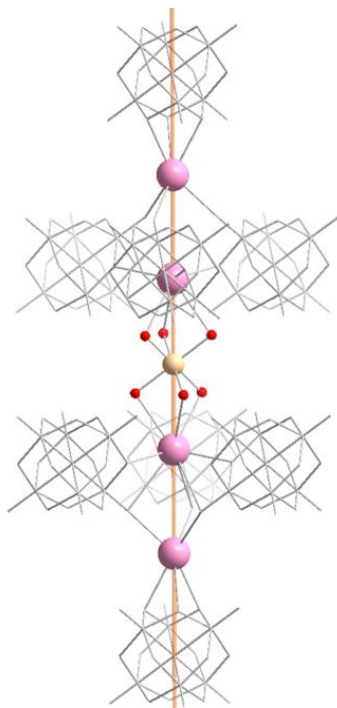


Fig S3. Representations of the crystal structure of $\text{CsNa}\{\text{Ta}_3\text{W}_3\}$. Colour code: $\{\text{MO}_6\}$ ($\text{M} = \text{W}, \text{Ta}$), grey wireframe; Cs^+ , pink spheres; Na^+ , teal spheres; O , red spheres. The Cs^+ counterions in $\text{CsNa}\{\text{Ta}_3\text{W}_3\}$ exhibit two different coordination environments in the crystal structure. In one of these environments, i.e. the Cs^+ located in the $\text{Cs}2$ crystallographic site, the cation is coordinated to the face of one of the $\{\text{Ta}_3\text{W}_3\}$ units, through bonds with three O_b oxo ligands ($\text{Cs}-\text{O} = 3.164(5)$ Å), and to other three $\{\text{Ta}_3\text{W}_3\}$ units via one $\text{Cs}-\text{O}_t$ bond for each unit ($\text{Cs}-\text{O} = 3.077(7)$ Å). Therefore, the coordination of this Cs^+ can be represented by the formula $[\text{Cs}(\mu_3\text{-}\{\text{Ta}_3\text{W}_3\})(\{\text{Ta}_3\text{W}_3\})_3]^{19}$. However, in the environment of the $\text{Cs}1$ crystallographic site, the Cs^+ is coordinated to the same three I units coordinated by $\text{Cs}2$ via bonds with an O_b ligand from each unit ($\text{Cs}-\text{O} = 3.047(4)$ Å). The remaining three bonds of $\text{Cs}1$ are with three solvent water molecules ($\text{Cs}-\text{O} = 3.326(8)$ Å). Hence, the coordination environment of $\text{Cs}1$ can be represented as $[\text{Cs}(\text{OH}_2)(\{\text{Ta}_3\text{W}_3\})_3]^{14}$. Moreover, a structural motif comprising four $\{\text{Ta}_3\text{W}_3\}$ units connected through coordination to both $\text{Cs}1$ and $\text{Cs}2$ can be identified and formulated as $[\text{Cs}_2(\text{OH}_2)_3(\{\text{Ta}_3\text{W}_3\})_4]^{18}$. The Na^+ counterion is exclusively coordinated by solvent water molecules and bridges two of these motifs. These coordination environments of the Na^+ and Cs^+ counterions in $\text{CsNa}\{\text{Ta}_3\text{W}_3\}$ closely resemble the equivalent environments in $\text{Cs}_6\text{Na}_2[\text{Nb}_6\text{O}_{19}] \cdot 18\text{H}_2\text{O}^7$ inasmuch as the Cs^+ are directly bonding to the faces of the $[\text{Nb}_6\text{O}_{19}]^{8-}$ superoctahedron while the Na^+ centres are coordinated solely by water molecules.

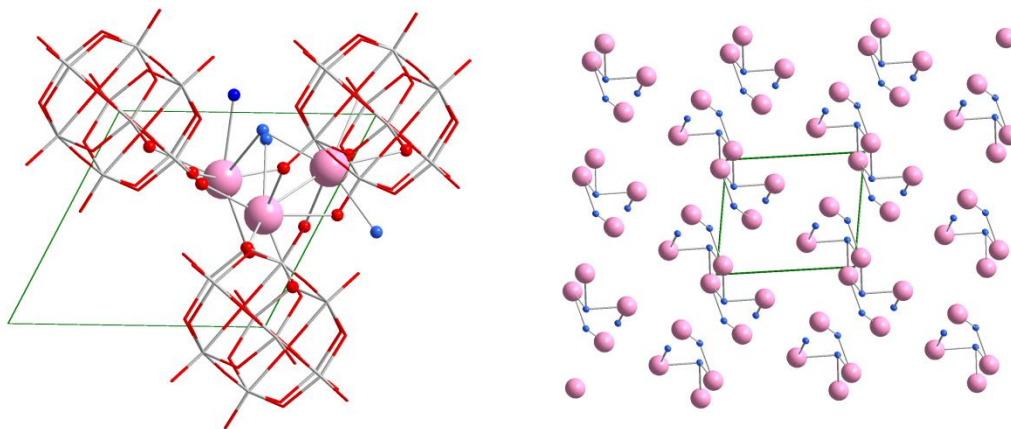


Fig S4. Representations of the crystal structure of $\text{Cs}\{\text{Ta}_2\text{W}_8\}$. Left: Representation viewed along the crystallographic ‘c’ axis highlighting the positions of the Cs^+ and waters of hydration in the unit cell. Right: Representation viewed along the crystallographic ‘a’ axis highlighting the coordination of the Cs^+ counterions by the solvent water molecules. The $\{\text{Ta}_2\text{W}_8\}$ clusters have been omitted for clarity. Colour code: W/Ta, grey wireframe; O, red wireframe, red spheres; H_2O , blue spheres; Cs^+ , pink spheres.

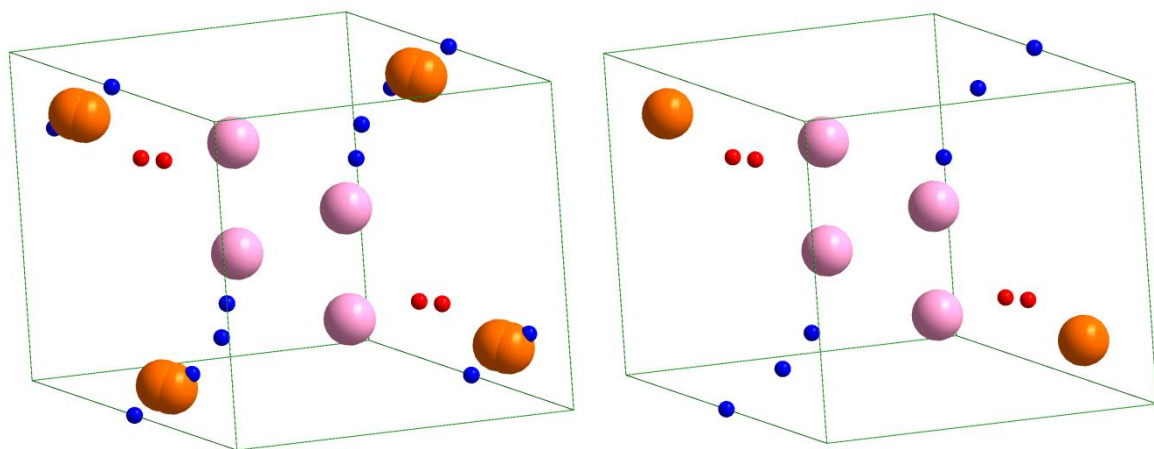


Fig S5. Representations of the contents of the unit cell of $\text{Cs}\{\text{NbW}_9\}$. Colour code: Cs site, S.O.F. = 1.00, pink; Cs site S.O.F. = 0.25, orange; O (solvent water molecules), SOF = 1.00, red; O (solvent waters), SOF = 0.50, blue. Left: All the crystallographic sites in the unit cell are shown. Right: Only some of the sites of each crystallographically dependent positions are shown.

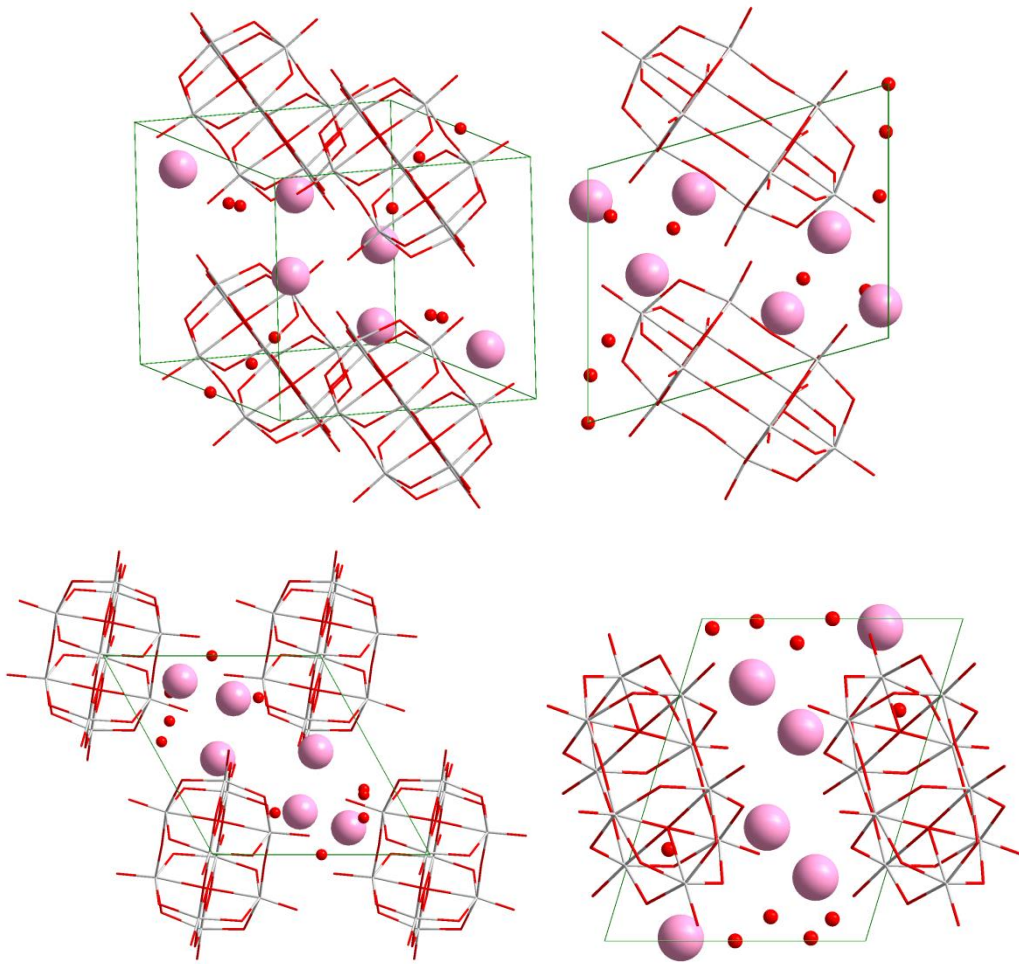


Fig S6. Representations of the crystal structure of $\text{Cs}\{\text{NbW}_9\}$ viewed along the same combination of crystallographic axes as in Fig S5 (top left), and along the a (top right), b (bottom left) and c (bottom right) crystallographic axes. The $\{\text{NbW}_9\}$ units are included in these representations. Colour code: W/Nb, grey wireframe; O, red wireframe, red spheres; Cs^+ , pink spheres.

BVS analysis

The bond-valence for each bond (BV) was calculated by using equation (1)⁸

$$\log(BV) = (d_0 - d)/B \quad (1)$$

where BV is the bond-valence for a particular bond, d is the bond length, while d_0 and B are empirical parameters. In the BVS analysis of $\{\text{Ta}_3\text{W}_3\}$, $d_0 = 1.9138$ and $B = 0.9482$, while in the BVS analysis of $\{\text{NbW}_9\}$, $\{\text{TaW}_9\}$ and $\{\text{Ta}_2\text{W}_8\}$; $d_0 = 1.91825$ and $B = 0.93838$. The values of those two sets of parameters correspond to the calculated values for $[\text{W}_6\text{O}_{19}]^{2-}$ and $[\text{W}_{10}\text{O}_{32}]^{4-}$ by Tytko and co-workers.⁸

The BVS on each particular atom is obtained from equation (2)⁸

$$BVS = \sum_{i=1}^k BV_i \quad (2)$$

where i is the index of a bond between that atom and another atom and k is the coordination number of the atom of which its BVS one wishes to calculate.

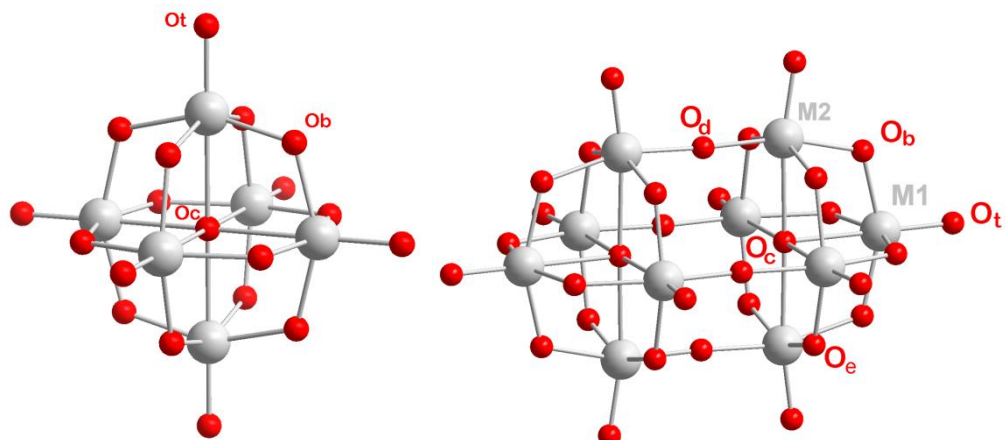


Fig S7. Representations of the molecular structures of $\{\text{Ta}_3\text{W}_3\}$ (left) and of $\{\text{NbW}_9\}$, $\{\text{TaW}_9\}$ and $\{\text{Ta}_2\text{W}_8\}$ (right). Colour code: W/Nb/Ta, grey; O, red. Selected oxygen and metal sites are labelled. This labelling scheme is used in tables S8-S15.

Table S8. Bond-Valence summation (BVS) analysis of the oxo ligands in $\{Ta_3W_3\}$.

Oxo type	Atom 1	Atom 2	d 1,2 [Å]	BVS	Assignment
O_c	O1	M1	2.3607		
			2.3607		
			2.3607	2.027	O^{2-}
			2.3607		
			2.3607		
O_b	O2	M1	1.9608	1.773	O^{2-}
			1.9661		
	O3	M1	1.9289	1.858	O^{2-}
			1.9598		
O_t	O4	M1	1.7686	1.465	O^{2-}

Table S9. Bond-Valence summation (BVS) analysis of the oxo ligands in $\{NbW_9\}$.

Oxo type	Atom 1	Atom 2	d (1-2) [Å]	BVS	Assignment
O_t	O13	M4	1.726	1.603	O^{2-}
	O11	M2	1.729	1.592	O^{2-}
	O10	M1	1.731	1.585	O^{2-}
	O12	M3	1.731	1.585	O^{2-}
	O14	M5	1.751	1.506	O^{2-}
O_b	O2	M1	1.920	1.861	O^{2-}
		M2	1.977		
	O3	M1	1.917	1.829	O^{2-}
		M3	1.996		
	O4	M1	1.935	1.815	O^{2-}
		M4	1.982		
	O5	M1	1.980	1.811	O^{2-}
		M5	1.938		
O_e	O6	M2	1.928	1.927	O^{2-}
		M3	1.938		
	O7	M3	1.942	1.836	O^{2-}
		M4	1.965		
	O8	M4	1.948	1.863	O^{2-}
		M5	1.946		
	O9	M2	1.941	1.914	O^{2-}
		M5	1.931		
O_d	O15	M3	1.895	1.990	O^{2-}
		M5	1.948		
	O16	M2	1.925	2.004	O^{2-}
		M4	1.910		
O_c	O1	M1	2.297		
		M2	2.374		
		M3	2.320	1.779	O^{2-}
		M4	2.370		
		M5	2.342		

Table S10. Bond-Valence summation (BVS) analysis of the oxo ligands in $\{TaW_9\}$.

Oxo type	Atom 1	Atom 2	d (1-2) [Å]	BVS	Assignment
O_t	O9	M1	1.722	1.608	O^{2-}
	O10	M2	1.731	1.576	O^{2-}
	O11	M3	1.724	1.603	O^{2-}
	O12	M4	1.717	1.628	O^{2-}
	O13	M5	1.718	1.624	O^{2-}
O_b	O1	M1	1.901	1.892	O^{2-}
		M2	1.986		
	O2	M1	1.919	1.897	O^{2-}
		M3	1.962		
	O3	M4	1.930	1.910	O^{2-}
		M1	1.944		
	O4	M1	1.919	1.918	O^{2-}
		M5	1.953		
O_e	O5	M2	1.924	1.928	O^{2-}
		M3	1.942		
	O6	M3	1.902	1.946	O^{2-}
		M4	1.959		
	O7	M5	1.917	1.986	O^{2-}
		M4	1.925		
	O8	M2	1.928	1.942	O^{2-}
		M5	1.933		
O_d	O15	M2	1.880	2.077	O^{2-}
		M4	1.928		
	O16	M3	1.884	2.074	O^{2-}
		M5	1.924		
O_c	O14	M1	2.293	1.859	O^{2-}
		M4	2.310		
		M2	2.311		
		M5	2.342		
		M3	2.354		

Table S11. Bond-Valence summation (BVS) analysis of the oxo ligands in $\{Ta_2W_8\}$.

Oxo type	Atom 1	Atom 2	d 1,2 [Å]	BVS	Assignment
O_t	O10	M1	1.708	1.664	O^{2-}
	O11	M2	1.731	1.576	O^{2-}
	O12	M3	1.734	1.564	O^{2-}
	O13	M4	1.788	1.372	O^{2-}
	O14	M5	1.705	1.677	O^{2-}
O_b	O5	M1	1.927	1.912	O^{2-}
		M5	1.947		
	O2	M1	1.932	1.932	O^{2-}
		M2	1.933		
	O3	M1	1.898	1.807	O^{2-}
		M3	2.032		
O_e	O4	M1	1.937	1.904	O^{2-}
		M4	1.939		
	O6	M3	1.941	1.882	O^{2-}
		M2	1.945		
	O7	M3	1.925	1.936	O^{2-}
		M4	1.938		
O_d	O8	M5	1.920	1.888	O^{2-}
		M4	1.965		
	O9	M2	1.934	1.901	O^{2-}
		M5	1.944		
	O15	M2	1.890	2.111	O^{2-}
		M4	1.902		
O_c	O16	M5	1.911	2.019	O^{2-}
		M3	1.918		
	O1	M4	2.276		
		M1	2.292		
		M2	2.315	1.835	O^{2-}
		M3	2.349		
		M5	2.417		

Table S12. Bond-Valence Summation (BVS) analysis of the metal site in $\{Ta_3W_3\}$.

Metal Site	BVS	Ta _{BVS} (%) ¹	W _{BVS} (%) ²
M1	5.392	60.8	39.2

Table S13. Bond-Valence Summation (BVS) analysis of the metal sites ligands in $\{NbW_9\}$.

Metal site	BVS	Nb _{BVS} (%) ³	W _{BVS} (%) ²
M1	5.798	20.2	79.8
M2	5.689	31.1	68.9
M3	5.740	26.0	74.0
M4	5.629	37.1	62.9
M5	5.646	35.4	64.6
Total (per cluster)⁴		30.0	70.0

Table S14. Bond-Valence Summation (BVS) analysis of the metal sites ligands in $\{TaW_9\}$.

Metal Site	BVS	Ta _{BVS} (%) ¹	W _{BVS} (%) ²
M1	5.994	0.6	99.4
M2	5.875	12.5	87.5
M3	5.926	7.4	92.6
M4	5.857	14.3	85.7
M5	5.861	13.9	86.1
Total (per cluster)		9.7	90.3

Table S15. Bond-Valence Summation (BVS) analysis of the metal sites ligands in $\{Ta_2W_8\}$.

Metal Site	BVS	Ta _{BVS} (%) ¹	W _{BVS} (%) ²
M1	6.025	-2.5	102.5
M2	5.898	10.2	89.8
M3	5.604	39.6	60.4
M4	5.630	37.0	63.0
M5	5.866	13.4	86.6
Total (per cluster)		19.5	80.5

¹ Ta_{BVS}(%) = (6 - BVS)*100

² W_{BVS}(%) = 100 - Ta_{BVS}(%)

³ Nb_{BVS}(%) = (6-BVS)*100

⁴ Total (per cluster) = ($\Sigma M_{BVS}(\%)$)*100). The large disparity in Nb content in $\{NbW_9\}$ as calculated by BVS and found by EDX is caused by the significant difference in Nb-O and W-O bond distances

Electrospray-ionisation mass spectrometry (ESI-MS)

Table S16. List of the assignments on the ESI-MS spectra of $\text{CsNa}\{\text{Ta}_3\text{W}_3\}$, $\text{Cs}\{\text{NbW}_9\}$, $\text{Cs}\{\text{TaW}_9\}$ and $\text{Cs}\{\text{Ta}_2\text{W}_8\}$.

Compound	Peak	m/z (obs.)	m/z (calc.)	Assignment
$\text{CsNa}\{\text{Ta}_3\text{W}_3\}$	1	460.9	460.9	$\{\text{H}_2\text{CsNa}_2[\text{Ta}_2\text{W}_3\text{O}_{18}]\}^{3-}$
	2	466.2	466.2	$\{\text{H}_2\text{Na}_3[\text{Ta}_2\text{W}_3\text{O}_{18}](\text{H}_2\text{O})_7\}^{3-}$
	3	691.8	691.8	$\{\text{H}_3\text{CsNa}_2[\text{Ta}_2\text{W}_3\text{O}_{18}]\}^{2-}$
	4	707.8	707.8	$\{\text{H}_4\text{CsNa}[\text{Ta}_2\text{W}_3\text{O}_{18}](\text{H}_2\text{O})_3\}^{2-}$
	5	757.8	757.7	$\{\text{H}_2\text{Cs}_2\text{Na}_2[\text{Ta}_2\text{W}_3\text{O}_{18}]\}^{2-}$
	6	801.8	801.7	$\{\text{H}_3\text{Cs}_3[\text{Ta}_2\text{W}_3\text{O}_{18}]\}^{2-}$
$\text{Cs}\{\text{NbW}_9\}$	1	758.4	759.4	$\{\text{H}_3\text{CsNa}_2[\text{NbW}_8\text{O}_{31}](\text{H}_2\text{O})_2\}^{3-}$
	2	798.4	798.1	$\{\text{HCs}[\text{NbW}_9\text{O}_{32}]\}^{3-}$
	3	802.4	802.8	$\{\text{HK}[\text{NbW}_9\text{O}_{32}](\text{H}_2\text{O})_6\}^{3-}$
	4	847.4	847.4	$\{\text{HCs}_3\text{Na}_2[\text{NbW}_8\text{O}_{31}](\text{H}_2\text{O})_2\}^{3-}$
	5	1272.6	1272.6	$\{\text{HCs}_2[\text{NbW}_9\text{O}_{32}](\text{H}_2\text{O})\}^{2-}$
	6	1338.0	1338.0	$\{\text{Cs}_3[\text{NbW}_9\text{O}_{32}](\text{H}_2\text{O})\}^{2-}$
$\text{Cs}\{\text{TaW}_9\}$	1	600.8	600.9	$\{\text{K}[\text{TaW}_9\text{O}_{32}](\text{H}_2\text{O})\}^{4-}$
	2	832.4	832.8	$\{\text{HNa}[\text{TaW}_9\text{O}_{32}](\text{H}_2\text{O})_7\}^{3-}$
	3	876.7	876.8	$\{\text{CsNa}[\text{TaW}_9\text{O}_{32}](\text{H}_2\text{O})_7\}^{3-}$
	4	1314.6	1315.6	$\{\text{H}_2\text{Cs}_3\text{Na}_2[\text{TaW}_8\text{O}_{31}](\text{H}_2\text{O})_2\}^{2-}$
$\text{Cs}\{\text{Ta}_2\text{W}_8\}$	1	780.8	781.5	$\{\text{H}_4\text{Na}_3[\text{Ta}_2\text{W}_7\text{O}_{31}](\text{H}_2\text{O})_7\}^{3-}$
	2	794.1	794.1	$\{\text{H}_4\text{CsNa}_2[\text{Ta}_2\text{W}_7\text{O}_{31}](\text{H}_2\text{O})_3\}^{3-}$
	3	837.1	836.8	$\{\text{H}_4\text{Cs}_2\text{Na}[\text{Ta}_2\text{W}_7\text{O}_{31}](\text{H}_2\text{O})_4\}^{3-}$
	4	881.7	881.4	$\{\text{H}_2\text{Cs}_2\text{Na}_3[\text{Ta}_2\text{W}_7\text{O}_{31}](\text{H}_2\text{O})_9\}^{3-}$
$\text{K}\{\text{W}_{10}\}$	1	587.3	587.3	$\{[\text{W}_{10}\text{O}_{32}]\}^{4-}$
	2	597.6	597.6	$\{[\text{W}_{10}\text{O}_{32}](\text{CH}_3\text{CN})\}^{4-}$
	3	608.3	608.4	$\{[\text{W}_{10}\text{O}_{32}](\text{CH}_3\text{CN})_2\}^{4-}$
	4	783.4	783.4	$\{\text{H}[\text{W}_{10}\text{O}_{32}]\}^{3-}$
	5	797.1	797.1	$\{\text{Na}[\text{W}_{10}\text{O}_{32}](\text{H}_2\text{O})\}^{3-}$
	6	1175.7	1175.7	$\text{H}_2[\text{W}_{10}\text{O}_{32}]^{2-}$
	7	1195.7	1195.7	$\{\text{NaH}[\text{W}_{10}\text{O}_{32}](\text{H}_2\text{O})\}^{2-}$

UV-Vis spectroscopy

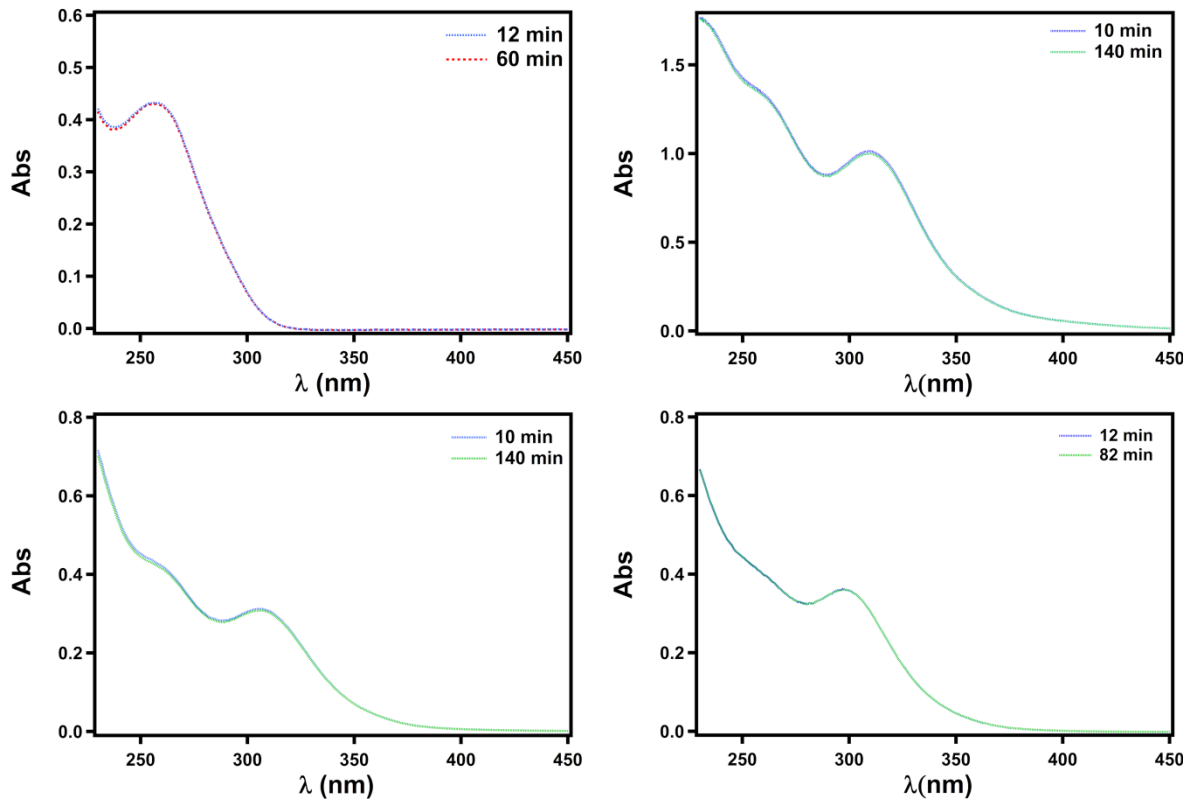


Fig S17. From top left to bottom right: UV-Vis spectra of aqueous $\text{CsNa}\{\text{Ta}_3\text{W}_3\}$ (0.1 mM), $\text{Cs}\{\text{NbW}_9\}$ (0.3 mM), $\text{Cs}\{\text{TaW}_9\}$ (0.1 mM) and $\text{Cs}\{\text{Ta}_2\text{W}_8\}$ (0.1 mM) taken at different time intervals after dissolution.

Electrochemistry

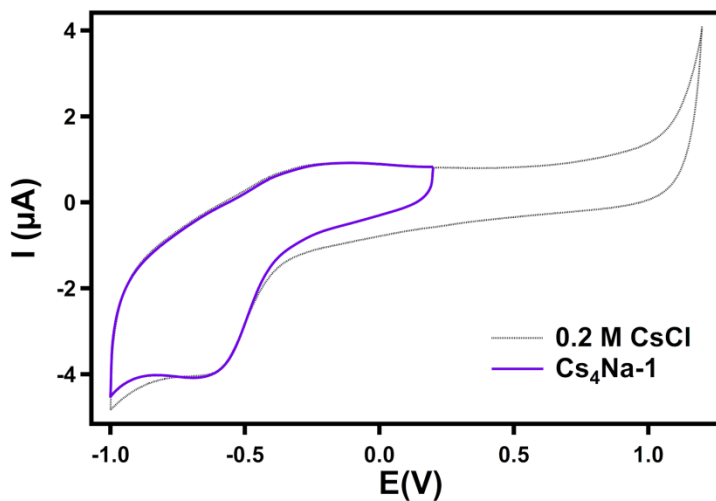


Fig S18. Cyclic voltammograms of aqueous 0.2 M CsCl (dotted black line) and of a 0.5 mM solution of $\text{CsNa}\{\text{Ta}_3\text{W}_3\}$ in 0.2 M CsCl (purple solid line). The scan speed was set at 100 mV s^{-1} .

Thermogravimetry (TGA)

The TG curves of the four reported compounds ($\text{CsNa}\{\text{Ta}_3\text{W}_3\}$, $\text{Cs}\{\text{NbW}_9\}$, $\text{Cs}\{\text{TaW}_9\}$ and $\text{Cs}\{\text{Ta}_2\text{W}_8\}$) show two well defined regions (*ca.* r.t. – 200 °C and 200 – 400 °C) of weight loss with as a function of the furnace temperature. The first region corresponds to the loss of lattice waters and the second one to the loss of water molecules caused by condensation of the clusters into their respective extended metal oxides (Cs_2O , Na_2O , Nb_2O_5 , Ta_2O_5 and WO_3).

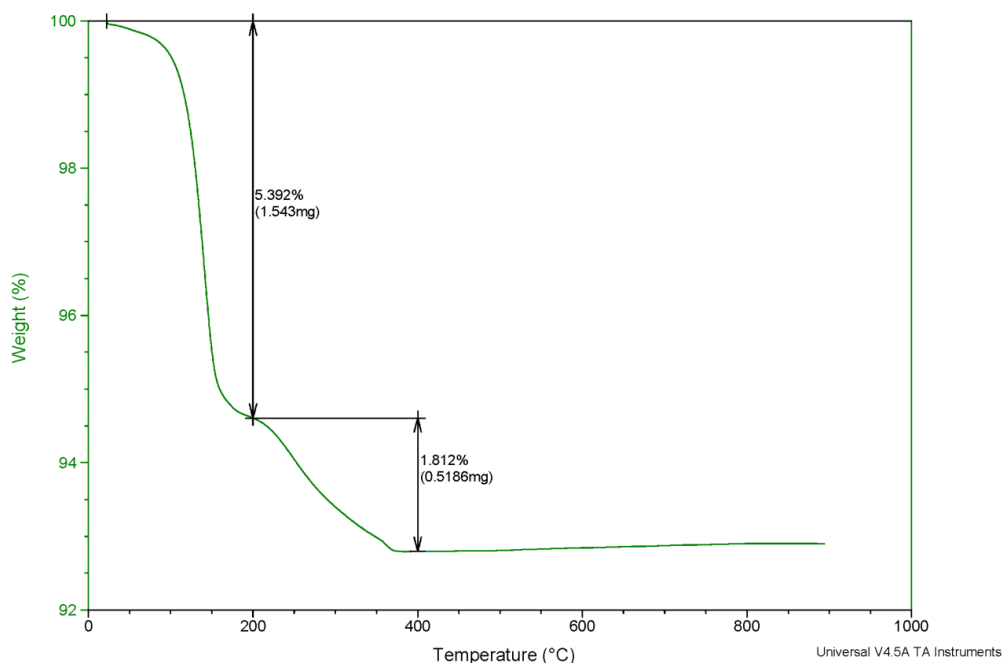


Fig S19. TGA/DSC plots of $\text{CsNa}\{\text{Ta}_3\text{W}_3\}$.

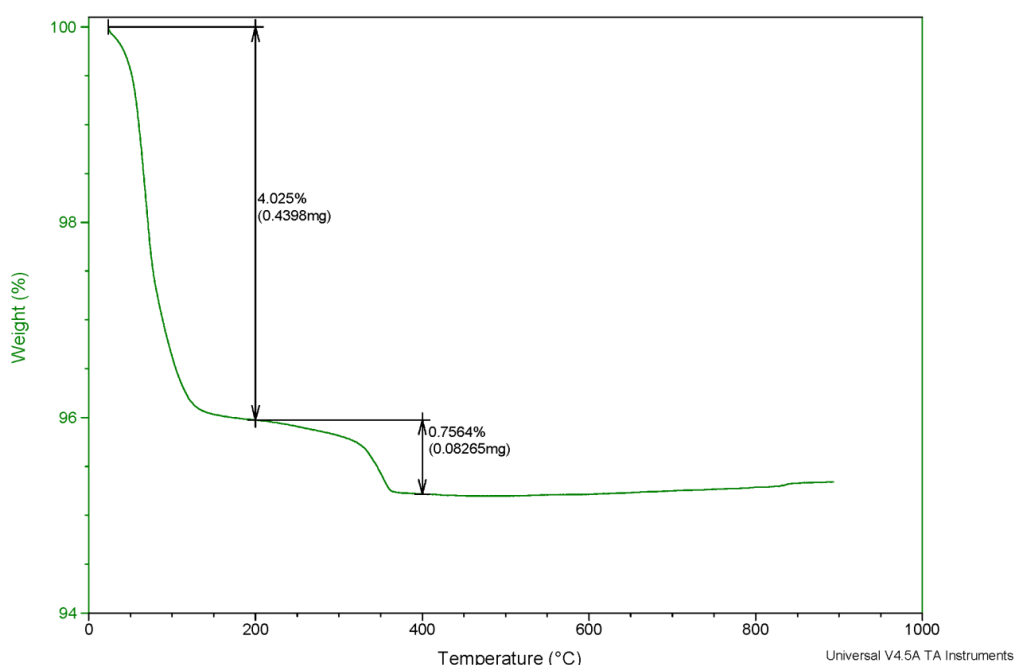


Fig S20. TGA/DSC plots of $\text{Cs}\{\text{NbW}_9\}$.

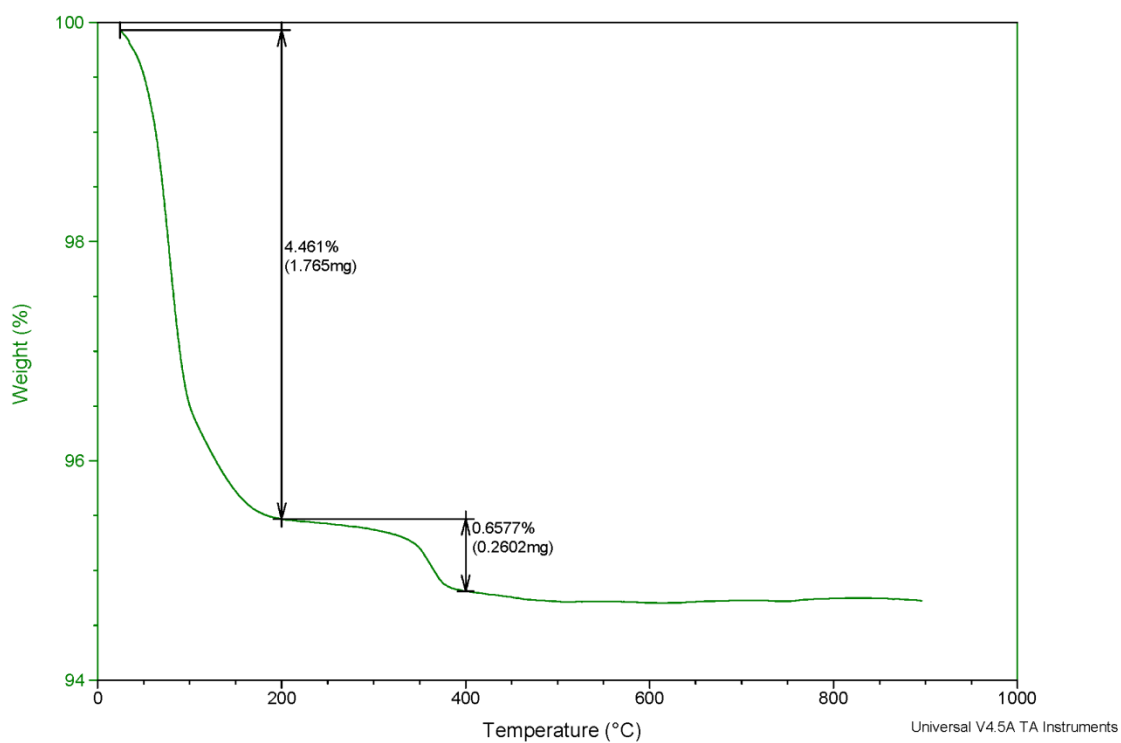


Fig S21. TGA/DSC plots of CsTaW_9 .

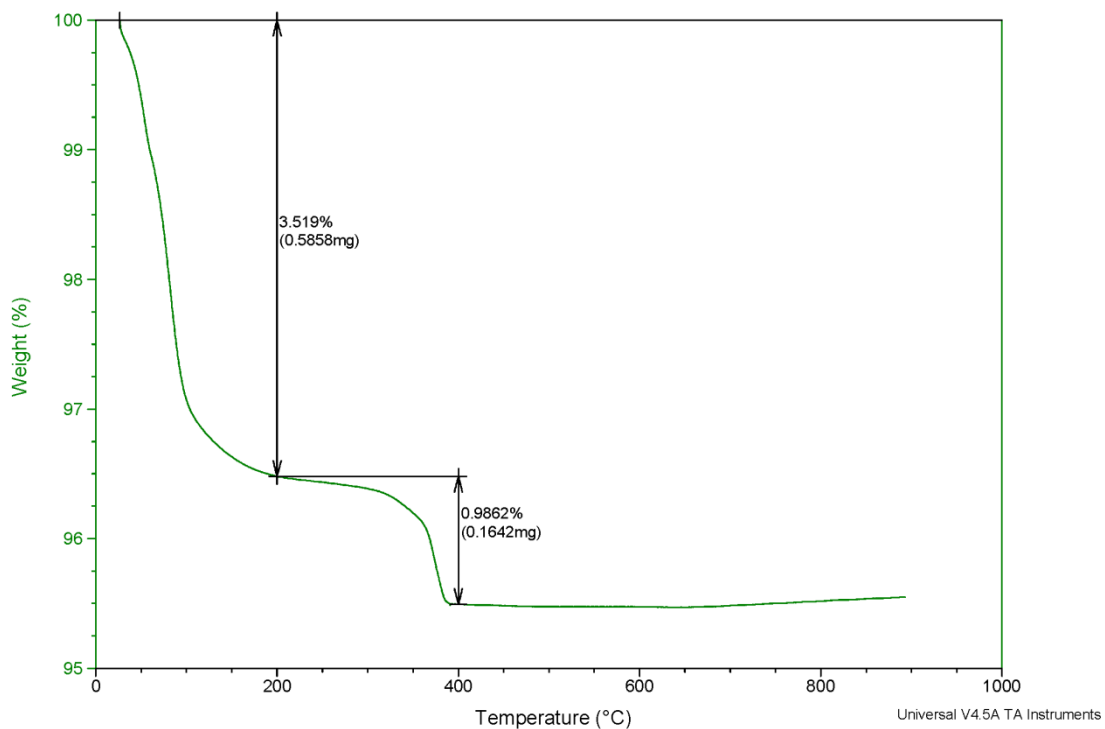


Fig S22. TGA/DSC plots of CsTa_2W_8 .

Scanning electron microscopy (SEM)

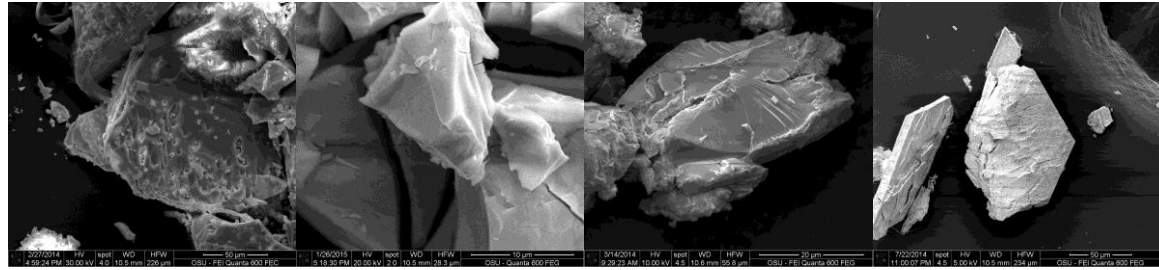


Fig S23. From left to right, scanning electron micrographs of $\text{CsNa}\{\text{Ta}_3\text{W}_3\}$, $\text{Cs}\{\text{NbW}_9\}$, $\text{Cs}\{\text{TaW}_9\}$ and $\text{Cs}\{\text{Ta}_2\text{W}_8\}$.

Energy-dispersive X-ray spectroscopy (EDX)

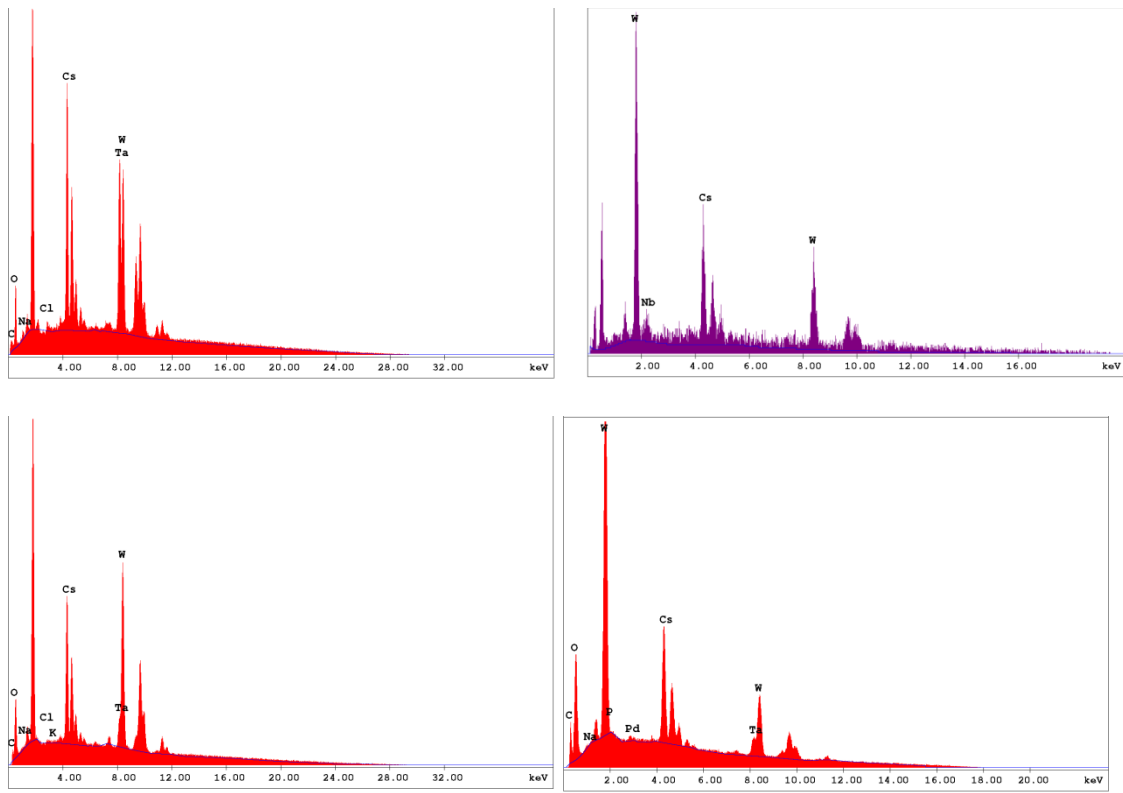


Fig S24. From top left to bottom right, EDX spectra of $\text{CsNa}\{\text{Ta}_3\text{W}_3\}$, $\text{Cs}\{\text{NbW}_9\}$, $\text{Cs}\{\text{TaW}_9\}$ and $\text{Cs}\{\text{Ta}_2\text{W}_8\}$.

Fourier-transformed infra-red spectroscopy (FTIR)

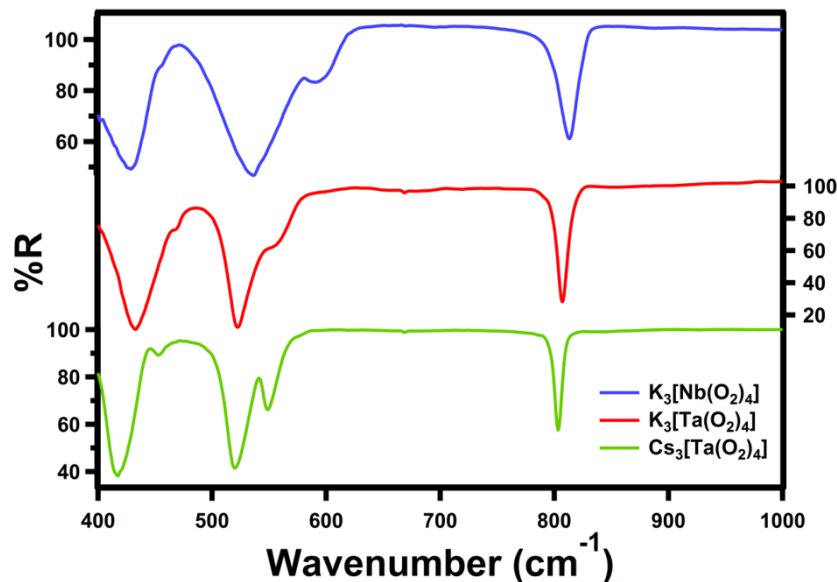


Fig S25. FTIR spectra of K₃[Nb(O₂)₄] (blue), K₃[Ta(O₂)₄] (red) and Cs₃[Ta(O₂)₄] (green).

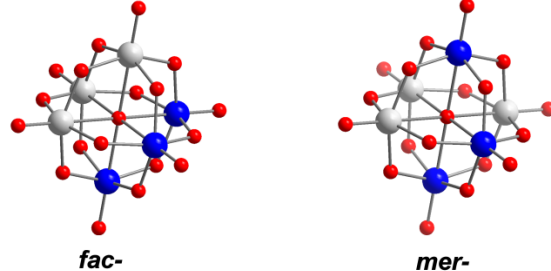
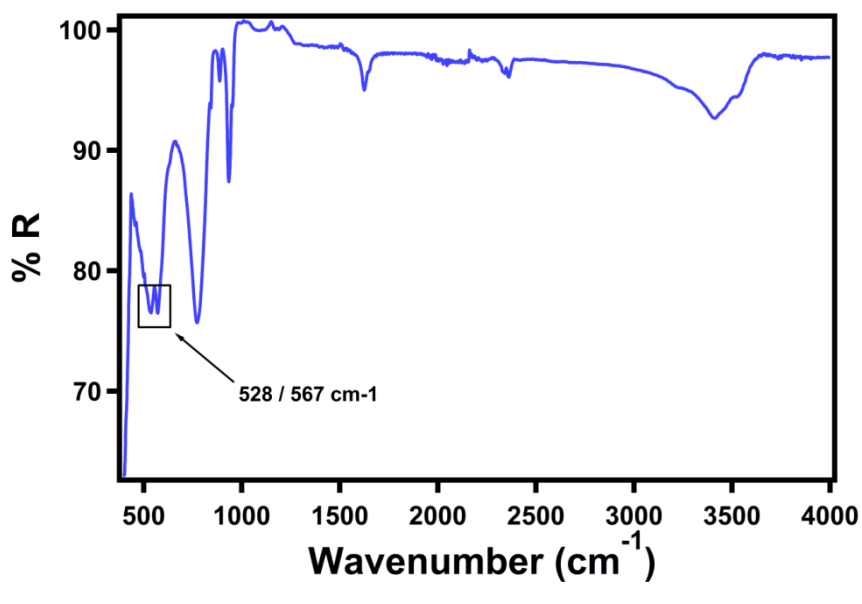


Fig S26. ATR-FTIR spectrum of CsNa[Ta₃W₃] (top) and molecular structure of the two {Ta₃W₃} isomers (bottom) The highlighted peaks indicate that {Ta₃W₃} is actually just the fac- isomer [fac-Ta₃W₃O₁₉]^{5,9}.

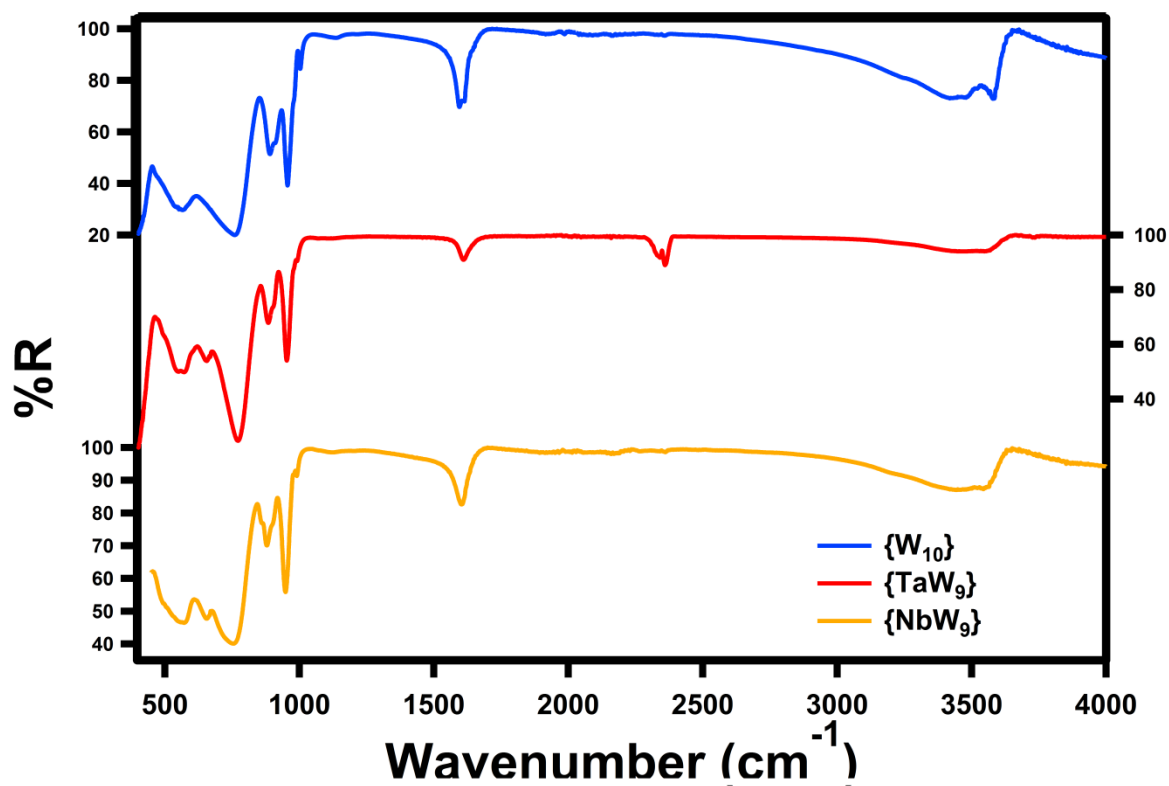


Fig S27. ATR-FTIR of $\{W_{10}\}$ (blue), $Cs\{NbW_9\}$ (orange) and $Cs\{TaW_9\}$ (red).

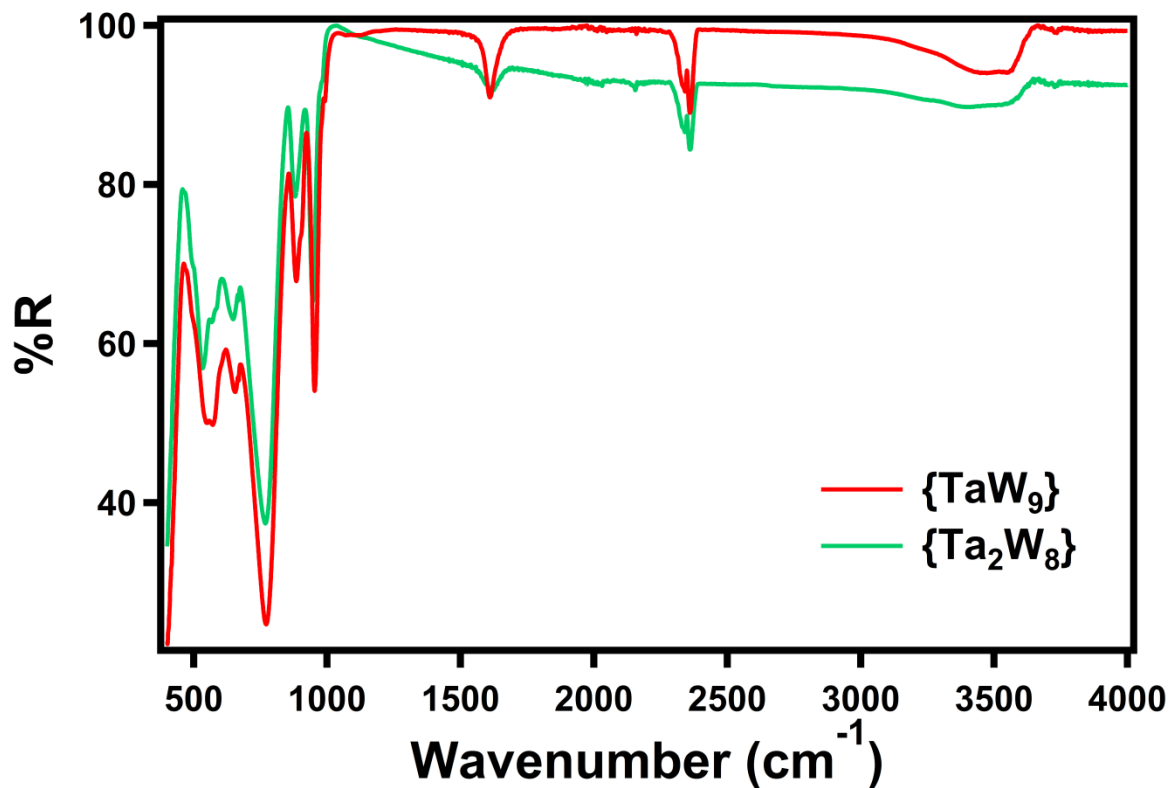


Fig S28. ATR-FTIR of $Cs\{TaW_9\}$ and $Cs\{Ta_2W_8\}$.

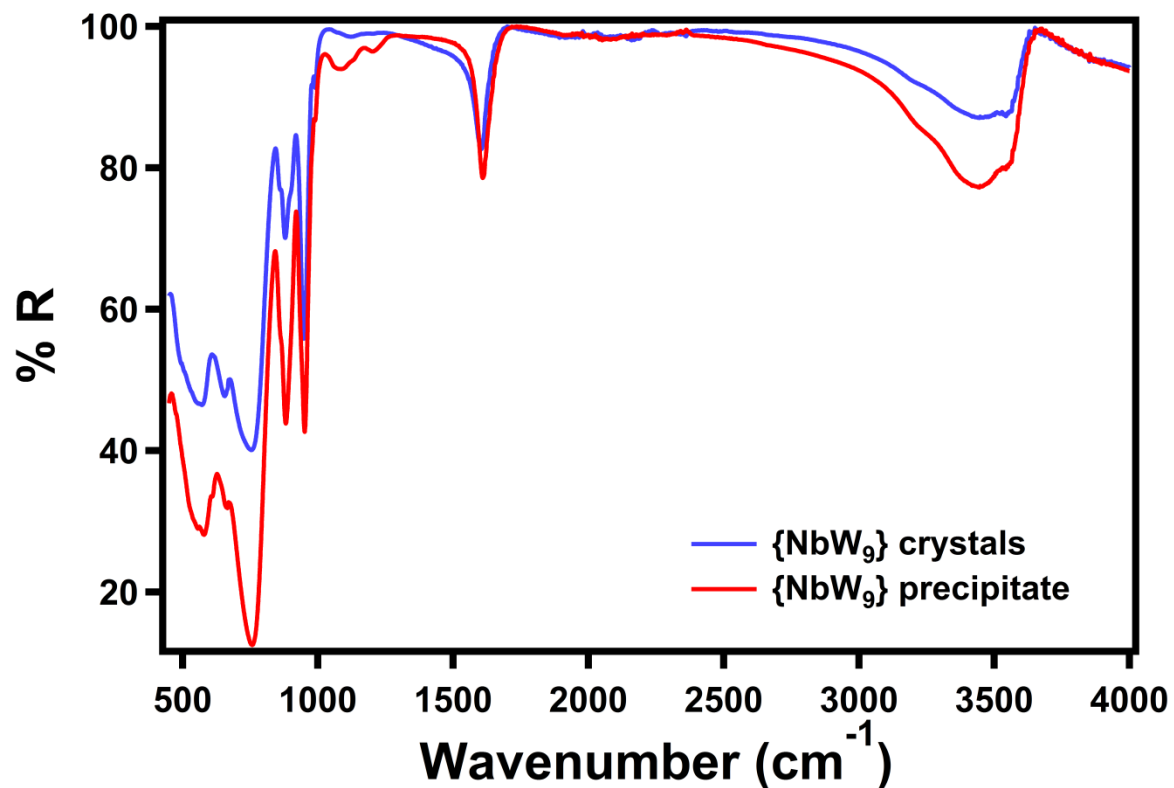


Fig S29. ATR-FTIR of crude and crystalline $\text{Cs}\{\text{NbW}_9\}$. The crude material (“precipitate”) is isolated as a powder upon the addition of CsCl to the refluxed reaction mixture.

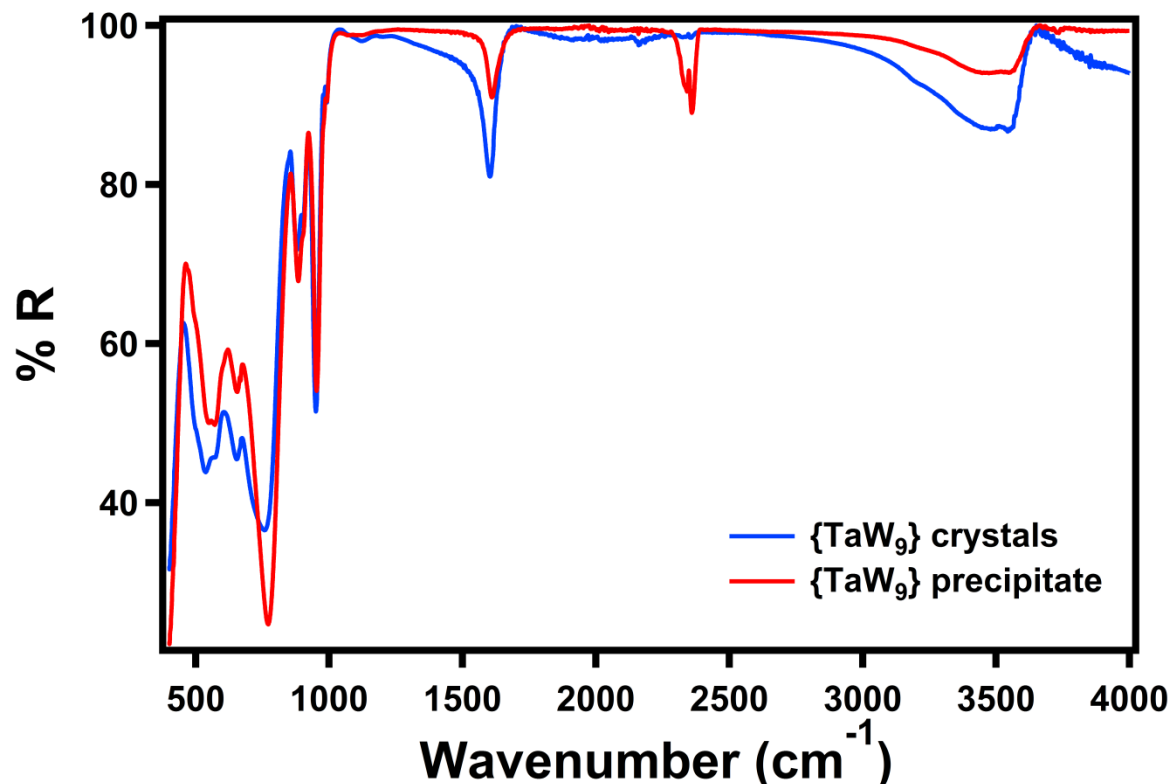


Fig S30. ATR-FTIR of crude and crystalline $\text{Cs}\{\text{TaW}_9\}$. The crude material (“precipitate”) is isolated as a powder upon the addition of CsCl to the refluxed reaction mixture.

Computational Details

Introduction

All species were fully optimized through first-principles calculations performed on the basis of density functional theory (DFT). The exchange and correlation terms were those in the generalized gradient approximation (GGA) Perdew-Burke-Ernzerhof functional including an empirical dispersion term (PBE-D3).¹⁰⁻¹² The calculations were performed using the Amsterdam Density Functional (ADF2013) package.¹³⁻¹⁵ Full electron triple- ζ plus two polarization function basis sets (TZ2P) were used on all atoms including relativistic corrections through the scalar-relativistic zero-order regular approximation (ZORA).¹⁶ Solvation effects were included using the conductor-like screening model (COSMO) in conjunction with the Allinger radii to create the dielectric cavity.^{17, 18} Single point calculations were performed using a hybrid functional (B3LYP).¹⁹ All geometries were optimized without symmetry constraints.

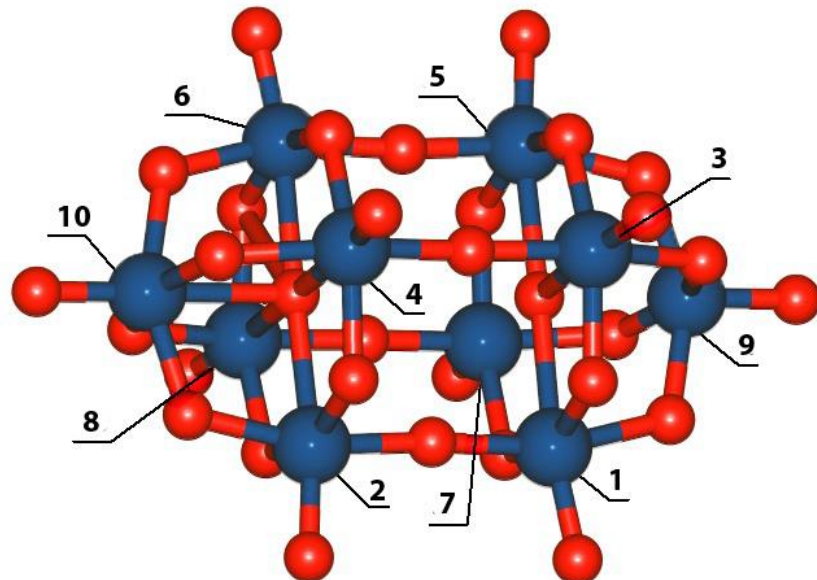


Fig S31. Labelled representation of the structure of $[W_{10}O_{32}]^4\{-W_{10}\}$. Color code: W, blue; O, red.

Fig S32. Molecular structures of the two substitutional isomers of $\{MW_9\}$ ($M = Nb, Ta$). Colour code: W, dark blue; O, red; Nb/Ta, cyan.

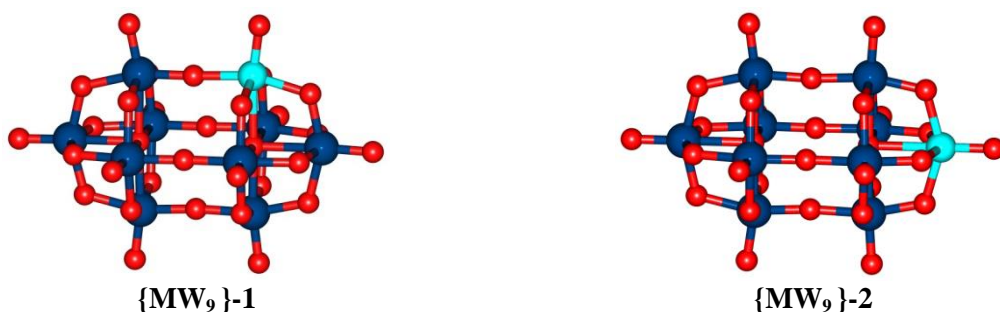
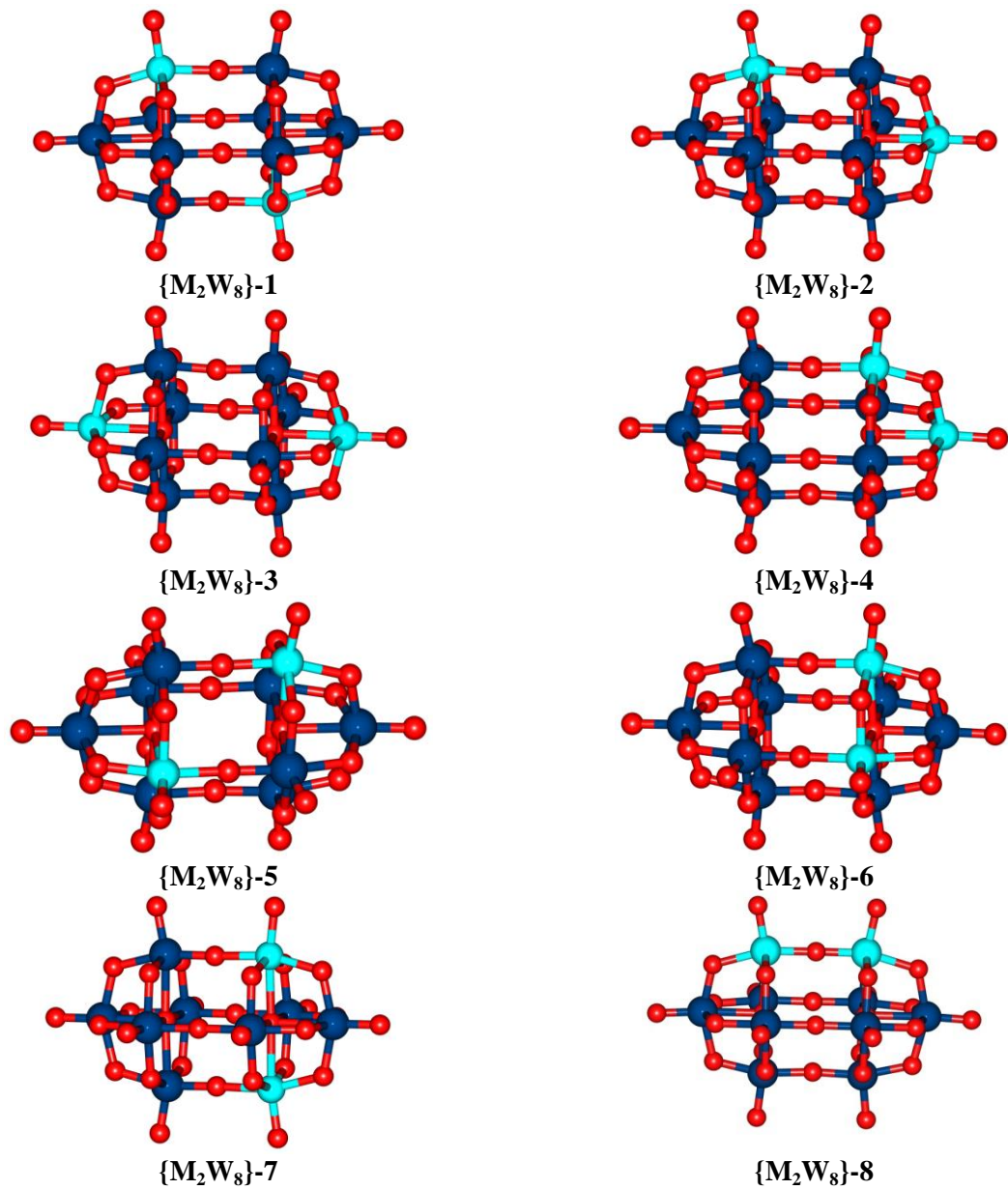


Fig S33. Molecular structures of the eight substitutional isomers of $\{M_2W_8\}$ ($M = Nb, Ta$). Colour code: W, dark blue; O, red; Nb/Ta, cyan.



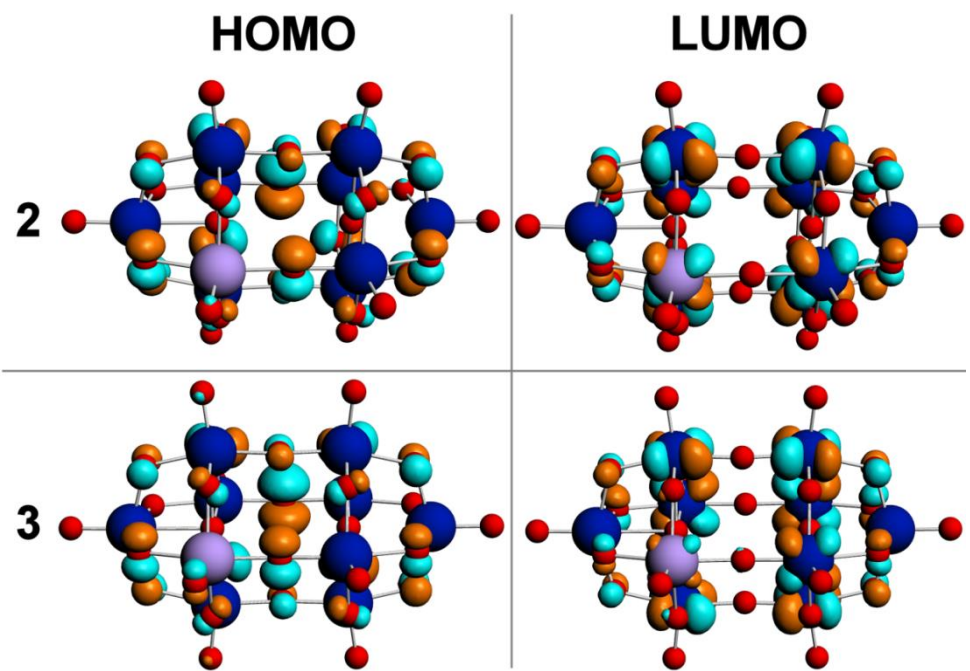
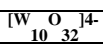
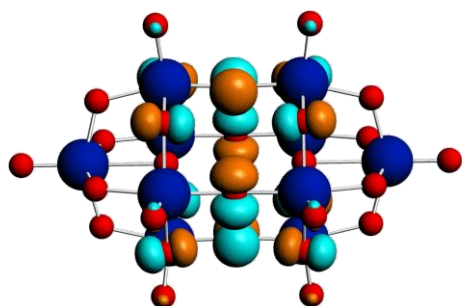


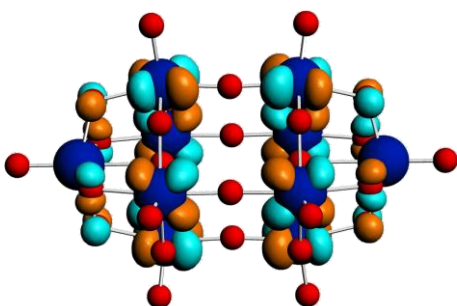
Fig S34. HOMO and LUMO for $\{NbW_9\}$ (2) and $\{TaW_9\}$ (3) at the B3LYP level of theory. Isosurface at 0.04. Colour code: W^{VI} , blue; O , red; Nb^V and Ta^V , purple. Isomeric structures are $\{MW_9\}$ -1.



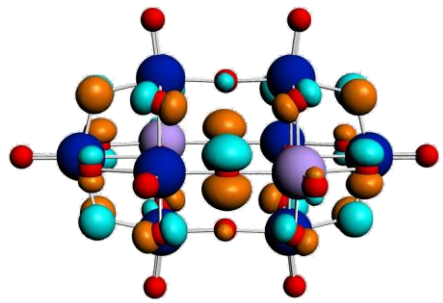
HOMO



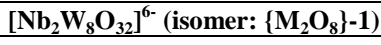
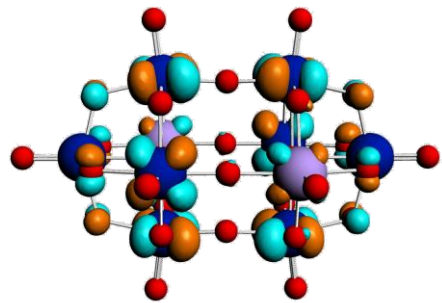
LUMO



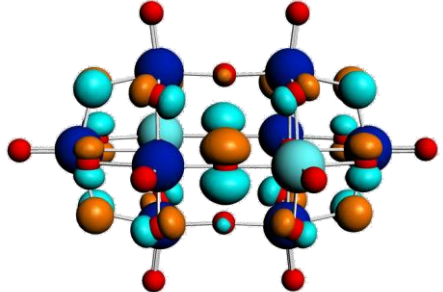
HOMO



LUMO



HOMO



LUMO

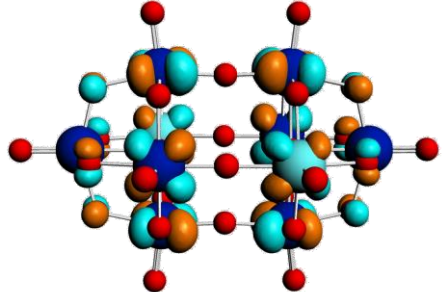


Fig S35. HOMO and LUMO for $[W_{10}O_{32}]^{4-}$, $[Ta_2W_8O_{32}]^{6-}$ (isomer: $\{M_2W_8\}\text{-1}$), and $[Nb_2W_8O_{32}]^{6-}$ (isomer: $\{M_2W_8\}\text{-1}$) species at B3LYP level of theory. Isosurface at 0.04. Color code: W, blue; O, red; Ta, purple; Nb, cyan.

Table S36. Mulliken spin density on the metal centres of $[W_{10}O_{32}]^{4-}$ ($\{W_{10}\}$) at different levels of theory (see atom labels in Figure S31).

Center	PBE-D3	B3LYP
W(1)	0.118	0.131
W(2)	0.118	0.131
W(3)	0.118	0.131
W(4)	0.118	0.131
W(5)	0.118	0.131
W(6)	0.118	0.131
W(7)	0.118	0.131
W(8)	0.118	0.131
W(9)	-0.015	-0.017
W(10)	-0.015	-0.017

Table S37. Mulliken spin density on the metal centres of $[NbW_9O_{32}]^{5-}$ (**2**) at different levels of theory (see atom labels in Figure S31).

Center	PBE-D3	B3LYP
W(1)	0.116	0.123
W(2)	0.131	0.146
Nb(3)	0.083	0.070
W(4)	0.099	0.098
W(5)	0.117	0.124
W(6)	0.132	0.148
W(7)	0.134	0.158
W(8)	0.148	0.182
W(9)	-0.012	-0.014
W(10)	-0.014	-0.017

Table S38. Mulliken spin density on the metal centres of $[TaW_9O_{32}]^{5-}$ (**3**) at different levels of theory (see atom labels in Figure S31).

Center	PBE-D3	B3LYP
W(1)	0.114	0.116
W(2)	0.132	0.144
Ta(3)	0.039	0.032
W(4)	0.081	0.075
W(5)	0.115	0.118
W(6)	0.134	0.146
W(7)	0.161	0.190
W(8)	0.176	0.220
W(9)	-0.012	-0.013
W(10)	-0.015	-0.017

Table S39. Highest occupied and lowest unoccupied molecular orbitals energies and the energy gap between them at different levels of theory for the $[W_{10}O_{32}]^{n-}$ species.

Species	State	PBE-D3			B3LYP		
		HOMO (eV)	LUMO (eV)	Gap (eV)	HOMO (eV)	LUMO (eV)	Gap (eV)
$[W_{10}O_{32}]^{4-}$	¹ A	-6.58	-4.02	2.56	-7.82	-3.63	4.18
$[W_{10}O_{32}]^{5-}$	² A	-3.75	-3.57	0.19 ^[a]	-4.20	-3.15	1.05 ^[a]
$[W_{10}O_{32}]^{6-}$	¹ A	-3.30	-2.51	0.79	-3.72	-2.17	1.55

^[a] HOMO is an alpha orbital and LUMO is a beta orbital.

Table S40. Highest occupied and lowest unoccupied molecular orbitals energies and the energy gap between them at different levels of theory for $[NbW_9O_{32}]^{n^-}$ and $[Nb_2W_8O_{32}]^{n^-}$ species.

Species	State	PBE-D3			B3LYP		
		HOMO (eV)	LUMO (eV)	Gap (eV)	HOMO (eV)	LUMO (eV)	Gap (eV)
$[NbW_9O_{32}]^{5^-}$	1A	-6.30	-3.61	2.69	-7.45	-3.20	4.25
$[NbW_9O_{32}]^{6^-}$	2A	-3.38	-3.19	0.19 ^[a]	-3.82	-2.75	1.07 ^[a]
$[NbW_9O_{32}]^{7^-}$	1A	-2.94	-2.21	0.73	-3.35	-1.88	1.47
$[Nb_2W_8O_{32}]^{6^-}$	1A	-5.97	-3.24	2.73	-7.11	-2.82	4.29
$[Nb_2W_8O_{32}]^{7^-}$	2A	-3.01	-2.81	0.20 ^[a]	-3.42	-2.36	1.06 ^[a]
$[Nb_2W_8O_{32}]^{8^-}$	1A	-2.58	-1.92	0.66	-2.96	-1.60	1.35

^[a] HOMO is an alpha orbital and LUMO is a beta orbital.

Table S41. Highest occupied and lowest unoccupied molecular orbitals energies and the energy gap between them at different levels of theory for $[TaW_9O_{32}]^{n^-}$ and $[Ta_2W_8O_{32}]^{n^-}$ species.

Species	State	PBE-D3			B3LYP		
		HOMO (eV)	LUMO (eV)	E _{gap} (eV)	HOMO (eV)	LUMO (eV)	E _{gap} (eV)
$[TaW_9O_{32}]^{5^-}$	1A	-6.30	-3.60	2.70	-7.47	-3.20	4.27
$[TaW_9O_{32}]^{6^-}$	2A	-3.38	-3.18	0.20 ^[a]	-3.84	-2.74	1.10 ^[a]
$[TaW_9O_{32}]^{7^-}$	1A	-2.94	-2.26	0.68	-3.35	-1.90	1.45
$[Ta_2W_8O_{32}]^{6^-}$	1A	-6.01	-3.20	2.81	-7.16	-2.78	4.38
$[Ta_2W_8O_{32}]^{7^-}$	2A	-2.97	-2.77	0.20 ^[a]	-3.40	-2.32	1.08 ^[a]
$[Ta_2W_8O_{32}]^{8^-}$	1A	-2.55	-1.96	0.59	-2.93	-1.66	1.27

^[a] HOMO is an alpha orbital and LUMO is a beta orbital.

Table S42. Experimental and calculated (B3LYP) gaps for different species. HOMO and LUMO energies are also presented for comparison.

Species	Calculated (B3LYP)			Experimental
	HOMO (eV)	LUMO (eV)	E _{gap} (eV)	E _{gap} (eV)
$[W_{10}O_{32}]^{4^-}$	-7.82	-3.63	4.18	3.85
$[NbW_9O_{32}]^{5^-}$	-7.45	-3.20	4.25	4.01
$[TaW_9O_{32}]^{5^-}$	-7.47	-3.20	4.27	4.07
$[Ta_2W_8O_{32}]^{6^-}$	-7.16	-2.78	4.38	4.16

Table S43. Relative energies (kcal mol⁻¹) of the different {MW₉} isomers (M=Nb, Ta) (Fig S32). Energies calculated at PBE-D3 level of theory. The cartesian coordinates of the structural models used in the calculations are shown in Tables S78, S82, S88-S89.

Species	Label	Rel. Energy (kcal mol ⁻¹)	
		M=Nb	M=Ta
$[MW_9O_{32}]^{5^-}$	{MW ₉ }-1	0.0	0.0
	{MW ₉ }-2	3.6	4.6

Table S44. Relative energies (kcal mol⁻¹) of the different {M₂W₈} isomers with (M=Nb, Ta) (Fig S33). Energies calculated at PBE-D3 level of theory. The cartesian coordinates of the structural models used in the calculations are shown in Tables S79, S83, S90-S103.

Species	Label	Rel. Energy (kcal mol ⁻¹)	
		M=Nb	M=Ta
[M ₂ W ₈ O ₃₂] ⁶⁻	{M ₂ W ₈ }-1	0.8 ^[a]	1.0 ^[a]
	{M ₂ W ₈ }-2	5.2	6.2
	{M ₂ W ₈ }-3	9.4	11.2
	{M ₂ W ₈ }-4	5.1	6.2
	{M ₂ W ₈ }-5	0.0 ^[a]	0.0 ^[a]
	{M ₂ W ₈ }-6	1.1 ^[a]	1.2 ^[a]
	{M ₂ W ₈ }-7	1.9	1.7
	{M ₂ W ₈ }-8	3.8	3.2

^[a] Considered degenerated at this level of theory.

Reduction potential calculations

Introduction

Nowadays computational prediction of redox potentials is a relatively straightforward procedure with errors within 200 mV with respect to experiment.²⁰ For a redox reaction with the general form:



The reduction potential relative to the standard hydrogen electrode (SHE) is expressed as:

$$E_{A/A^-}^0 = -\frac{\Delta G_{A/A^-}^0 - \Delta G_{SHE}^0}{nF} \quad (2)$$

where $\Delta G_{A/A^-}^0$ and ΔG_{SHE}^0 are the free-energy changes associated with Equation 1 and the SHE respectively, n is the number of electrons, and F is the Faraday constant. The value of ΔG_{SHE}^0 has been experimentally measured and has a generally accepted value of -4.28 V.²¹⁻²³ Once E_{A/A^-}^0 is obtained with respect to the SHE, it can be easily adjusted to other reference electrodes. For Ag/AgCl, the potential is shifted up by 0.197 V.²⁴

Calculation tables

Table S45. Calculated redox potentials for the stepwise one- and two- electron reductions of $[W_{10}O_{32}]^n$, $[TaW_9O_{32}]^n$, $[NbW_9O_{32}]^n$, $[Ta_2W_8O_{32}]^n$ and $[Nb_2W_8O_{32}]^n$.

Reduction	Redox Potential vs Ag/AgCl (V) ^[a]	
	PBE-D3	B3LYP
$[W_{10}O_{32}]^{4-} + 1e^- \rightarrow [W_{10}O_{32}]^{5-}$	-0.13	-0.14
$[TaW_9O_{32}]^{5-} + 1e^- \rightarrow [TaW_9O_{32}]^{6-}$	-0.52	-0.55
$[Ta_2W_8O_{32}]^{6-} + 1e^- \rightarrow [Ta_2W_8O_{32}]^{7-}$	-0.90	-0.96
$[NbW_9O_{32}]^{5-} + 1e^- \rightarrow [NbW_9O_{32}]^{6-}$	-0.51	-0.54
$[Nb_2W_8O_{32}]^{6-} + 1e^- \rightarrow [Nb_2W_8O_{32}]^{7-}$	-0.85	-0.96
$[W_{10}O_{32}]^{5-} + 1e^- \rightarrow [W_{10}O_{32}]^{6-}$	-0.56	-0.61
$[TaW_9O_{32}]^{6-} + 1e^- \rightarrow [TaW_9O_{32}]^{7-}$	-0.93	-0.98
$[Ta_2W_8O_{32}]^{7-} + 1e^- \rightarrow [Ta_2W_8O_{32}]^{8-}$	-1.30	-1.38
$[NbW_9O_{32}]^{6-} + 1e^- \rightarrow [NbW_9O_{32}]^{7-}$	-0.92	-0.97
$[Nb_2W_8O_{32}]^{7-} + 1e^- \rightarrow [Nb_2W_8O_{32}]^{8-}$	-1.25	-1.34

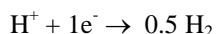
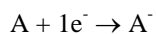
^[a] The calculated redox potential does not include zero point energy or entropy contributions to the polyoxometalate species since their contribution to the calculated redox potential is on the order of 20meV (e.g. -0.34V vs -0.36 V for $[W_{10}O_{32}]^{4-} + 2e^- \rightarrow [W_{10}O_{32}]^{6-}$).

Table S46. Experimental and calculated (B3LYP) redox potentials for $[W_{10}O_{32}]^{4-}$, $[TaW_9O_{32}]^{5-}$, $[NbW_9O_{32}]^{5-}$, (vs. Ag/AgCl). LUMO energy is also presented as it is correlated with the redox potential.

Reduction	Calculated (B3LYP)		Experimental
	LUMO (eV)	Redox Potential (V)	Redox Potential (V)
$[W_{10}O_{32}]^{4-} + 1e^- \rightarrow [W_{10}O_{32}]^{5-}$	-3.63	-0.14	-0.15
$[TaW_9O_{32}]^{5-} + 1e^- \rightarrow [TaW_9O_{32}]^{6-}$	-3.20	-0.55	-0.54
$[NbW_9O_{32}]^{5-} + 1e^- \rightarrow [NbW_9O_{32}]^{6-}$	-3.20	-0.54	-0.56

Expressions used in the reduction potential calculations

Half reactions



Gibbs free energies and reduction potentials

$$\Delta G^0(A/A^-) = -nFE^0(A/A^-)$$

$$E^0(A/A^-) = -\Delta G(A/A^-)/nF$$

$$\Delta G^0(NHE) = -nFE^0(NHE)$$

$$E^0(NHE) = -\Delta G(NHE)/nF = -(4.28) V$$

Reference electrode (NHE to Ag/AgCl)

$$E^0(NHE) = E^0(Ag/AgCl) + 0.197 V$$

$$E^0(Ag/AgCl) = E^0(NHE) - 0.197 V = 4.28 V - 0.197 V = 4.083 V$$

Reduction potential vs Ag/AgCl

$$E^0(A/A^-) \text{ vs Ag/AgCl} = E^0(A/A^-) - E^0(Ag/AgCl) = -\Delta G(A/A^-) - 4.083 V$$

Density of states

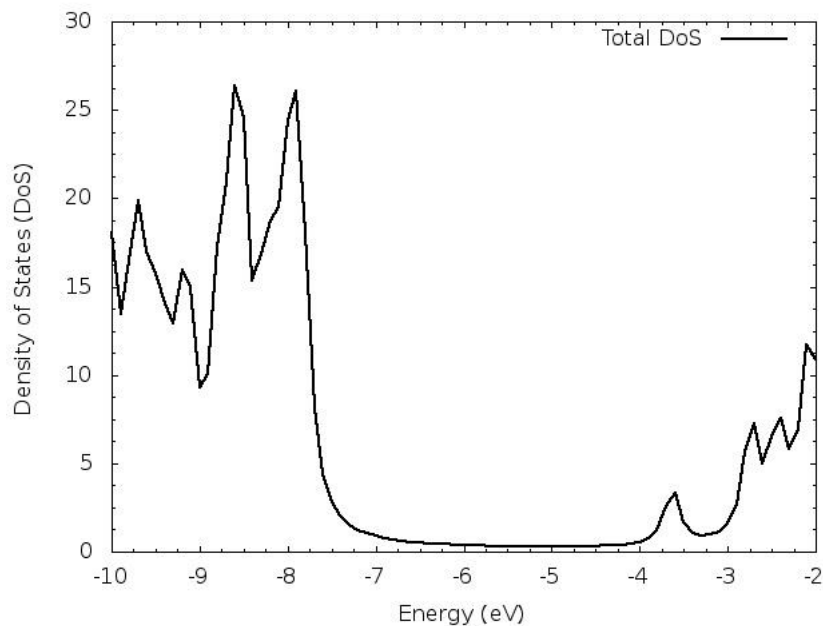


Figure S47. Total Density of States at B3LYP/TZ2P level of theory of $[W_{10}O_{32}]^4$. Fermi level ($0.5*(HOMO+LUMO)$) is located at -5.724 eV.

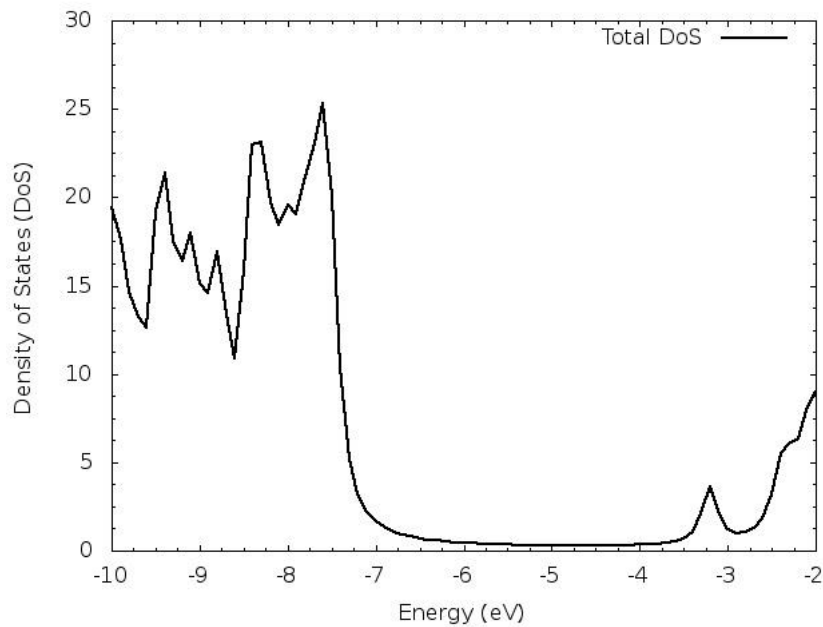


Figure S48. Total Density of States at B3LYP/TZ2P level of theory of $[NbW_9O_{32}]^5$. Fermi level ($0.5*(HOMO+LUMO)$) is located at -5.327 eV.

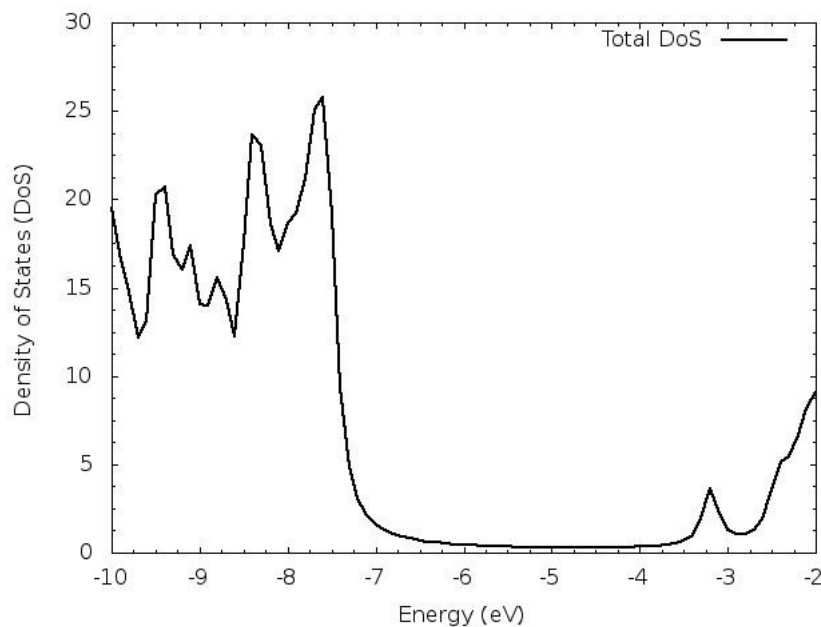


Figure S49. Total Density of States at B3LYP/TZ2P level of theory of $[TaW_9O_{32}]^{5-}$. Fermi level ($0.5*(HOMO+LUMO)$) is located at -5.333 eV.

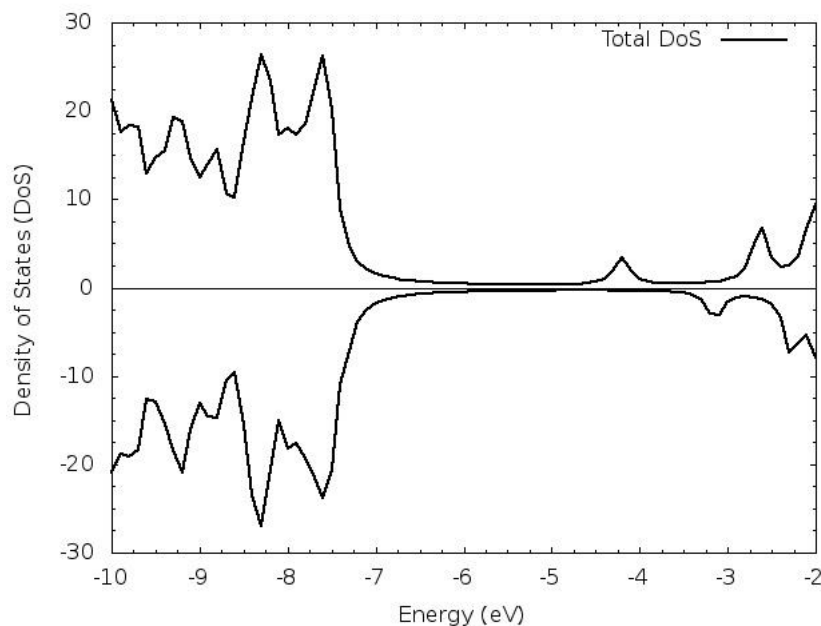


Figure S50. Total Density of States at B3LYP/TZ2P level of theory of $[W_{10}O_{32}]^{5-}$. Alpha and beta orbitals are presented as positive and negative DOS respectively. Fermi level ($0.5*(HOMO+LUMO)$) are located at -3.416 and -5.243 eV for alpha and beta orbitals.

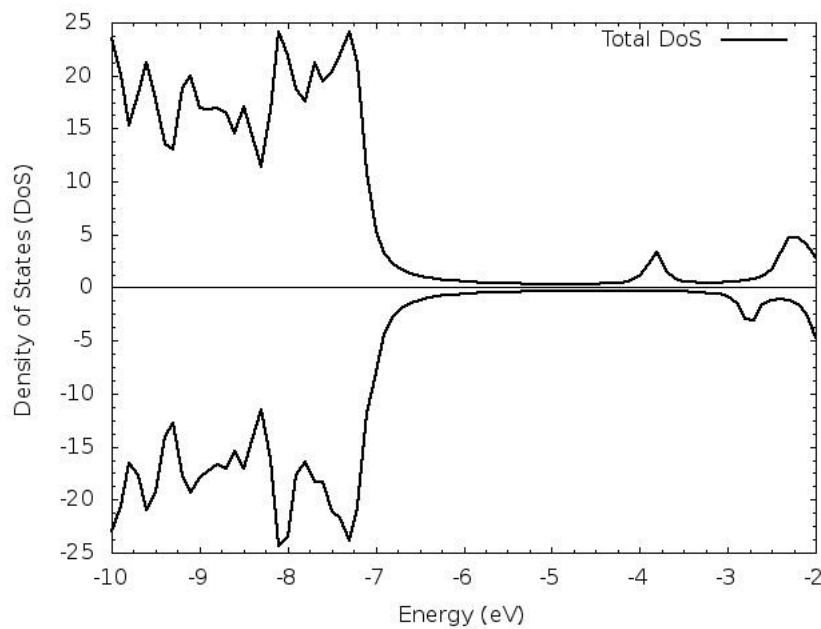


Figure S51. Total Density of States at B3LYP/TZ2P level of theory of $[NbW_9O_{32}]^{6-}$. Alpha and beta orbitals are presented as positive and negative DOS respectively. Fermi level ($0.5*(HOMO+LUMO)$) are located at -3.076 and -4.883 eV for alpha and beta orbitals.

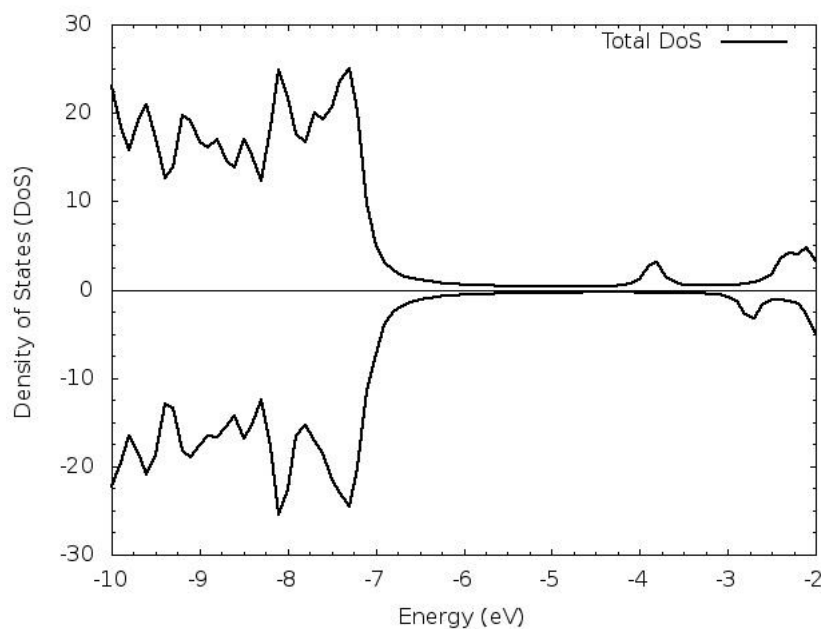


Figure S52. Total Density of States at B3LYP/TZ2P level of theory of $[TaW_9O_{32}]^{6-}$. Alpha and beta orbitals are presented as positive and negative DOS respectively. Fermi level ($0.5*(HOMO+LUMO)$) are located at -3.094 and -4.890 eV for alpha and beta orbitals.

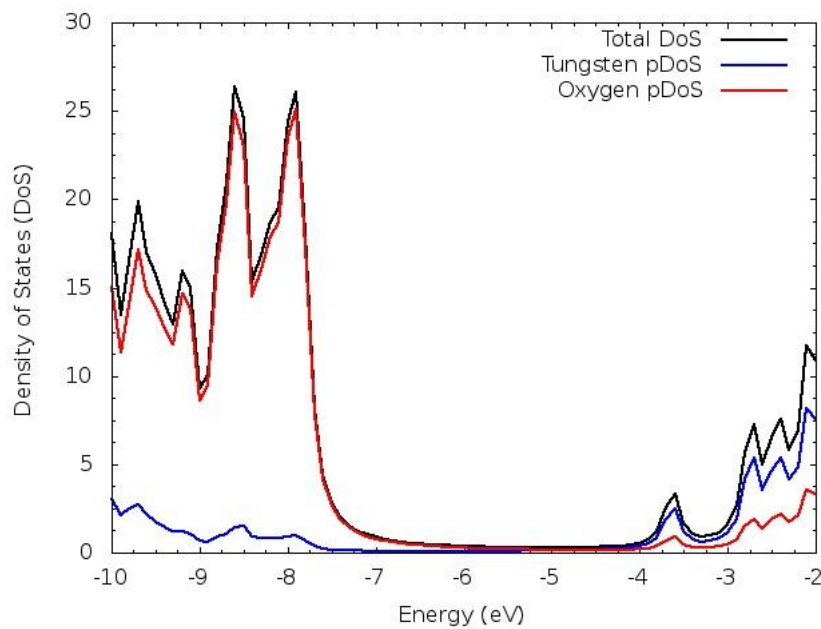


Figure S53. Total and partial Density of States at B3LYP/TZ2P level of theory of States of $[W_{10}O_{32}]^4$. Fermi level ($0.5*(HOMO+LUMO)$) is located at -5.724 eV.

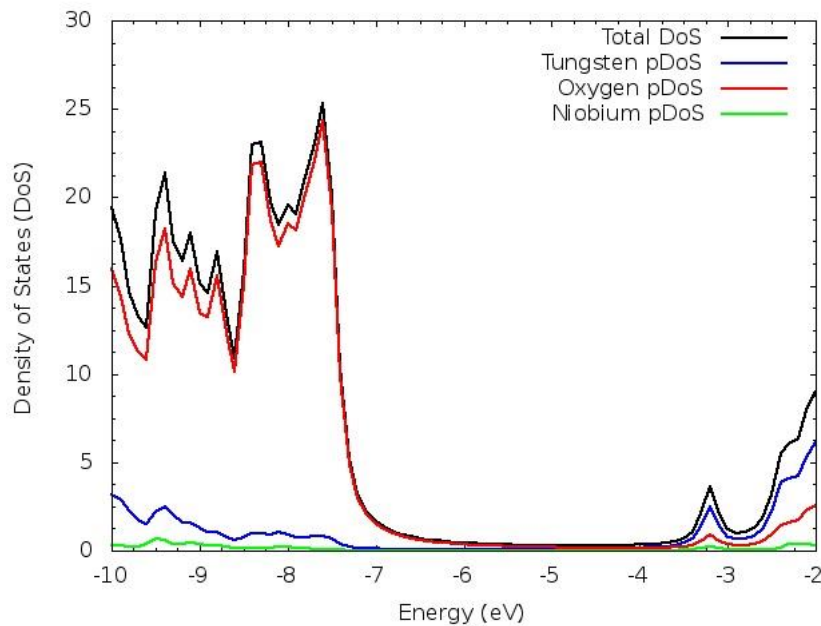


Figure S54. Total and partial Density of States at B3LYP/TZ2P level of theory at B3LYP/TZ2P level of theory of $[NbW_9O_{32}]^5$. Fermi level ($0.5*(HOMO+LUMO)$) is located at -5.327 eV.

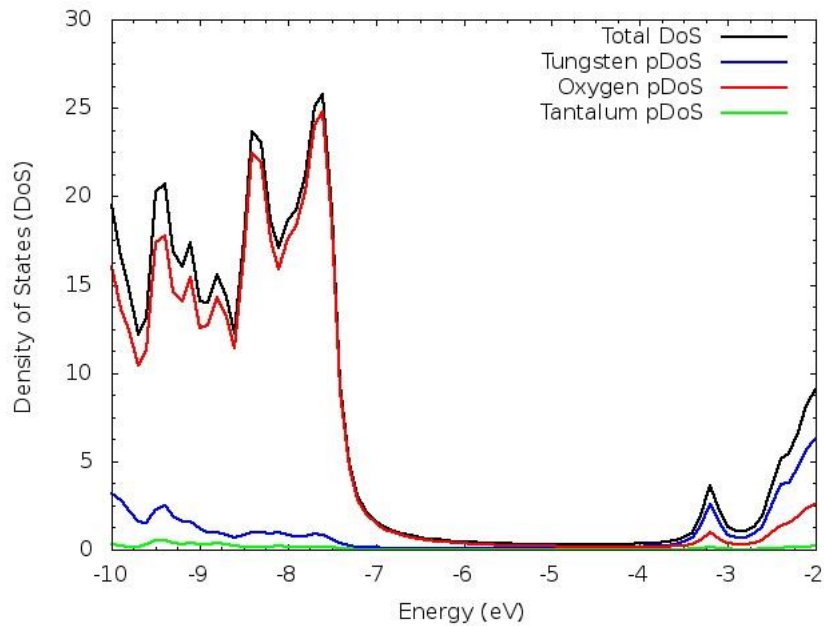


Figure S55. Total and partial Density of States at B3LYP/TZ2P level of theory of $[TaW_9O_{32}]^{5-}$. Fermi level ($0.5*(HOMO+LUMO)$) is located at -5.333 eV.

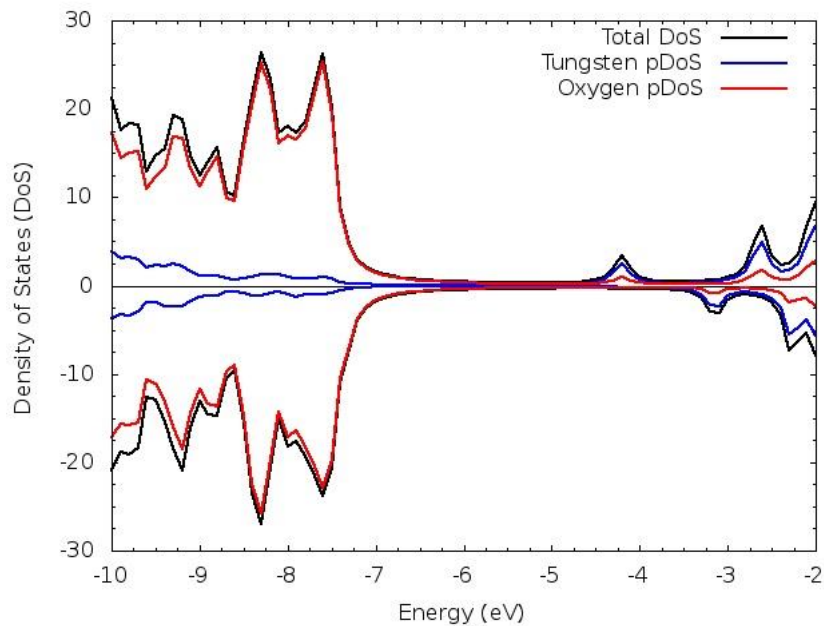


Figure S56. Total and partial Density of States at B3LYP/TZ2P level of theory of $[W_{10}O_{32}]^{5-}$. Alpha and beta orbitals are presented as positive and negative DOS respectively. Fermi level ($0.5*(HOMO+LUMO)$) are located at -3.416 and -5.243 eV for alpha and beta orbitals.

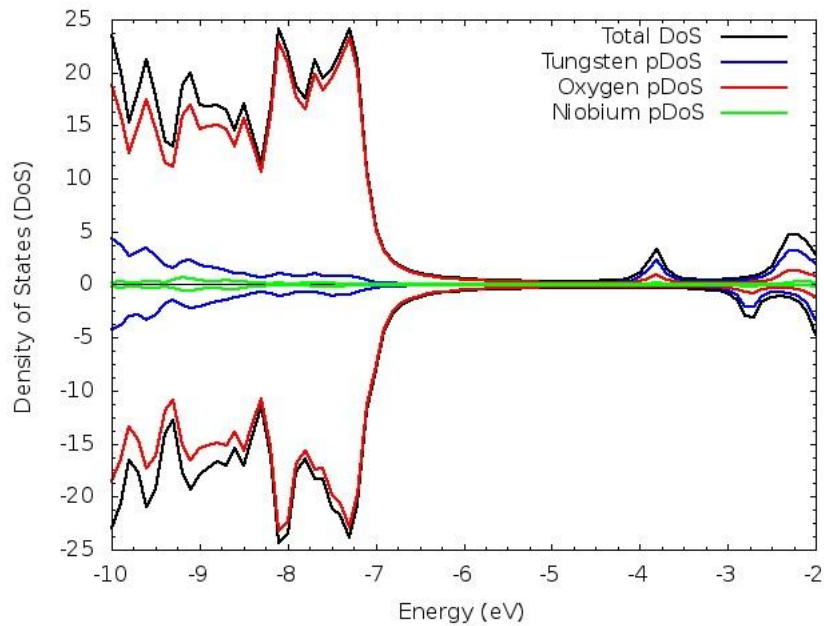


Figure S57. Total and partial Density of States at B3LYP/TZ2P level of theory of $[NbW_9O_{32}]^{6-}$. Alpha and beta orbitals are presented as positive and negative DOS respectively. Fermi level ($0.5*(HOMO+LUMO)$) are located at -3.076 and -4.883 eV for alpha and beta orbitals.

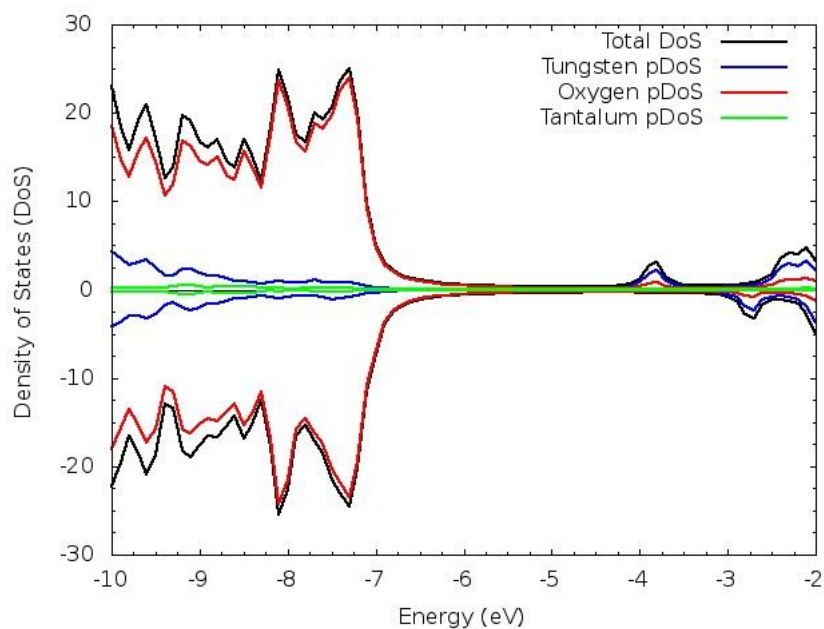


Figure S58. Total and partial Density of States at B3LYP/TZ2P level of theory of $[TaW_9O_{32}]^{6-}$. Alpha and beta orbitals are presented as positive and negative DOS respectively. Fermi level ($0.5*(HOMO+LUMO)$) are located at -3.094 and -4.890 eV for alpha and beta orbitals.

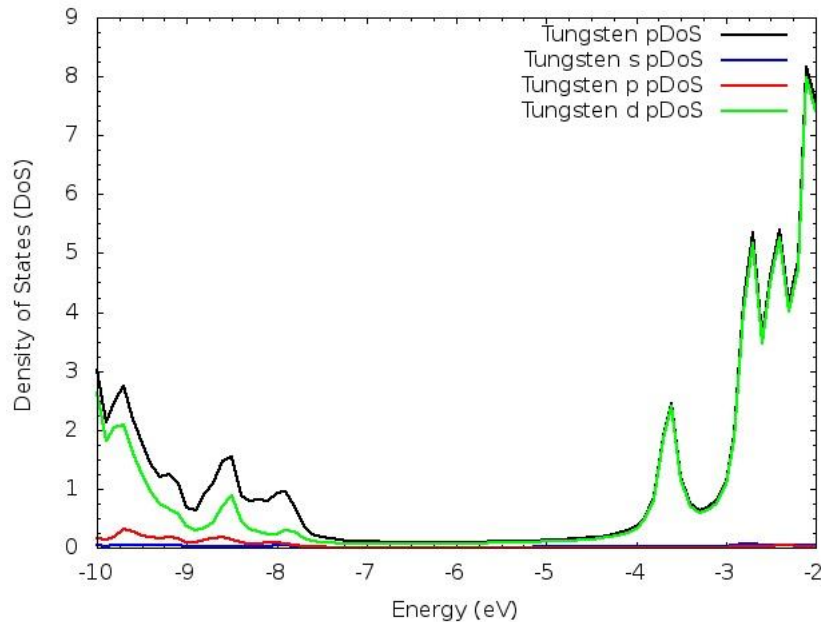


Figure S59. Tungsten partial Density of States decomposed for *s*, *p* and *d* orbitals at B3LYP/TZ2P level of theory of States of $[W_{10}O_{32}]^{4-}$. Fermi level ($0.5*(HOMO+LUMO)$) is located at -5.724 eV.

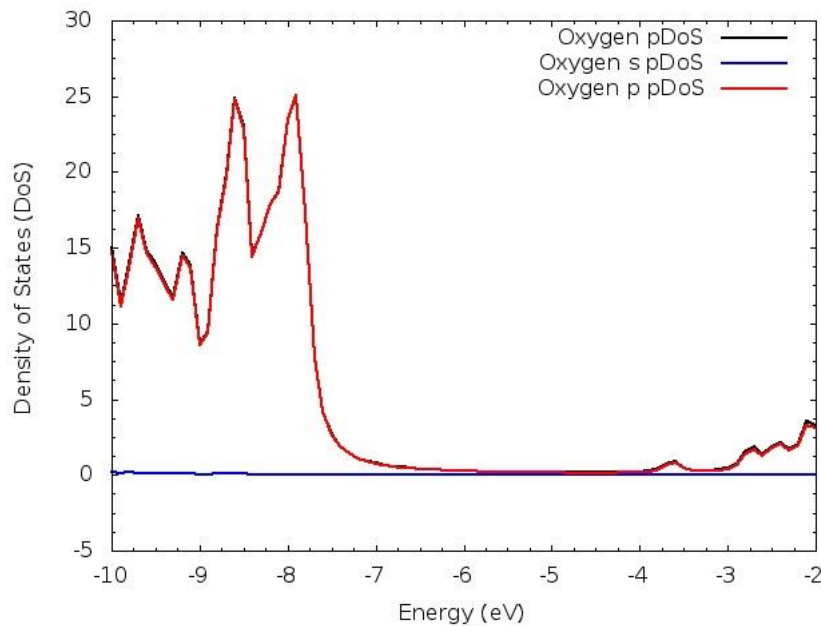


Figure S60. Oxygen partial Density of States decomposed for *s* and *p* orbitals at B3LYP/TZ2P level of theory of States of $[W_{10}O_{32}]^{4-}$. Fermi level ($0.5*(HOMO+LUMO)$) is located at -5.724 eV.

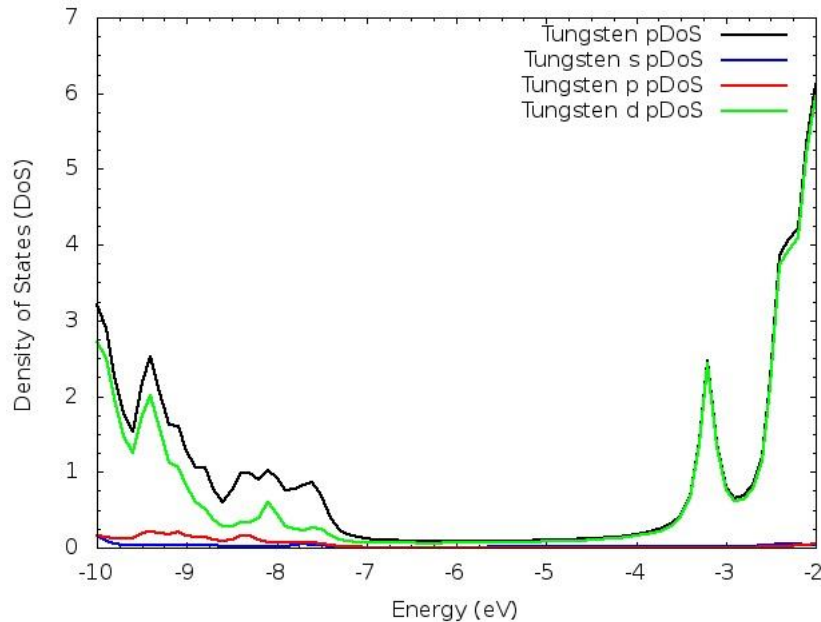


Figure S61. Tungsten partial Density of States decomposed for *s*, *p* and *d* orbitals at B3LYP/TZ2P level of theory of $[NbW_9O_{32}]^{5-}$. Fermi level ($0.5*(HOMO+LUMO)$) is located at -5.327 eV.

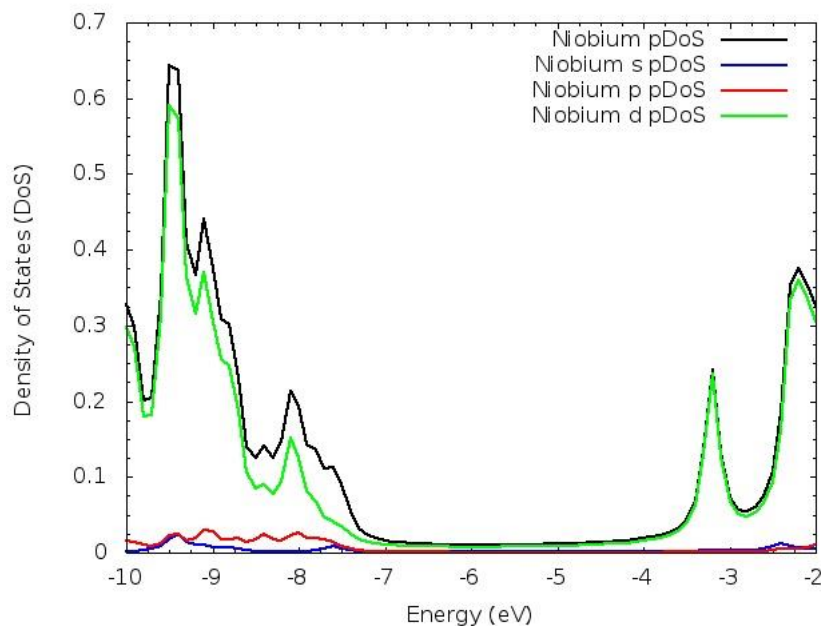


Figure S62. Niobium partial Density of States decomposed for *s*, *p* and *d* orbitals at B3LYP/TZ2P level of theory of $[NbW_9O_{32}]^{5-}$. Fermi level ($0.5*(HOMO+LUMO)$) is located at -5.327 eV.

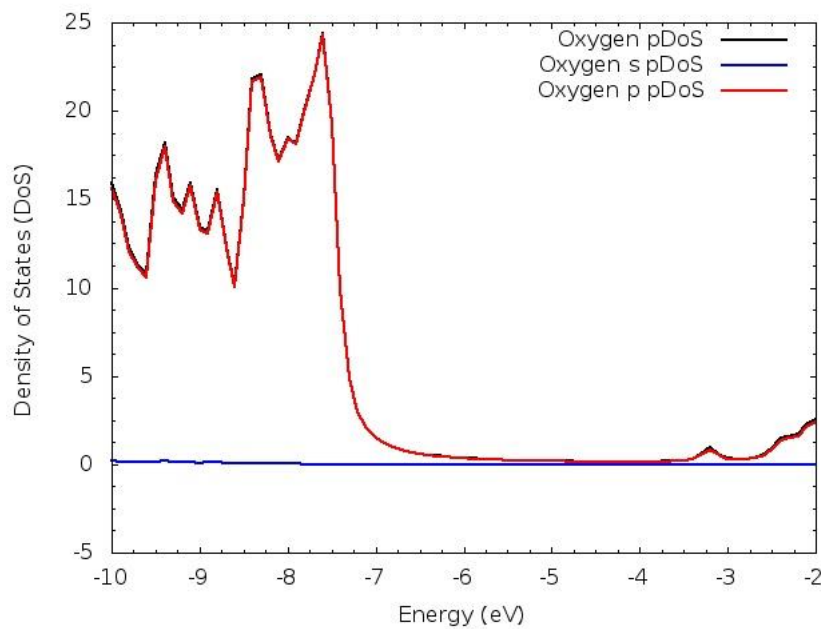


Figure S63. Oxygen partial Density of States decomposed for *s* and *p* orbitals at B3LYP/TZ2P level of theory of $[NbW_9O_{32}]^5$. Fermi level ($0.5*(HOMO+LUMO)$) is located at -5.327 eV.

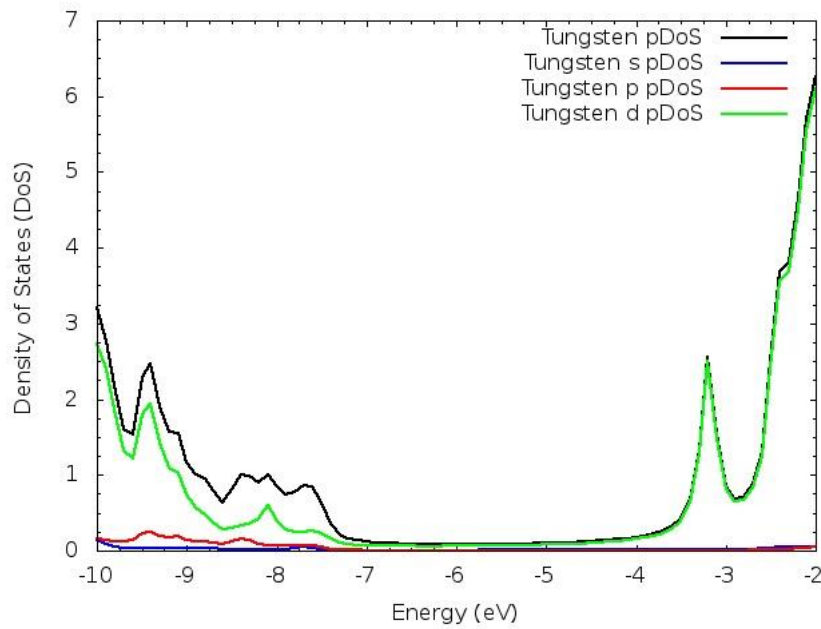


Figure S64. Tungsten partial Density of States decomposed for *s*, *p* and *d* orbitals at B3LYP/TZ2P level of theory of $[TaW_9O_{32}]^5$. Fermi level ($0.5*(HOMO+LUMO)$) is located at -5.333 eV.

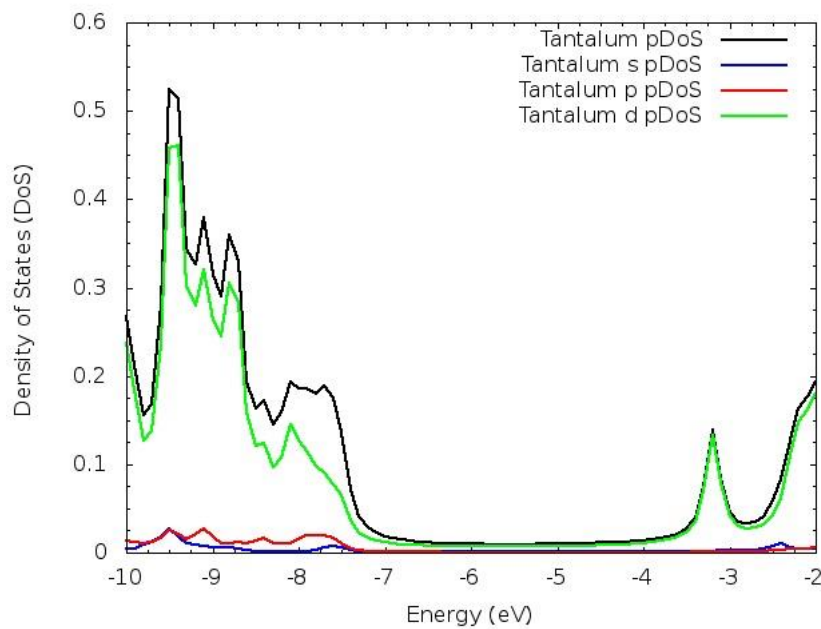


Figure S65. Tantalum partial Density of States decomposed for *s*, *p* and *d* orbitals at B3LYP/TZ2P level of theory of $[TaW_9O_{32}]^{5-}$. Fermi level ($0.5*(HOMO+LUMO)$) is located at -5.333 eV.

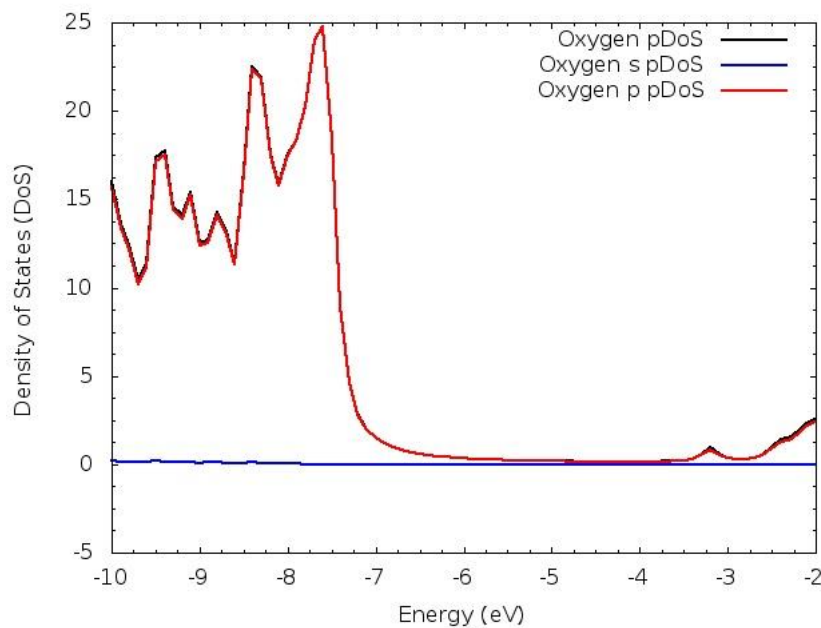


Figure S66. Oxygen partial Density of States decomposed for *s* and *p* orbitals at B3LYP/TZ2P level of theory of $[TaW_9O_{32}]^{5-}$. Fermi level ($0.5*(HOMO+LUMO)$) is located at -5.333 eV.

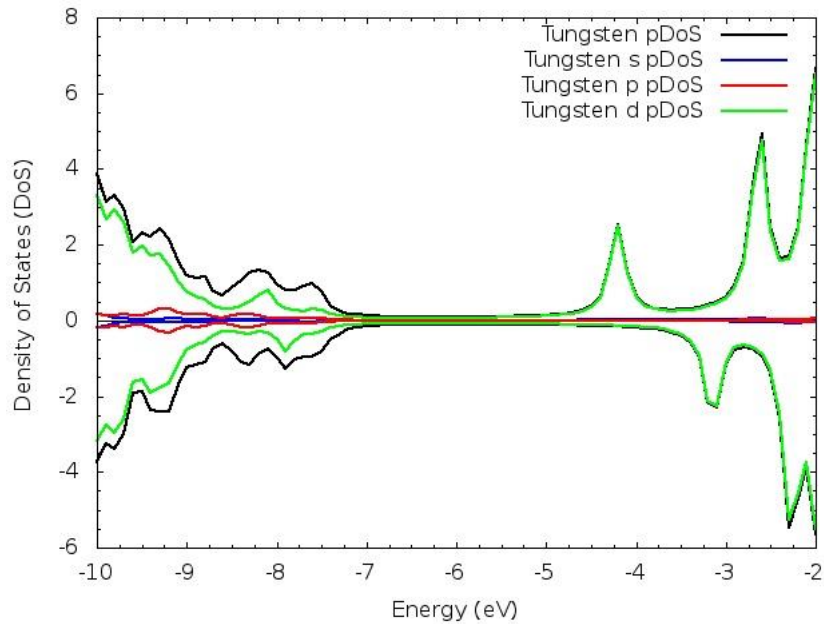


Figure S67. Tungsten partial Density of States decomposed for *s*, *p* and *d* orbitals at B3LYP/TZ2P level of theory of States of $[W_{10}O_{32}]^{5-}$. Alpha and beta orbitals are presented as positive and negative DOS respectively. Fermi level ($0.5*(HOMO+LUMO)$) are located at -3.416 and -5.243 eV for alpha and beta orbitals.

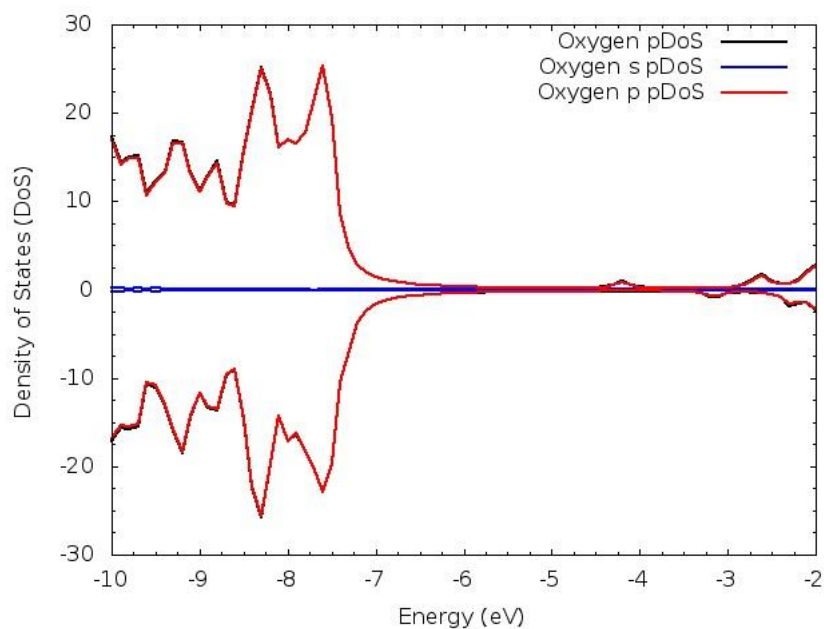


Figure S68. Oxygen partial Density of States decomposed for *s* and *p* orbitals at B3LYP/TZ2P level of theory of States of $[W_{10}O_{32}]^{5-}$. Alpha and beta orbitals are presented as positive and negative DOS respectively. Fermi level ($0.5*(HOMO+LUMO)$) are located at -3.416 and -5.243 eV for alpha and beta orbitals.

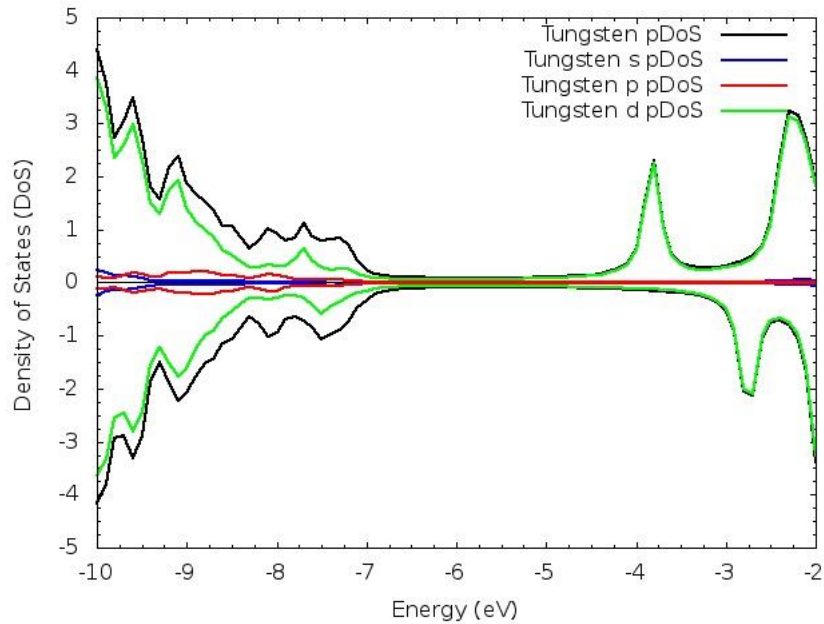


Figure S69. Tungsten partial Density of States decomposed for *s*, *p* and *d* orbitals at B3LYP/TZ2P level of theory of $[NbW_9O_{32}]^6-$. Alpha and beta orbitals are presented as positive and negative DOS respectively. Fermi level ($0.5*(HOMO+LUMO)$) are located at -3.076 and -4.884 eV for alpha and beta orbitals.

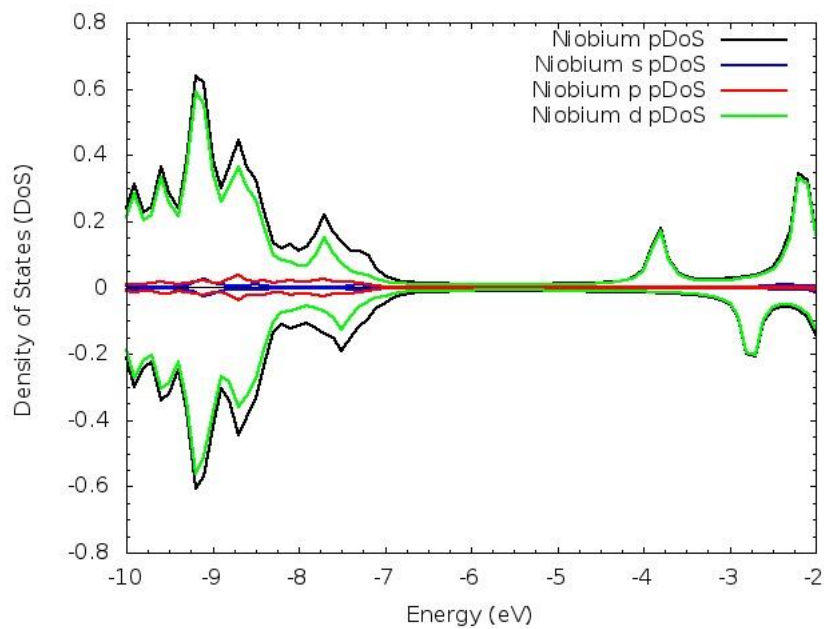


Figure S70. Niobium partial Density of States decomposed for *s*, *p* and *d* orbitals at B3LYP/TZ2P level of theory of $[NbW_9O_{32}]^6-$. Alpha and beta orbitals are presented as positive and negative DOS respectively. Fermi level ($0.5*(HOMO+LUMO)$) are located at -3.076 and -4.884 eV for alpha and beta orbitals.

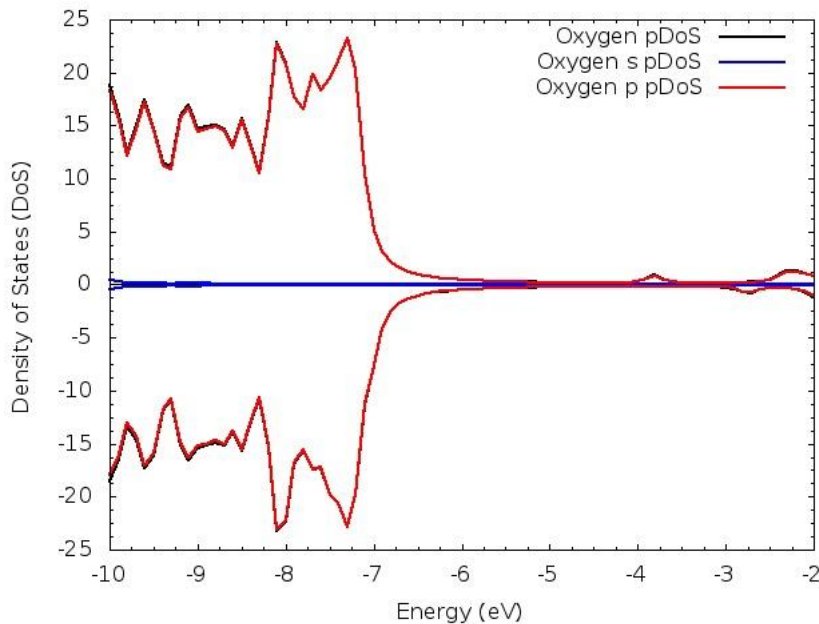


Figure S71. Oxygen partial Density of States decomposed for *s* and *p* orbitals at B3LYP/TZ2P level of theory of $[NbW_9O_{32}]^6^-$. Alpha and beta orbitals are presented as positive and negative DOS respectively. Fermi level ($0.5*(HOMO+LUMO)$) are located at -3.076 and -4.884 eV for alpha and beta orbitals.

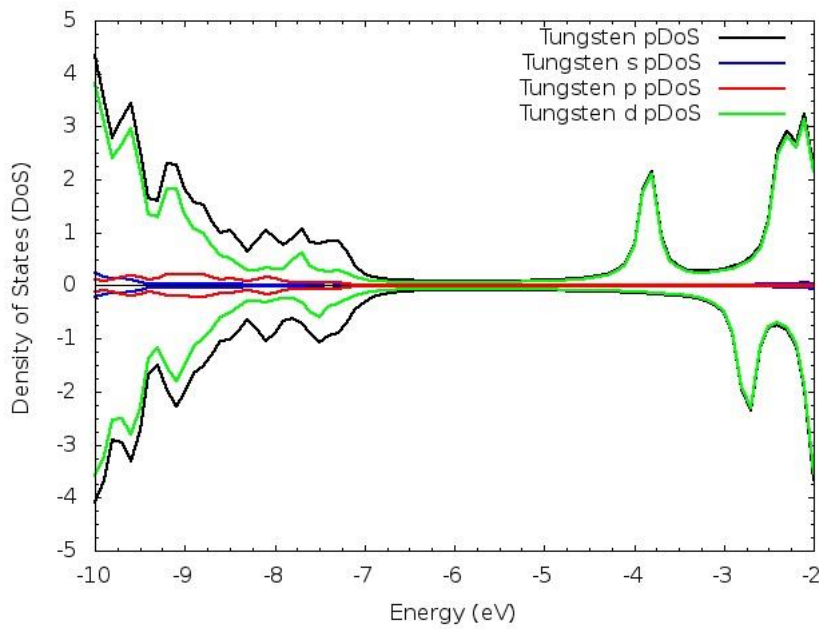


Figure S72. Tungsten partial Density of States decomposed for *s*, *p* and *d* orbitals at B3LYP/TZ2P level of theory of $[TaW_9O_{32}]^6^-$. Alpha and beta orbitals are presented as positive and negative DOS respectively. Fermi level ($0.5*(HOMO+LUMO)$) are located at -3.094 and -4.890 eV for alpha and beta orbitals.

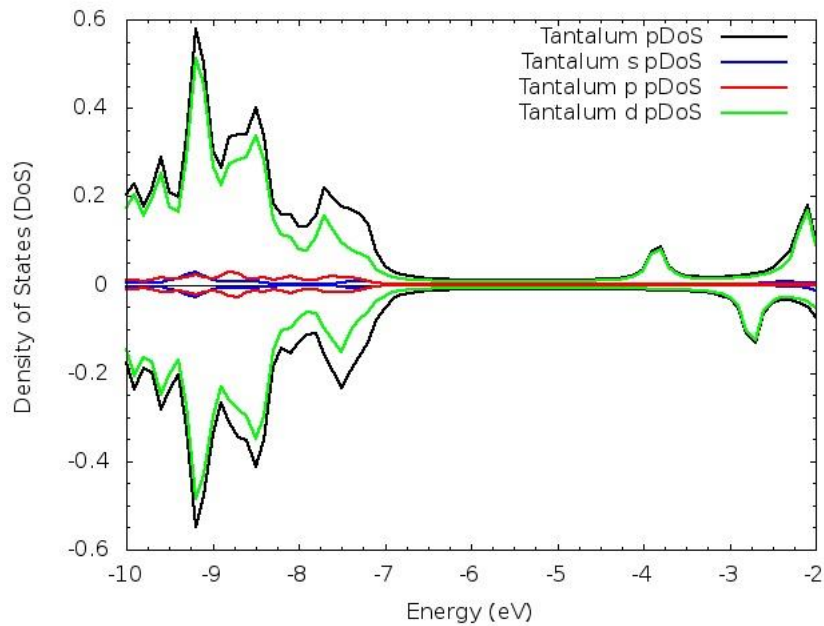


Figure S73. Tantalum partial Density of States decomposed for *s*, *p* and *d* orbitals at B3LYP/TZ2P level of theory of $[TaW_9O_{32}]^{6-}$. Alpha and beta orbitals are presented as positive and negative DOS respectively. Fermi level ($0.5*(HOMO+LUMO)$) are located at -3.094 and -4.890 eV for alpha and beta orbitals.

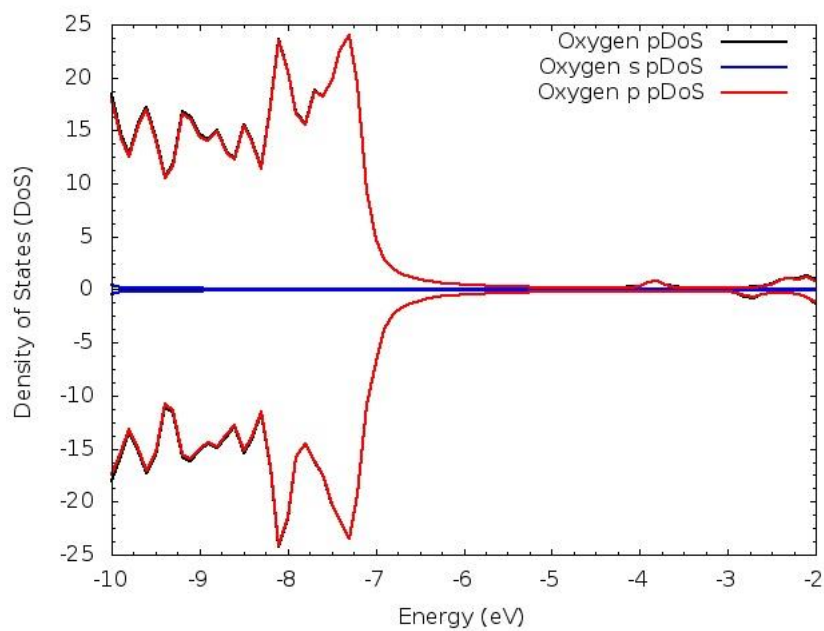


Figure S74. Oxygen partial Density of States decomposed for *s* and *p* orbitals at B3LYP/TZ2P level of theory of $[TaW_9O_{32}]^{6-}$. Alpha and beta orbitals are presented as positive and negative DOS respectively. Fermi level ($0.5*(HOMO+LUMO)$) are located at -3.094 and -4.890 eV for alpha and beta orbitals.

Cartesian coordinates⁵ tables

Table S75. Cartesian coordinates (\AA) of $[W_{10}O_{32}]^{4-}$ (1A).

W	2.328493	-2.335593	0.005194
W	2.328745	-2.335599	-3.806281
W	-0.007878	-0.000029	-3.806393
W	2.328561	0.000013	2.365896
W	-0.007726	0.000016	0.005468
O	2.328726	-0.000006	-3.833174
O	0.451220	-0.000043	-5.712550
O	0.068101	-0.000006	-1.900484
O	0.449316	-1.879041	-3.789073
O	4.208103	-1.879121	-3.789189
O	0.451454	0.000025	1.911635
O	2.328547	0.000023	0.032098
O	4.206021	0.000011	1.911516
O	2.328619	-2.259520	-1.900529
O	0.449041	-1.879098	-0.011944
O	0.449267	1.878981	-3.789047
O	2.328555	1.877048	1.911511
O	2.328474	0.000001	4.103396
O	2.328437	-1.877044	1.911460
O	-1.724543	-0.000054	-4.023493
O	2.328464	-4.052255	0.222022
O	2.328755	-4.052260	-4.023118
O	-1.724477	0.000022	0.222597
O	2.328650	2.259468	-1.900532
O	4.208088	1.879105	-3.789219

⁵ Optimized at PBE-D3 level of theory

O	4.207934	-1.879003	-0.012038
O	2.328795	-1.877053	-5.712571
O	2.328716	0.000001	-7.904484
O	2.328712	1.877032	-5.712558
O	6.381896	0.000035	0.222542
O	2.328660	4.052249	-4.023060
W	2.328704	2.335569	-3.806249
W	2.328599	2.335621	0.005223
W	4.665242	0.000034	0.005373
W	2.328678	-0.000006	-6.166981
W	4.665087	0.000018	-3.806637
O	2.328641	4.052272	0.222099
O	6.381805	0.000036	-4.023911
O	4.589492	0.000026	-1.900598
O	4.208012	1.879004	-0.011849
O	0.449112	1.879108	-0.011959
O	4.205782	0.000010	-5.712788

Table S76. Cartesian coordinates(Å) of $[W_{10}O_{32}]^{5-}$ (²A).

W	2.328405	-2.336562	0.004243
W	2.328812	-2.336637	-3.805289
W	-0.009630	-0.000076	-3.805315
W	2.328680	0.000039	2.374412
W	-0.009354	0.000183	0.004640
O	2.328779	-0.000079	-3.836631
O	0.449735	-0.000109	-5.733989
O	0.058658	0.000056	-1.900416
O	0.449334	-1.878888	-3.806928

O	4.208281	-1.879066	-3.807001
O	0.449653	0.000146	1.933385
O	2.328463	0.000176	0.035591
O	4.207487	-0.000087	1.932917
O	2.328608	-2.268176	-1.900507
O	0.448971	-1.878877	0.005950
O	0.449259	1.878766	-3.806993
O	2.328527	1.878646	1.933185
O	2.329059	-0.000132	4.119072
O	2.328525	-1.878581	1.933091
O	-1.730664	-0.000128	-4.029671
O	2.328442	-4.057692	0.227763
O	2.328848	-4.057772	-4.028848
O	-1.730519	0.000238	0.228208
O	2.328628	2.267910	-1.900473
O	4.208099	1.878886	-3.807149
O	4.207930	-1.878674	0.005625
O	2.328699	-1.878668	-5.734239
O	2.328122	-0.000077	-7.920185
O	2.328628	1.878529	-5.734240
O	6.388035	0.000114	0.228980
O	2.328674	4.057666	-4.028650
W	2.328710	2.336496	-3.805278
W	2.328573	2.336660	0.004260
W	4.667052	0.000200	0.004328
W	2.328486	-0.000072	-6.175530
W	4.666755	-0.000058	-3.805906
O	2.328555	4.057811	0.227737

O	6.387866	-0.000035	-4.029751
O	4.599044	0.000070	-1.900660
O	4.208020	1.878842	0.006190
O	0.449064	1.879096	0.005961
O	4.207580	-0.000083	-5.734570

Table S77. Cartesian coordinates(Å) of $[W_{10}O_{32}]^{6-}$ (1A).

W	2.328356	-2.337955	0.003037
W	2.328866	-2.338023	-3.804128
W	-0.010421	-0.000099	-3.804034
W	2.328618	0.000042	2.384243
W	-0.010352	0.000143	0.003390
O	2.328775	-0.000077	-3.845789
O	0.446222	-0.000136	-5.759065
O	0.053169	0.000024	-1.900308
O	0.450572	-1.877898	-3.813394
O	4.207105	-1.877954	-3.813471
O	0.446203	0.000187	1.958396
O	2.328501	0.000153	0.044700
O	4.211000	-0.000056	1.958079
O	2.328612	-2.274598	-1.900505
O	0.450158	-1.877760	0.012466
O	0.450353	1.877781	-3.813445
O	2.328536	1.881781	1.958016
O	2.329022	-0.000051	4.136898
O	2.328340	-1.881707	1.957837
O	-1.737472	-0.000161	-4.024799
O	2.328282	-4.065048	0.223353

O	2.329001	-4.065122	-4.024533
O	-1.737482	0.000171	0.223505
O	2.328664	2.274072	-1.900432
O	4.206740	1.877698	-3.813750
O	4.206689	-1.877655	0.012007
O	2.328875	-1.881804	-5.759065
O	2.328043	-0.000012	-7.937983
O	2.328642	1.881715	-5.759098
O	6.394782	0.000147	0.224414
O	2.328668	4.064989	-4.024363
W	2.328698	2.337847	-3.804158
W	2.328648	2.338050	0.003131
W	4.667815	0.000179	0.003175
W	2.328522	-0.000054	-6.185339
W	4.667717	-0.000048	-3.804712
O	2.328697	4.065127	0.223474
O	6.394818	-0.000037	-4.025217
O	4.604753	0.000063	-1.900717
O	4.206950	1.877939	0.012613
O	0.450193	1.878202	0.012482
O	4.211005	-0.000057	-5.759591

Table S78. Cartesian coordinates (\AA) of $[\text{TaW}_9\text{O}_{32}]^{5-}$ (isomer: $\{\text{MW}_9\}\text{-}1$) (^1A) (Fig S41).

W	2.306514	2.329203	3.882853
W	2.329367	2.325573	0.063372
W	4.678400	-0.000066	0.104400
W	2.240765	0.000019	6.243436
Ta	4.675229	0.000060	3.953119

O	2.342166	-0.000002	0.026979
O	4.214534	-0.000101	-1.860319
O	4.642034	-0.000005	1.952713
O	4.212284	1.882158	0.059470
O	0.444909	1.880440	0.052238
O	4.105787	0.000095	5.899548
O	2.268203	-0.000013	3.920217
O	0.345436	-0.000087	5.745105
O	2.319398	2.255866	1.957328
O	4.158867	1.939877	3.904190
O	4.212222	-1.882355	0.059491
O	2.209737	-1.882792	5.790394
O	2.144270	0.000042	7.985062
O	2.209600	1.882828	5.790271
O	6.390404	-0.000142	-0.190776
O	2.252775	4.053100	4.087460
O	2.329434	4.045611	-0.163144
O	6.434170	0.000097	4.219313
O	2.319381	-2.256104	1.957300
O	0.444937	-1.880282	0.052112
O	0.405402	1.872328	3.800057
O	2.328213	1.877417	-1.856438
O	2.359101	0.000059	-4.053645
O	2.328105	-1.877362	-1.856456
O	-1.778985	-0.000178	4.010729
O	2.329292	-4.045674	-0.163256
W	2.329305	-2.325648	0.063328
W	2.306555	-2.329099	3.882855

W	-0.048787	-0.000097	3.840190
W	2.368055	0.000031	-2.310431
W	-0.017264	0.000071	0.024145
O	2.252862	-4.052995	4.087467
O	-1.736281	0.000118	-0.208066
O	0.047024	-0.000016	1.918293
O	0.405601	-1.872364	3.800124
O	4.158995	-1.939738	3.904170
O	0.466868	0.000130	-1.866138

Table S77. Cartesian coordinates(Å) of $[TaW_9O_{32}]^{6-}$ (isomer: {MW₉}-I) (²A) (Fig S41).

W	2.291202	2.332008	3.875441
W	2.329817	2.328137	0.059867
W	4.684933	-0.000398	0.099338
W	2.231842	-0.000417	6.250253
Ta	4.666515	-0.000155	3.949493
O	2.332032	-0.000066	0.019819
O	4.223865	0.000451	-1.870481
O	4.644040	-0.000254	1.957352
O	4.215870	1.876744	0.063254
O	0.451000	1.882674	0.033627
O	4.104938	0.000299	5.908089
O	2.249398	-0.000164	3.920288
O	0.342327	0.000586	5.776189
O	2.313438	2.269077	1.960748
O	4.154097	1.933073	3.914023
O	4.215699	-1.877101	0.062472
O	2.222709	-1.883666	5.810000

O	2.150464	-0.000422	8.000735
O	2.223055	1.883683	5.809720
O	6.404405	-0.000538	-0.181895
O	2.246563	4.060814	4.090182
O	2.334043	4.053230	-0.165575
O	6.433366	0.000065	4.218924
O	2.313320	-2.268606	1.960579
O	0.450717	-1.882137	0.032729
O	0.397133	1.878370	3.828149
O	2.351725	1.880891	-1.880064
O	2.377011	0.000207	-4.071527
O	2.351582	-1.880392	-1.880569
O	-1.790611	-0.000830	4.020006
O	2.332539	-4.053055	-0.165835
W	2.329088	-2.327972	0.059942
W	2.291538	-2.331992	3.874707
W	-0.056135	-0.000551	3.835886
W	2.366244	0.000076	-2.320967
W	-0.011738	-0.000064	0.027275
O	2.246898	-4.060793	4.089734
O	-1.733116	-0.000002	-0.226523
O	0.025940	-0.000097	1.923070
O	0.397461	-1.878510	3.828923
O	4.153986	-1.932843	3.915104
O	0.475684	0.000642	-1.903424

Table S78. Cartesian coordinates (\AA) of $[TaW_9O_{32}]^{7-}$ (isomer: {MW₉}-1) (^lA) (Fig S41).

W	2.283658	2.335253	3.871415
---	----------	----------	----------

W	2.327587	2.328251	0.059475
W	4.685375	-0.000185	0.093744
W	2.228359	-0.000365	6.260598
Ta	4.660997	-0.000368	3.945375
O	2.335244	-0.000051	0.012945
O	4.232073	0.000553	-1.892476
O	4.651981	-0.000258	1.961235
O	4.217662	1.873626	0.062506
O	0.453230	1.879966	0.023032
O	4.110157	-0.000450	5.917760
O	2.241385	-0.000158	3.925277
O	0.345244	0.000821	5.810903
O	2.308096	2.279196	1.964475
O	4.154820	1.929105	3.920397
O	4.217555	-1.873535	0.061529
O	2.235244	-1.884229	5.831497
O	2.163309	-0.000379	8.019981
O	2.236447	1.884493	5.831292
O	6.411020	-0.000131	-0.188060
O	2.239568	4.068132	4.094664
O	2.331404	4.057455	-0.172386
O	6.435166	-0.000179	4.222595
O	2.307916	-2.278294	1.964318
O	0.453033	-1.879597	0.021941
O	0.394771	1.880639	3.848184
O	2.364080	1.882535	-1.906063
O	2.383177	0.000238	-4.093308
O	2.363851	-1.881831	-1.906531

O	-1.797802	-0.000693	4.037996
O	2.330357	-4.057218	-0.172045
W	2.327017	-2.327950	0.059655
W	2.283703	-2.335396	3.870596
W	-0.060415	-0.000442	3.832516
W	2.365323	0.000110	-2.334738
W	-0.018603	-0.000210	0.028693
O	2.239635	-4.068305	4.094186
O	-1.742177	-0.000223	-0.236969
O	0.006016	-0.000177	1.927080
O	0.394891	-1.880633	3.849034
O	4.154817	-1.929813	3.921888
O	0.479716	0.000694	-1.935147

Table S79 Cartesian coordinates(Å) of $[Ta_2W_8O_{32}]^{6-}$ (isomer: $\{M_2W_8\}$ -I) (1A) (Fig S42).

W	0.003008	1.913519	-2.324696
W	-0.003027	-1.913563	-2.324699
W	2.362017	-1.862563	0.000015
W	-0.062033	4.285880	0.000020
Ta	2.375003	1.985492	0.000040
O	0.039172	-1.956660	-0.000010
O	1.929008	-3.815422	-0.000004
O	2.334653	-0.002885	0.000027
O	1.899805	-1.880289	-1.878260
O	-1.861579	-1.934076	-1.941997
O	1.816756	3.926733	0.000025
O	-0.039174	1.956676	0.000015
O	-1.929013	3.815402	0.000008

O	-0.000009	-0.000018	-2.261356
O	1.861505	1.934064	-1.941894
O	1.899858	-1.880236	1.878271
O	-0.061952	3.833917	1.885551
O	-0.125191	6.034445	0.000023
O	-0.061976	3.833911	-1.885567
O	4.084513	-2.142654	0.000023
O	-0.047775	2.130389	-4.051612
O	0.047753	-2.130456	-4.051616
O	4.140245	2.248354	0.000068
O	0.000039	0.000008	2.261366
O	-1.861472	-1.934046	1.941854
O	-1.899825	1.880213	-1.878246
O	0.061929	-3.833918	-1.885549
O	0.125181	-6.034442	-0.000012
O	0.062016	-3.833895	1.885563
O	-4.084523	2.142657	-0.000018
O	0.047870	-2.130343	4.051610
W	-0.002956	-1.913497	2.324684
W	0.003035	1.913541	2.324701
W	-2.362031	1.862563	-0.000008
W	0.062035	-4.285876	-0.000012
Ta	-2.375028	-1.985500	-0.000032
O	-0.047742	2.130416	4.051625
O	-4.140264	-2.248375	-0.000052
O	-2.334728	0.002879	-0.000019
O	-1.899823	1.880258	1.878247
O	1.861487	1.934119	1.941945

O -1.816766 -3.926719 -0.000022

Table S80. Cartesian coordinates (\AA) of $[\text{Ta}_2\text{W}_8\text{O}_{32}]^{7-}$ (isomer: $\{\text{M}_2\text{W}_8\}\text{-}1)$ (^2A) (Fig S42).

W	-0.014967	1.908553	-2.322749
W	0.015329	-1.909862	-2.323020
W	2.378761	-1.872869	-0.000049
W	-0.067709	4.295859	-0.000140
Ta	2.364942	1.975203	0.000295
O	0.056341	-1.964336	-0.000478
O	1.943690	-3.845809	0.000071
O	2.345232	-0.000936	0.000077
O	1.917677	-1.894354	-1.876368
O	-1.853550	-1.949765	-1.934935
O	1.810602	3.944016	-0.001539
O	-0.055858	1.964249	0.000420
O	-1.943620	3.845491	-0.000314
O	0.000142	-0.000558	-2.259613
O	1.853020	1.949730	-1.934223
O	1.917929	-1.893621	1.876231
O	-0.067822	3.857075	1.884733
O	-0.128862	6.052705	-0.000716
O	-0.069246	3.855829	-1.885456
O	4.108018	-2.143683	-0.000211
O	-0.063276	2.124953	-4.054780
O	0.063348	-2.126254	-4.054985
O	4.136513	2.252932	0.001576
O	0.000333	0.000554	2.260268
O	-1.852553	-1.949508	1.933480
O	-1.917634	1.892137	-1.875479

O	0.067667	-3.857000	-1.885149
O	0.128543	-6.052719	0.000664
O	0.068614	-3.856165	1.885151
O	-4.108259	2.144775	0.001143
O	0.063255	-2.125410	4.054971
W	0.015588	-1.908610	2.322938
W	-0.014794	1.909656	2.323123
W	-2.379137	1.873141	0.000635
W	0.067703	-4.295877	0.000112
Ta	-2.365230	-1.975325	-0.000718
O	-0.062410	2.126506	4.055010
O	-4.136594	-2.253719	-0.002018
O	-2.347157	0.001075	0.000755
O	-1.917250	1.894071	1.876491
O	1.853306	1.951484	1.934350
O	-1.810624	-3.943614	0.000444

Table S81. Cartesian coordinates(Å) of $[Ta_2W_8O_{32}]^{8-}$ (isomer: $\{M_2W_8\}\text{-}I$) (1A) (Fig S42).

W	-0.021946	1.906009	-2.322542
W	0.021876	-1.906785	-2.322445
W	2.386485	-1.881834	0.000297
W	-0.069673	4.310952	-0.000182
Ta	2.365383	1.969537	0.000150
O	0.068145	-1.970984	-0.000482
O	1.948163	-3.885887	-0.000727
O	2.373539	-0.000426	0.000221
O	1.924047	-1.904513	-1.872655
O	-1.855308	-1.954808	-1.928238

O	1.812901	3.958942	0.000058
O	-0.067784	1.971335	0.000270
O	-1.948229	3.885603	0.000895
O	-0.000078	-0.000276	-2.271119
O	1.854207	1.954559	-1.927647
O	1.924427	-1.905993	1.872831
O	-0.063591	3.881138	1.883991
O	-0.113937	6.075744	-0.000626
O	-0.064341	3.880603	-1.883877
O	4.119321	-2.169101	0.000619
O	-0.071379	2.132427	-4.058577
O	0.071720	-2.133356	-4.058346
O	4.141768	2.266768	0.000484
O	0.000636	0.000202	2.271288
O	-1.853247	-1.954536	1.926284
O	-1.923945	1.904508	-1.872258
O	0.063976	-3.880349	-1.883219
O	0.113174	-6.075653	0.001151
O	0.064121	-3.880374	1.883566
O	-4.119496	2.170311	0.000308
O	0.071611	-2.132016	4.058361
W	0.022980	-1.905883	2.322342
W	-0.021661	1.905913	2.322839
W	-2.386887	1.881868	0.000223
W	0.069655	-4.310997	0.000408
Ta	-2.365651	-1.969753	-0.000747
O	-0.071579	2.132907	4.058688
O	-4.141758	-2.267882	-0.000899

O	-2.376175	0.000366	-0.000225
O	-1.923377	1.904131	1.872585
O	1.854536	1.955912	1.927218
O	-1.812629	-3.958327	-0.000263

Table S82. Cartesian coordinates (\AA) of $[NbW_9O_{32}]^{5-}$ (isomer: {MW₉}-1) (^lA) (Fig S41).

W	2.306704	2.321760	3.881459
W	2.329791	2.322346	0.063033
W	4.682414	-0.000116	0.102679
W	2.240619	-0.000047	6.242451
Nb	4.696689	0.000013	3.961595
O	2.342068	-0.000006	0.024862
O	4.212319	-0.000073	-1.864888
O	4.656344	-0.000049	1.947880
O	4.213661	1.882038	0.056725
O	0.444178	1.880472	0.050687
O	4.106204	0.000324	5.906437
O	2.257253	-0.000090	3.926891
O	0.339854	-0.000146	5.749664
O	2.319685	2.248091	1.956237
O	4.159738	1.937812	3.905198
O	4.213537	-1.882132	0.056482
O	2.209404	-1.883555	5.792408
O	2.139147	-0.000016	7.984759
O	2.209331	1.883609	5.792175
O	6.393842	-0.000215	-0.199382
O	2.255733	4.046987	4.083254
O	2.330338	4.043095	-0.161609

O	6.431814	0.000367	4.228118
O	2.319744	-2.248190	1.956202
O	0.444070	-1.880262	0.050562
O	0.401218	1.873194	3.799781
O	2.327314	1.877608	-1.857998
O	2.354277	0.000015	-4.055630
O	2.327046	-1.877531	-1.858021
O	-1.780769	-0.000407	4.012392
O	2.330046	-4.043093	-0.161673
W	2.329677	-2.322358	0.063127
W	2.306972	-2.321743	3.881382
W	-0.049061	-0.000228	3.844750
W	2.365901	0.000004	-2.311819
W	-0.019529	0.000114	0.026581
O	2.256153	-4.046987	4.083346
O	-1.738523	0.000244	-0.209069
O	0.042981	-0.000065	1.918125
O	0.401418	-1.873390	3.799825
O	4.159655	-1.937577	3.905873
O	0.465630	0.000181	-1.865791

Table S83. Cartesian coordinates (\AA) of $[NbW_9O_{32}]^{6-}$ (isomer: {MW₉}-I) (²A) (Fig S41).

W	2.294238	2.324159	3.875096
W	2.333226	2.324621	0.060605
W	4.690805	-0.000444	0.098910
W	2.233750	-0.000329	6.249793
Nb	4.690644	-0.000072	3.952123
O	2.334922	-0.000054	0.017982
O	4.221031	0.000355	-1.880096

O	4.665902	-0.000238	1.952502
O	4.218393	1.876549	0.057628
O	0.450330	1.881117	0.035444
O	4.100628	0.000391	5.921613
O	2.238229	-0.000184	3.923133
O	0.333303	0.000294	5.774838
O	2.316859	2.258817	1.959094
O	4.153498	1.929885	3.922349
O	4.218019	-1.877012	0.057030
O	2.213691	-1.884363	5.811757
O	2.137733	-0.000190	8.000529
O	2.213779	1.884426	5.811603
O	6.407745	-0.000668	-0.197487
O	2.249941	4.054345	4.084415
O	2.337059	4.050298	-0.162533
O	6.433541	0.000174	4.231020
O	2.316687	-2.258410	1.958913
O	0.449961	-1.880441	0.034541
O	0.392821	1.878459	3.824529
O	2.345434	1.880808	-1.880897
O	2.368028	0.000154	-4.072829
O	2.345167	-1.880306	-1.881313
O	-1.791746	-0.000990	4.019166
O	2.335352	-4.050051	-0.162718
W	2.332384	-2.324390	0.060815
W	2.294589	-2.324147	3.874327
W	-0.054960	-0.000614	3.841307
W	2.367245	0.000043	-2.321688

W	-0.013250	0.000013	0.027716
O	2.250262	-4.054293	4.083953
O	-1.735062	0.000104	-0.225726
O	0.025271	-0.000087	1.921830
O	0.393138	-1.878804	3.825121
O	4.153482	-1.929659	3.923044
O	0.472819	0.000733	-1.898377

Table S84. Cartesian coordinates (\AA) of $[\text{NbW}_9\text{O}_{32}]^{7-}$ (isomer: {MW₉}-I) (¹A) (Fig S4I).

W	2.286252	2.326169	3.872150
W	2.330646	2.324088	0.060690
W	4.692543	-0.000704	0.091568
W	2.232584	-0.000474	6.260983
Nb	4.690360	0.000043	3.944233
O	2.334939	-0.000020	0.010030
O	4.228241	-0.000018	-1.903685
O	4.676711	-0.000322	1.955084
O	4.218640	1.872240	0.056948
O	0.451140	1.878746	0.024789
O	4.105182	0.001539	5.936537
O	2.228056	-0.000164	3.931215
O	0.336488	-0.000017	5.807341
O	2.311153	2.269057	1.962689
O	4.152624	1.925572	3.926920
O	4.217915	-1.873084	0.056649
O	2.227090	-1.886388	5.833907
O	2.149488	-0.000502	8.020871
O	2.225764	1.886319	5.833392

O	6.415570	-0.001243	-0.204358
O	2.245440	4.060859	4.090308
O	2.335052	4.053926	-0.169390
O	6.441100	0.000360	4.235053
O	2.310985	-2.268620	1.962490
O	0.450261	-1.877726	0.023921
O	0.389258	1.881258	3.843646
O	2.357782	1.882334	-1.907033
O	2.373463	0.000278	-4.094693
O	2.356769	-1.881633	-1.907476
O	-1.797930	-0.001334	4.037948
O	2.332362	-4.053607	-0.169486
W	2.329285	-2.323799	0.060953
W	2.287122	-2.326292	3.871343
W	-0.057861	-0.000861	3.838237
W	2.364737	0.000137	-2.335891
W	-0.019689	0.000210	0.028201
O	2.246574	-4.060983	4.089641
O	-1.744223	0.000449	-0.235487
O	0.005413	-0.000167	1.926424
O	0.390217	-1.881758	3.844378
O	4.152969	-1.925054	3.927502
O	0.474418	0.001187	-1.929483

Table S85 Cartesian coordinates (Å) of $[Nb_2W_8O_{32}]^6^-$ (isomer: $\{M_2W_8\}\text{-}I$) (lA) (Fig S42).

W	0.005959	1.912101	-2.312392
W	-0.005071	-1.912210	-2.312329
W	2.363245	-1.859943	-0.000068

W	-0.065605	4.287289	0.000006
Nb	2.403393	1.997856	0.000240
O	0.057929	-1.960579	-0.000372
O	1.930490	-3.825879	-0.000584
O	2.354462	-0.004142	0.000054
O	1.905042	-1.884641	-1.879867
O	-1.864061	-1.935550	-1.938762
O	1.818052	3.929794	0.000148
O	-0.057756	1.960949	0.000265
O	-1.930683	3.825790	0.000298
O	0.000475	-0.000025	-2.240298
O	1.864062	1.936423	-1.938331
O	1.905255	-1.884236	1.879434
O	-0.057152	3.836688	1.885719
O	-0.126725	6.037209	-0.000276
O	-0.058023	3.836501	-1.885687
O	4.085487	-2.156625	0.000384
O	-0.043675	2.119473	-4.042056
O	0.043709	-2.120043	-4.042020
O	4.145225	2.259587	0.001419
O	0.000056	0.000083	2.240440
O	-1.863357	-1.935680	1.937966
O	-1.904456	1.883476	-1.879225
O	0.056479	-3.836655	-1.885643
O	0.126259	-6.037395	-0.000054
O	0.057993	-3.836503	1.885560
O	-4.085385	2.157173	-0.001001
O	0.044787	-2.119301	4.041776

W	-0.004935	-1.912175	2.312055
W	0.005180	1.911852	2.312811
W	-2.363216	1.859736	-0.000022
W	0.065273	-4.287504	-0.000242
Nb	-2.403747	-1.998047	-0.000227
O	-0.044219	2.120075	4.042418
O	-4.145497	-2.259996	-0.000098
O	-2.355972	0.004014	-0.000086
O	-1.904925	1.884163	1.879568
O	1.863515	1.936197	1.938511
O	-1.817864	-3.929300	0.000571

Table S86. Cartesian coordinates (\AA) of $[Nb_2W_8O_{32}]^{7-}$ (isomer: $\{M_2W_8\}\text{-}1$) (^2A) (Fig S42).

W	-0.013152	1.908526	-2.312530
W	0.013777	-1.909795	-2.312633
W	2.380327	-1.874114	-0.000164
W	-0.068492	4.297388	-0.000415
Nb	2.390828	1.978792	-0.000045
O	0.072728	-1.967328	-0.000490
O	1.947616	-3.849014	0.000351
O	2.370505	-0.004787	-0.000129
O	1.922585	-1.893599	-1.879072
O	-1.851638	-1.954589	-1.932447
O	1.805621	3.955359	-0.000375
O	-0.072324	1.967597	0.000483
O	-1.947889	3.848878	-0.000175
O	0.000273	-0.000461	-2.242034
O	1.851250	1.955254	-1.932355

O	1.922746	-1.892900	1.878838
O	-0.072864	3.858000	1.886548
O	-0.136581	6.055140	-0.001313
O	-0.073858	3.856980	-1.887319
O	4.109724	-2.158290	-0.000188
O	-0.060287	2.117086	-4.047071
O	0.060118	-2.118293	-4.047100
O	4.137738	2.270021	0.000938
O	0.000289	0.000421	2.242327
O	-1.850720	-1.954764	1.931220
O	-1.922223	1.891634	-1.877640
O	0.072828	-3.857561	-1.886403
O	0.135858	-6.055363	0.000838
O	0.073077	-3.857153	1.887021
O	-4.109860	2.159819	0.001350
O	0.060160	-2.117272	4.046965
W	0.013858	-1.908783	2.312378
W	-0.013106	1.909123	2.312941
W	-2.380740	1.874285	0.000963
W	0.068248	-4.297595	0.000175
Nb	-2.391066	-1.978848	-0.000732
O	-0.058966	2.118269	4.047322
O	-4.137771	-2.271316	-0.002248
O	-2.372714	0.004846	0.001056
O	-1.921931	1.893412	1.879346
O	1.851379	1.955806	1.931575
O	-1.805351	-3.954811	0.000244

Table S87. Cartesian coordinates (\AA) of $[Nb_2W_8O_{32}]^{8-}$ (isomer: $\{M_2W_8\}\text{-}1$) (^1A) (Fig S42).

W	-0.018743	1.906148	-2.311837
W	0.018752	-1.906793	-2.311764
W	2.385877	-1.885600	0.000140
W	-0.063320	4.312580	-0.000223
Nb	2.393127	1.967177	0.000143
O	0.081297	-1.975627	-0.000138
O	1.948501	-3.886268	-0.001093
O	2.394883	-0.009638	0.000150
O	1.926121	-1.903779	-1.876880
O	-1.851904	-1.957916	-1.923529
O	1.811051	3.974393	0.000724
O	-0.080974	1.975772	0.000177
O	-1.948310	3.886387	0.000290
O	-0.000052	-0.000195	-2.252795
O	1.851502	1.957879	-1.923784
O	1.927082	-1.905103	1.876984
O	-0.067918	3.882435	1.887020
O	-0.124565	6.078538	-0.000764
O	-0.066808	3.881537	-1.886119
O	4.119355	-2.184773	0.000110
O	-0.062035	2.124971	-4.050859
O	0.062015	-2.125721	-4.050630
O	4.146826	2.272213	0.001248
O	0.000525	0.000094	2.252261
O	-1.850452	-1.958083	1.923055
O	-1.926122	1.904089	-1.876628
O	0.066909	-3.882297	-1.886902

O	0.124253	-6.078437	0.000965
O	0.067609	-3.881622	1.886460
O	-4.119334	2.186699	-0.000164
O	0.063071	-2.124207	4.050744
W	0.020145	-1.905844	2.311672
W	-0.018988	1.905853	2.311844
W	-2.386230	1.885738	-0.000042
W	0.063274	-4.312518	0.000412
Nb	-2.393491	-1.967429	-0.000189
O	-0.062595	2.124800	4.050697
O	-4.146925	-2.273993	-0.000903
O	-2.398478	0.009647	-0.000002
O	-1.926107	1.903737	1.876529
O	1.851476	1.958622	1.923406
O	-1.810301	-3.973466	0.000217

Table S88. Cartesian coordinates (\AA) of the $\{\text{NbW}_9\}\text{-}2$ isomer (Fig S41).

W	2.328181	-2.327170	0.043524
W	2.329191	-2.331448	-3.783885
W	-0.006188	-0.000147	-3.784148
Nb	2.328802	0.000016	2.438575
W	-0.001187	0.000290	0.044365
O	2.329190	-0.000109	-3.836133
O	0.452311	-0.000066	-5.712991
O	0.081971	0.000079	-1.911106
O	0.443604	-1.884278	-3.802558
O	4.214831	-1.885025	-3.802422
O	0.382601	0.000283	1.910479
O	2.328285	0.000051	0.029643

O	4.274361	-0.000194	1.910007
O	2.328697	-2.241767	-1.911133
O	0.444082	-1.883011	-0.034972
O	0.443524	1.884110	-3.802480
O	2.328188	1.945406	1.910232
O	2.328512	-0.000122	4.204467
O	2.328152	-1.945299	1.910039
O	-1.727068	-0.000268	-4.020129
O	2.327993	-4.060837	0.161785
O	2.329252	-4.052787	-4.017506
O	-1.734704	0.000582	0.163465
O	2.328801	2.241680	-1.911029
O	4.214714	1.884905	-3.802364
O	4.211681	-1.882994	-0.034939
O	2.328993	-1.876285	-5.713108
O	2.328277	0.000043	-7.906802
O	2.328877	1.876204	-5.713133
O	6.392262	-0.000492	0.164158
O	2.328707	4.052700	-4.017671
W	2.328988	2.331437	-3.783992
W	2.328602	2.327488	0.043537
W	4.658885	-0.000211	0.043746
W	2.328728	-0.000055	-6.161693
W	4.662720	-0.000068	-3.784557
O	2.328853	4.061084	0.161570
O	6.383933	0.000044	-4.019125
O	4.575107	-0.000127	-1.911307
O	4.212405	1.882953	-0.034719

O	0.444451	1.883387	-0.034955
O	4.205316	0.000014	-5.713412

Table S89. Cartesian coordinates (\AA) of the $\{\text{TaW}_9\}\text{-}2$ isomer (Fig S41).

W	2.328149	-2.330049	0.038819
W	2.329296	-2.332027	-3.784854
W	-0.006743	-0.000237	-3.784918
Ta	2.328538	0.000009	2.420008
W	-0.004120	0.000411	0.040066
O	2.329128	-0.000070	-3.835176
O	0.451630	-0.000236	-5.710951
O	0.082396	0.000090	-1.908936
O	0.444185	-1.883903	-3.798704
O	4.214423	-1.884386	-3.798580
O	0.385826	0.000371	1.908325
O	2.328367	0.000044	0.030490
O	4.270707	-0.000341	1.907554
O	2.328731	-2.241701	-1.909258
O	0.444447	-1.882504	-0.037454
O	0.443878	1.883547	-3.798693
O	2.328331	1.942070	1.907530
O	2.328629	0.000001	4.207386
O	2.328143	-1.942030	1.907359
O	-1.727492	-0.000510	-4.016629
O	2.327948	-4.062684	0.162555
O	2.329528	-4.053159	-4.014497
O	-1.736426	0.000912	0.165880
O	2.328760	2.241528	-1.909133

O	4.214053	1.884534	-3.798456
O	4.211255	-1.882567	-0.037783
O	2.329164	-1.876820	-5.711042
O	2.328383	-0.000073	-7.903697
O	2.328682	1.876832	-5.711160
O	6.393902	-0.000944	0.166895
O	2.328437	4.053048	-4.014599
W	2.328818	2.331962	-3.784899
W	2.328693	2.330307	0.038773
W	4.661724	-0.000333	0.039323
W	2.328768	-0.000038	-6.159551
W	4.663354	0.000097	-3.785319
O	2.329093	4.062853	0.162284
O	6.384302	0.000364	-4.016080
O	4.575132	-0.000109	-1.909318
O	4.212058	1.882536	-0.037513
O	0.444869	1.883022	-0.037403
O	4.205935	0.000181	-5.711323

Table S90. Cartesian coordinates (\AA) of the $\{Nb_2W_8\}\text{-}2$ isomer (Fig S42).

W	2.327896	-2.338557	0.024547
W	2.328693	-2.318326	-3.802833
W	0.008883	0.035308	-3.782954
Nb	2.330231	-0.008656	2.437867
W	0.007669	-0.004973	0.047151
O	2.328793	-0.012489	-3.860514
O	0.449734	-0.025269	-5.723594
O	0.094463	0.014921	-1.900416

O	0.449368	-1.878707	-3.785946
O	4.207373	-1.878866	-3.785443
O	0.377352	-0.034825	1.920388
O	2.328390	-0.009052	0.037126
O	4.280371	-0.035171	1.918515
O	2.328302	-2.244537	-1.905952
O	0.440331	-1.894081	-0.038838
O	0.384787	1.894520	-3.822940
O	2.328266	1.906192	1.936557
O	2.330043	-0.036150	4.212738
O	2.329231	-1.964595	1.897831
O	-1.719721	-0.016875	-4.012744
O	2.327364	-4.077216	0.151794
O	2.328934	-4.051731	-4.016475
O	-1.730968	-0.006905	0.165504
O	2.328792	2.316590	-1.849681
O	4.273948	1.894216	-3.822844
O	4.215802	-1.894442	-0.039787
O	2.328130	-1.898280	-5.719664
O	2.327591	-0.059801	-7.922089
O	2.329846	1.873346	-5.805669
O	6.387906	-0.008252	0.163991
O	2.328583	4.163299	-4.073780
Nb	2.329124	2.416581	-3.828558
W	2.328707	2.343144	0.026909
W	4.649404	-0.005801	0.043296
W	2.327390	0.011823	-6.170303
W	4.648471	0.034841	-3.785830

O	2.328616	4.071125	0.265045
O	6.377474	-0.020802	-4.013183
O	4.562870	0.014483	-1.901817
O	4.218719	1.880314	0.011547
O	0.438416	1.880274	0.012437
O	4.207303	-0.026620	-5.724070

Table S91. Cartesian coordinates (\AA) of the $\{Nb_2W_8\}\text{-}3$ isomer (Fig S42).

W	2.328424	-2.326998	0.015522
W	2.329067	-2.327317	-3.816733
W	-0.000734	-0.000159	-3.816588
Nb	2.328573	-0.000127	2.419394
W	-0.000496	0.000094	0.016585
O	2.328860	0.000005	-3.827551
O	0.384880	0.000089	-5.702556
O	0.095903	-0.000021	-1.900238
O	0.438665	-1.889873	-3.774957
O	4.219695	-1.889879	-3.775466
O	0.384794	0.000100	1.902190
O	2.328464	-0.000080	0.026313
O	4.271905	-0.000338	1.901643
O	2.328738	-2.229439	-1.900606
O	0.437504	-1.890101	-0.026072
O	0.438387	1.889857	-3.774819
O	2.328538	1.943105	1.901860
O	2.328888	-0.000150	4.195451
O	2.328348	-1.943049	1.901615
O	-1.739055	-0.000365	-3.963832

O	2.328462	-4.065636	0.160973
O	2.329510	-4.065868	-3.962692
O	-1.739133	0.000210	0.162149
O	2.328631	2.229762	-1.900446
O	4.219603	1.890205	-3.775281
O	4.218992	-1.890348	-0.025982
O	2.328783	-1.943141	-5.702858
O	2.327708	-0.000219	-7.996427
O	2.328747	1.943157	-5.702933
O	6.396123	-0.000802	0.163063
O	2.328569	4.065832	-3.962035
W	2.328635	2.327305	-3.816653
W	2.328621	2.327521	0.015683
W	4.657802	-0.000380	0.015589
Nb	2.328247	-0.000137	-6.220357
W	4.658018	0.000136	-3.817527
O	2.328637	4.066076	0.160899
O	6.396541	0.000617	-3.963279
O	4.561830	-0.000109	-1.900793
O	4.219163	1.889847	-0.025907
O	0.437873	1.890249	-0.025666
O	4.272173	0.000369	-5.703356

Table S92. Cartesian coordinates (\AA) of the $\{\text{Nb}_2\text{W}_8\}\text{-}4$ isomer (Fig S42).

W	2.327992	-2.321099	0.055576
W	2.329013	-2.339208	-3.785694
W	0.009226	0.004441	-3.779620
Nb	2.329543	0.004726	2.448195

W	0.011092	0.023741	0.060773
O	2.328932	0.011425	-3.847606
O	0.451743	-0.013584	-5.725354
O	0.098604	0.014778	-1.919628
O	0.441852	-1.886339	-3.811255
O	4.216236	-1.885563	-3.811225
O	0.371711	-0.049644	1.929490
O	2.328410	-0.025215	0.061656
O	4.285611	-0.048959	1.928233
O	2.328645	-2.246154	-1.931926
O	0.453981	-1.885980	-0.062900
O	0.442767	1.894419	-3.839043
O	2.328187	1.922735	2.024061
O	2.330281	-0.073820	4.222664
O	2.329231	-1.983833	1.914669
O	-1.716294	0.001598	-4.017743
O	2.328023	-4.067420	0.136865
O	2.329363	-4.064647	-4.024985
O	-1.730726	-0.036266	0.154021
O	2.328359	2.333756	-1.953631
O	4.214746	1.894447	-3.839479
O	4.202553	-1.885858	-0.063120
O	2.329185	-1.880237	-5.715743
O	2.327928	-0.018423	-7.926910
O	2.328859	1.865013	-5.754812
O	6.387131	-0.036579	0.154554
O	2.328421	4.069273	-4.105535
W	2.328593	2.354861	-3.784009

Nb	2.327988	2.400213	0.103495
W	4.645676	0.023216	0.057901
W	2.327514	0.005179	-6.175564
W	4.648465	0.004917	-3.782633
O	2.327510	4.158992	0.254017
O	6.374225	0.001507	-4.020448
O	4.560900	0.014957	-1.921110
O	4.274533	1.879059	-0.001927
O	0.381708	1.878677	-0.000508
O	4.205164	-0.013104	-5.726442

Table S93. Cartesian coordinates (\AA) of the $\{Nb_2W_8\}\text{-}5$ isomer (Fig S42).

W	2.334698	-2.311862	0.025892
W	2.289705	-2.334416	-3.796987
Nb	-0.087262	-0.004855	-3.867824
W	2.336707	0.010510	2.387084
W	0.000104	0.036615	-0.007612
O	2.341385	0.003555	-3.867773
O	0.453514	-0.041868	-5.827481
O	-0.010742	0.016015	-1.858274
O	0.433646	-1.946936	-3.807380
O	4.199979	-1.881831	-3.760797
O	0.483991	-0.030450	1.972247
O	2.323315	-0.012913	0.066945
O	4.230292	-0.029238	1.910242
O	2.311022	-2.250862	-1.896674
O	0.458735	-1.875543	0.018354
O	0.434098	1.934635	-3.866785

O	2.370603	1.875242	2.025315
O	2.376414	-0.065864	4.136747
O	2.370058	-1.905299	1.929827
O	-1.833986	-0.005256	-4.097854
O	2.338276	-4.046046	0.218993
O	2.338599	-4.064341	-4.004842
O	-1.712818	-0.016555	0.327168
O	2.312661	2.340196	-1.943994
O	4.203621	1.869454	-3.818957
O	4.210943	-1.871836	-0.040222
O	2.357835	-1.901965	-5.711389
O	2.396191	-0.048669	-7.938001
O	2.358676	1.843241	-5.771907
O	6.394085	-0.010482	0.205478
O	2.343711	4.042664	-4.127609
W	2.292233	2.329508	-3.796295
Nb	2.333519	2.415674	0.063991
W	4.664549	0.037937	-0.002838
W	2.319727	-0.010011	-6.188328
W	4.640754	-0.006309	-3.825894
O	2.334225	4.161760	0.297006
O	6.374911	-0.009230	-4.018994
O	4.580847	0.017442	-1.903737
O	4.276171	1.894112	0.005495
O	0.393459	1.894540	0.065634
O	4.234429	-0.040467	-5.730650

Table S94. Cartesian coordinates (\AA) of the $\{\text{Nb}_2\text{W}_8\}\text{-}6$ isomer (Fig S42).

W	2.300892	-2.310802	0.043762
W	2.328733	-2.332497	-3.786505
W	-0.013460	-0.000179	-3.811694
W	2.314896	0.014260	2.394479
Nb	-0.070906	0.039132	0.054686
O	2.322042	0.006112	-3.851193
O	0.479005	-0.030351	-5.771881
O	-0.008454	0.020278	-1.968425
O	0.442254	-1.886985	-3.833692
O	4.216346	-1.887012	-3.785750
O	0.460051	-0.042270	2.035208
O	2.343917	-0.014913	0.096870
O	4.243721	-0.040379	1.935164
O	2.313168	-2.244194	-1.916326
O	0.452704	-1.932044	-0.011791
O	0.441993	1.885128	-3.887450
O	2.369856	1.869547	2.034680
O	2.398855	-0.069253	4.143384
O	2.371097	-1.914740	1.935743
O	-1.726450	-0.004434	-4.130287
O	2.355631	-4.049688	0.205521
O	2.331473	-4.058781	-4.008911
O	-1.819685	-0.009412	0.289661
O	2.307763	2.335806	-1.968393
O	4.215512	1.885638	-3.834095
O	4.198655	-1.868436	-0.065339
O	2.357008	-1.898216	-5.713374
O	2.376950	-0.049607	-7.939204

O	2.358980	1.848458	-5.772294
O	6.379232	-0.025299	0.206403
O	2.331605	4.052204	-4.131069
W	2.327389	2.339307	-3.811917
Nb	2.289297	2.399559	0.054866
W	4.640526	0.028463	0.042882
W	2.342257	-0.014638	-6.189602
W	4.662933	0.000368	-3.787669
O	2.337157	4.148501	0.288946
O	6.389131	-0.001651	-4.010392
O	4.575843	0.016133	-1.916961
O	4.259939	1.877027	-0.012606
O	0.378735	1.949416	0.045793
O	4.226286	-0.029557	-5.713910

Table S95. Cartesian coordinates (\AA) of the $\{\text{Nb}_2\text{W}_8\}\text{-}7$ isomer (Fig S42).

Nb	2.328433	-2.395548	0.065329
W	2.328635	-2.363012	-3.802897
W	0.017046	-0.000259	-3.795259
W	2.329466	-0.000146	2.393379
W	0.016172	0.000004	0.034687
O	2.328491	-0.000112	-3.847133
O	0.450791	-0.000311	-5.732961
O	0.086893	-0.000122	-1.917166
O	0.445234	-1.889851	-3.833944
O	4.212527	-1.889449	-3.834376
O	0.435347	-0.000137	1.950700
O	2.328542	-0.000009	0.093183
O	4.223232	-0.000267	1.949455

O	2.328601	-2.343045	-1.965363
O	0.396216	-1.875289	-0.014374
O	0.445062	1.889433	-3.833841
O	2.328841	1.884743	2.015768
O	2.330832	-0.000224	4.146040
O	2.328964	-1.885106	2.015994
O	-1.707533	-0.000446	-4.027969
O	2.328940	-4.150384	0.281511
O	2.328732	-4.078134	-4.111005
O	-1.718745	0.000095	0.219109
O	2.328329	2.345136	-1.965400
O	4.211809	1.889391	-3.834243
O	4.260959	-1.875406	-0.015705
O	2.328537	-1.868549	-5.750140
O	2.326951	-0.000248	-7.939776
O	2.328213	1.868176	-5.750247
O	6.376139	-0.000007	0.218978
O	2.327736	4.078005	-4.112361
W	2.328132	2.363181	-3.803065
Nb	2.328305	2.396054	0.065303
W	4.641408	0.000079	0.033279
W	2.327463	-0.000178	-6.189821
W	4.640203	0.000053	-3.797486
O	2.328664	4.150721	0.283403
O	6.364861	0.000298	-4.031295
O	4.571839	0.000043	-1.918571
O	4.260883	1.875629	-0.015841
O	0.396516	1.875268	-0.014531

O	4.205214	-0.000073	-5.734027
---	----------	-----------	-----------

Table S96. Cartesian coordinates (\AA) of the $\{\text{Nb}_2\text{W}_8\}\text{-}8$ isomer (Fig S42).

W	2.297521	-2.309658	0.010232
W	2.299339	-2.308817	-3.811149
Nb	-0.114328	-0.000150	-3.831048
W	2.327201	-0.000023	2.383497
Nb	-0.113958	0.000292	0.029022
O	2.344444	0.000011	-3.865751
O	0.490030	-0.000035	-5.844698
O	-0.135203	0.000068	-1.901447
O	0.444141	-1.942287	-3.855240
O	4.213500	-1.873503	-3.764947
O	0.488195	0.000257	2.042759
O	2.341579	0.000293	0.063862
O	4.250200	0.000050	1.907059
O	2.298656	-2.236917	-1.900407
O	0.442118	-1.943248	0.052892
O	0.444071	1.942003	-3.855103
O	2.388853	1.883702	1.935171
O	2.433584	-0.000083	4.131796
O	2.388856	-1.883499	1.935119
O	-1.840230	-0.000199	-4.196076
O	2.358787	-4.038804	0.219737
O	2.359968	-4.038004	-4.020213
O	-1.840209	0.000315	0.395863
O	2.298702	2.236650	-1.900372
O	4.213506	1.873453	-3.764909

O	4.211209	-1.873332	-0.034569
O	2.391629	-1.883064	-5.736291
O	2.437835	-0.000191	-7.933197
O	2.391594	1.882834	-5.736246
O	6.400366	-0.000176	0.209768
O	2.359733	4.037841	-4.020057
W	2.299083	2.308585	-3.811340
W	2.297960	2.309453	0.009962
W	4.667186	0.000012	0.009769
W	2.329164	-0.000162	-6.184898
W	4.669067	0.000063	-3.812391
O	2.359629	4.038647	0.219443
O	6.402925	0.000338	-4.007905
O	4.598942	-0.000114	-1.900426
O	4.211648	1.873603	-0.034493
O	0.441930	1.943847	0.052924
O	4.253658	-0.000054	-5.708382

Table S97. Cartesian coordinates (\AA) of the $\{\text{Ta}_2\text{W}_8\}\text{-}2$ isomer (Fig S42).

W	2.328301	-2.339711	0.022758
W	2.328943	-2.321831	-3.800478
W	0.001608	0.032368	-3.786725
Ta	2.329587	-0.010023	2.416153
W	0.001738	-0.002945	0.041563
O	2.328920	0.000005	-3.856290
O	0.449304	-0.028363	-5.721719
O	0.087775	0.013976	-1.900685
O	0.451638	-1.875985	-3.782195

O	4.205589	-1.875414	-3.781947
O	0.379876	-0.031946	1.917953
O	2.328555	-0.008530	0.041838
O	4.277280	-0.032541	1.916439
O	2.328625	-2.238227	-1.904503
O	0.441247	-1.891359	-0.039504
O	0.383206	1.892067	-3.819863
O	2.328240	1.911911	1.931523
O	2.330070	-0.028753	4.211913
O	2.329018	-1.964059	1.897809
O	-1.725385	-0.021915	-4.015445
O	2.327808	-4.077243	0.148907
O	2.329162	-4.053606	-4.008248
O	-1.734762	-0.005849	0.167153
O	2.328650	2.303247	-1.850348
O	4.274656	1.891886	-3.819759
O	4.215327	-1.891922	-0.040124
O	2.328160	-1.895125	-5.712340
O	2.328078	-0.056810	-7.919744
O	2.328901	1.872242	-5.799010
O	6.391747	-0.007223	0.166318
O	2.327873	4.164249	-4.060705
Ta	2.328572	2.394512	-3.822397
W	2.329079	2.346358	0.026020
W	4.655390	-0.003510	0.038599
W	2.328094	0.011537	-6.169518
W	4.655561	0.032669	-3.788505
O	2.328818	4.074486	0.255006

O	6.382931	-0.023680	-4.015083
O	4.568919	0.013959	-1.901688
O	4.219362	1.880130	0.008289
O	0.438035	1.879768	0.008428
O	4.208384	-0.028806	-5.722525

Table S98. Cartesian coordinates (\AA) of the $\{\text{Ta}_2\text{W}_8\}\text{-}3$ isomer (Fig S42).

W	2.328519	-2.330601	0.012950
W	2.328967	-2.330860	-3.814072
W	-0.004640	-0.000059	-3.813996
Ta	2.328703	-0.000072	2.398473
W	-0.004176	0.000000	0.014005
O	2.328867	-0.000001	-3.836947
O	0.383886	0.000249	-5.700363
O	0.102969	-0.000021	-1.900166
O	0.439031	-1.889225	-3.772902
O	4.219065	-1.889262	-3.773516
O	0.383946	0.000025	1.900009
O	2.328486	-0.000180	0.035770
O	4.273044	-0.000246	1.899749
O	2.328737	-2.221518	-1.900505
O	0.438077	-1.889554	-0.028192
O	0.438850	1.889294	-3.772593
O	2.328574	1.944256	1.899841
O	2.329030	-0.000027	4.195204
O	2.328379	-1.944160	1.899532
O	-1.741639	-0.000165	-3.956588
O	2.328636	-4.067915	0.153300

O	2.329285	-4.067998	-3.954910
O	-1.741511	0.000054	0.154764
O	2.328641	2.221847	-1.900381
O	4.219126	1.889507	-3.773261
O	4.218858	-1.890214	-0.028123
O	2.328578	-1.944189	-5.700498
O	2.327656	-0.000289	-7.995999
O	2.328716	1.944246	-5.700687
O	6.398892	-0.000751	0.155482
O	2.328647	4.068141	-3.954280
W	2.328682	2.330920	-3.814004
W	2.328586	2.331222	0.013082
W	4.661714	-0.000432	0.012780
Ta	2.328177	-0.000110	-6.199222
W	4.661662	0.000039	-3.815066
O	2.328511	4.068503	0.153191
O	6.398828	0.000540	-3.956269
O	4.554430	-0.000185	-1.901017
O	4.218733	1.889502	-0.028107
O	0.438303	1.889439	-0.027908
O	4.273055	0.000245	-5.701239

Table S99. Cartesian coordinates (\AA) of the $\{\text{Ta}_2\text{W}_8\}\text{-}4$ isomer (Fig S42).

W	2.328072	-2.323552	0.045259
W	2.329240	-2.336346	-3.787795
W	0.005368	0.002407	-3.779816
Ta	2.329172	0.003644	2.428008
W	-0.000673	0.024162	0.058299

O	2.328952	0.008286	-3.842563
O	0.452693	-0.013829	-5.722011
O	0.090971	0.013172	-1.916963
O	0.441620	-1.886863	-3.808735
O	4.216931	-1.886186	-3.808179
O	0.373318	-0.050682	1.926546
O	2.328065	-0.011187	0.062492
O	4.283118	-0.050164	1.925996
O	2.328673	-2.237987	-1.929331
O	0.454915	-1.879866	-0.064129
O	0.442876	1.890975	-3.835541
O	2.327513	1.923645	2.014409
O	2.329570	-0.064316	4.223417
O	2.328264	-1.974561	1.907026
O	-1.719140	0.001862	-4.018647
O	2.328550	-4.066379	0.133754
O	2.330011	-4.061749	-4.020061
O	-1.739887	-0.031995	0.160951
O	2.328258	2.309323	-1.946781
O	4.214475	1.891016	-3.835442
O	4.200811	-1.879354	-0.063931
O	2.329678	-1.881734	-5.714591
O	2.328781	-0.019959	-7.921884
O	2.328971	1.865676	-5.746702
O	6.396421	-0.032823	0.162261
O	2.328600	4.065914	-4.085897
W	2.328467	2.349837	-3.782654
Ta	2.328323	2.384222	0.087671

W	4.657547	0.024180	0.055977
W	2.327955	0.004526	-6.172027
W	4.652199	0.003007	-3.781748
O	2.328055	4.164425	0.242414
O	6.377058	0.001671	-4.019230
O	4.567826	0.013683	-1.917485
O	4.275821	1.878702	-0.006051
O	0.380424	1.878270	-0.006630
O	4.205021	-0.013074	-5.722336

Table S100. Cartesian coordinates (\AA) of the $\{\text{Ta}_2\text{W}_8\}\text{-}5$ isomer (Fig S42).

W	2.332775	-2.316279	0.017209
W	2.293003	-2.338364	-3.804427
Ta	-0.064146	-0.003383	-3.854826
W	2.332573	0.008240	2.386499
W	-0.008066	0.034771	-0.003230
O	2.326631	0.002512	-3.862386
O	0.457489	-0.035422	-5.819006
O	-0.003103	0.015813	-1.859579
O	0.436283	-1.947970	-3.809548
O	4.198658	-1.877960	-3.760768
O	0.478155	-0.034531	1.964952
O	2.324583	0.001834	0.061246
O	4.228713	-0.032005	1.912722
O	2.312056	-2.252034	-1.900394
O	0.459664	-1.872811	0.012860
O	0.435710	1.939188	-3.863147
O	2.364105	1.871399	2.017975

O	2.367559	-0.065374	4.134670
O	2.364870	-1.901053	1.920381
O	-1.833549	-0.006462	-4.089629
O	2.337226	-4.047974	0.214210
O	2.345827	-4.067231	-4.009251
O	-1.721237	-0.022827	0.318466
O	2.312388	2.330293	-1.941952
O	4.201000	1.869154	-3.814152
O	4.207286	-1.869961	-0.040751
O	2.361131	-1.899871	-5.714325
O	2.395003	-0.039514	-7.936045
O	2.361836	1.849813	-5.764940
O	6.397492	-0.017350	0.208636
O	2.349331	4.050902	-4.117092
W	2.293508	2.337214	-3.799510
Ta	2.331443	2.392473	0.052577
W	4.668744	0.034741	0.004179
W	2.321556	-0.005400	-6.187690
W	4.645524	-0.004134	-3.817534
O	2.336628	4.161370	0.286913
O	6.377234	-0.007869	-4.014093
O	4.581948	0.016530	-1.900514
O	4.276787	1.891537	0.007248
O	0.388441	1.892553	0.062800
O	4.229824	-0.034562	-5.721432

Table S101. Cartesian coordinates (\AA) of the $\{\text{Ta}_2\text{W}_8\}\text{-}6$ isomer (Fig S42).

W	2.300713	-2.318476	0.042380
W	2.330544	-2.334001	-3.786287

W	-0.012565	-0.001594	-3.811354
W	2.311063	0.017575	2.392557
Ta	-0.059491	0.038021	0.045749
O	2.325669	0.003184	-3.845614
O	0.479188	-0.029619	-5.764014
O	-0.000068	0.018553	-1.962233
O	0.444562	-1.886873	-3.828581
O	4.217342	-1.887803	-3.782788
O	0.457054	-0.041531	2.022491
O	2.331000	-0.002353	0.086619
O	4.235325	-0.039982	1.929709
O	2.314297	-2.249000	-1.913490
O	0.453512	-1.929551	-0.014125
O	0.444918	1.882541	-3.879801
O	2.370017	1.871844	2.023004
O	2.387151	-0.058990	4.140543
O	2.368756	-1.907027	1.929923
O	-1.725294	-0.004439	-4.123620
O	2.352044	-4.054209	0.210235
O	2.331787	-4.059448	-4.009513
O	-1.830377	-0.012794	0.280000
O	2.310193	2.328321	-1.962078
O	4.215670	1.883666	-3.829232
O	4.192137	-1.863582	-0.063149
O	2.356686	-1.897843	-5.711708
O	2.375016	-0.047205	-7.934411
O	2.358238	1.848789	-5.764414
O	6.383722	-0.024295	0.211768

O	2.331177	4.051228	-4.124620
W	2.329267	2.338364	-3.811153
Ta	2.291590	2.388156	0.046353
W	4.648186	0.027007	0.042044
W	2.343607	-0.015602	-6.185890
W	4.664736	-0.001021	-3.787215
O	2.343445	4.159165	0.281124
O	6.389927	-0.001447	-4.011604
O	4.581105	0.014400	-1.914166
O	4.258357	1.874007	-0.013710
O	0.376422	1.952652	0.039848
O	4.226253	-0.028793	-5.712257

Table S102. Cartesian coordinates (\AA) of the $\{\text{Ta}_2\text{W}_8\}\text{-}7$ isomer (Fig S42).

Ta	2.328015	-2.375183	0.048985
W	2.328582	-2.357521	-3.805251
W	0.011469	-0.000140	-3.792605
W	2.328784	-0.000114	2.393408
W	-0.001946	0.000103	0.039936
O	2.328614	0.000011	-3.843956
O	0.452958	-0.000062	-5.730160
O	0.071715	-0.000018	-1.914189
O	0.445083	-1.888327	-3.831351
O	4.212527	-1.887714	-3.831053
O	0.433195	-0.000085	1.949234
O	2.328417	0.000209	0.082667
O	4.224370	-0.000384	1.948172
O	2.328399	-2.322630	-1.961055
O	0.392167	-1.870309	-0.014486

O	0.444896	1.888128	-3.831315
O	2.328807	1.879209	2.003954
O	2.330898	-0.000337	4.144777
O	2.328637	-1.879497	2.003723
O	-1.711329	-0.000387	-4.034047
O	2.327703	-4.150883	0.269768
O	2.328413	-4.073524	-4.100322
O	-1.734928	0.000209	0.228317
O	2.328476	2.321725	-1.960780
O	4.212373	1.887862	-3.831174
O	4.264299	-1.870318	-0.016259
O	2.328772	-1.870425	-5.746174
O	2.327756	0.000322	-7.935450
O	2.328666	1.870640	-5.745933
O	6.392145	0.000348	0.229105
O	2.327896	4.073503	-4.099420
W	2.328378	2.357383	-3.804806
Ta	2.328442	2.375099	0.049042
W	4.659386	0.000468	0.038913
W	2.328026	0.000189	-6.186412
W	4.646594	0.000189	-3.794295
O	2.328122	4.150877	0.269568
O	6.369328	0.000285	-4.036808
O	4.588013	0.000292	-1.915288
O	4.264589	1.870302	-0.014534
O	0.392310	1.870404	-0.014250
O	4.203863	0.000098	-5.730873

Table S103. Cartesian coordinates (\AA) of the $\{\text{Ta}_2\text{W}_8\}\text{-}8$ isomer (Fig S42).

W	2.299797	-2.317821	0.011626
W	2.300115	-2.317166	-3.811824
Ta	-0.092476	-0.000174	-3.829490
W	2.328138	0.000090	2.383320
Ta	-0.090722	-0.000136	0.027389
O	2.331762	-0.000038	-3.863856
O	0.487709	-0.000029	-5.835267
O	-0.102190	-0.000169	-1.901265
O	0.444873	-1.943573	-3.855247
O	4.208481	-1.872367	-3.764964
O	0.487769	-0.000184	2.032904
O	2.330669	0.000065	0.062525
O	4.246546	0.000011	1.903905
O	2.300059	-2.248214	-1.900471
O	0.444997	-1.943495	0.052140
O	0.444799	1.943212	-3.855166
O	2.389179	1.883464	1.934455
O	2.425448	-0.000061	4.130919
O	2.389608	-1.883372	1.934451
O	-1.844978	-0.000237	-4.177336
O	2.360056	-4.045327	0.225630
O	2.360532	-4.044433	-4.025867
O	-1.843507	-0.000393	0.376207
O	2.299892	2.248234	-1.900161
O	4.208601	1.872319	-3.764870
O	4.207504	-1.872637	-0.035102
O	2.390666	-1.882724	-5.735641

O	2.427978	0.000045	-7.932199
O	2.390629	1.882734	-5.735409
O	6.398773	0.000570	0.201247
O	2.360346	4.044265	-4.025670
W	2.300041	2.317024	-3.811619
W	2.299485	2.318100	0.011759
W	4.666591	0.000386	0.008313
W	2.329015	0.000027	-6.184739
W	4.667647	0.000003	-3.810723
O	2.359363	4.045323	0.225696
O	6.400639	0.000172	-4.000713
O	4.588791	0.000059	-1.900392
O	4.207166	1.873062	-0.034566
O	0.444607	1.943394	0.052235
O	4.248481	-0.000015	-5.704841

References

1. L. B. Fullmer, P. I. Molina, M. R. Antonio and M. Nyman, *Dalton Trans.*, 2014, **43**, 15295-15299.
2. W. G. Klemperer, *Inorg. Synth.*, 1990, **27**, 74-85.
3. G. M. Sheldrick, Bruker AXS, Madison, WI, 1998, p. Bruker/Siemens Area Detector Absorption Correction Program.
4. SHELXTL-6.10, Bruker AXS, Madison, WI, pp. Program for Structure Solution, Refinement and Presentation.
5. D. Bayot and M. Devillers, *Coord. Chem. Rev.*, 2006, **250**, 2610-2626.
6. F. Chauveau, M. Boyer and B. Le Meur, *C. R. Acad. Sci., Paris, Ser. C*, 1969, **268**, 479-482.
7. M. Nyman, T. M. Alam, F. Bonhomme, M. A. Rodriguez, C. S. Frazer and M. E. Welk, *J. Cluster Sci.*, 2006, **17**, 197-219.
8. K. H. Tytko, J. Mehmke and S. Fischer, *Struct. Bonding* 1999, **93**, 129-321.
9. C. Rocchiccioli-Deltcheff, R. Thouvenot and M. Dabbabi, *Spectrochim. Acta, Part A*, 1977, **33A**, 143-153.
10. D. C. Duncan and C. L. Hill, *Inorg. Chem.*, 1996, **35**, 5828-5835.
11. J. P. Perdew, K. Burke and M. Ernzerhof, *Phys. Rev. Lett.*, 1997, **78**, 1396.
12. S. Grimme, J. Antony, S. Ehrlich and H. Krieg, *J. Chem. Phys.*, 2010, **132**, 154104/154101-154104/154119.
13. G. Te Velde, F. M. Bickelhaupt, E. J. Baerends, C. Fonseca Guerra, S. J. A. Van Gisbergen, J. G. Snijders and T. Ziegler, *J. Comput. Chem.*, 2001, **22**, 931-967.
14. C. F. Guerra, J. G. Snijders, G. Te Velde and E. J. Baerends, *Theor. Chem. Acc.*, 1998, **99**, 391-403.

15. ADF, *Theoretical Chemistry*, 2013, <http://www.scm.com>, Vrije Universiteit, Amsterdam, The Netherlands.
16. E. van Lenthe, A. Ehlers and E.-J. Baerends, *J. Chem. Phys.*, 1999, **110**, 8943-8953.
17. A. Klamt and G. Schueuermann, *J. Chem. Soc., Perkin Trans. 2*, 1993, 799-805.
18. N. L. Allinger, X. Zhou and J. Bergsma, *J. Mol. Struct.: THEOCHEM*, 1994, **118**, 69-83.
19. P. J. Stephens, F. J. Devlin, C. F. Chabalowski and M. J. Frisch, *J. Phys. Chem.*, 1994, **98**, 11623-11627.
20. C. P. Kelly, C. J. Cramer and D. G. Truhlar, *J. Phys. Chem. B*, 2006, **110**, 16066-16081.
21. A. Lewis, J. A. Bumpus, D. G. Truhlar and C. J. Cramer, *J. Chem. Educ.*, 2004, **81**, 596-604.
22. P. Winget, C. J. Cramer and D. G. Truhlar, *Theor. Chem. Acc.*, 2004, **112**, 217-227.
23. C. J. Cramer, A. Kinal, M. Wloch, P. Piecuch and L. Gagliardi, *J. Phys. Chem. A*, 2007, **111**, 4871.
24. A. J. Esswein, Y. Surendranath, S. Y. Reece and D. G. Nocera, *Energy Environ. Sci.*, 2011, **4**, 499-504.